The Novel Anti-Infective BDM-I: Clinical Utility and Mechanism of Action

Michael Radzieta

Supervisor: A/Prof Slade Jensen

School of Medicine

Western Sydney University

March 2019

A thesis presented to

Western Sydney University

In fulfilment of requirements

for the Degree of

Doctor of Philosophy (Ph.D.)

Table of Contents

List of Figures

Chapter 5

Chapter 6

Chapter 7

List of Tables

List of Abbreviations

Abbreviation	Full Term
Δ	deletion
°C	degrees Celsius
(v/v)	volume per volume
(w/v)	weight per volume
%	percent
Ala	alanine
AMP	ampicillin
Arg	arginine
ARG	antibiotic resistant gene
Asn	asparagine
Asp	aspartic acid
ATP	adenosine-5'-triphosphate
bp	base pairs
BCP	bacterial cytological profiling
BHIA	brain heart infusion agar
BHIB	brain heart infusion broth
$CaCl_2$	calcium chloride
CA-MRSA	community-acquired methicillin-resistant *Staphylococcus aureus*
CAMP	cationic antimicrobial peptide
CFU	colony forming units
CML	chloramphenicol
Cys	cysteine
Da	Dalton(s)
DAPI	4',6-diamidino-2-phenylindole
DARTS	drug affinity responsive target stability
DMSO	dimethyl sulfoxide
DNA	deoxyribonucleic acid
dNTP	deoxynucleoside triphosphate
EDTA	ethylene diamine tetraacetic acid
e.g.	exempli gratia; 'for example'
et al.	et alia; 'and others'
FM4-64	FM® Lipophilic Styryl Dye
g	grams
g	unit of gravity
GFP	green fluorescent protein
Gln	glutamine
Glu	glutamic acid
Gly	glycine
h	hour(s)
HA-MRSA	hospital acquired methicillin-resistant *Staphylococcus aureus*
hVISA	heterogeneous vancomycin-intermediate *Staphylococcus aureus*
i.e.	id est; 'that is'
IS	insertion sequence

Ile	isoleucine
kb	kilobase(s)
kDa	kiloDalton(s)
L	litre(s)
LBA	Luria-Bertani agar
LBB	Luria-Bertani broth
LC/MS	liquid chromatography-mass spectrometry
Leu	leucine
Lys	lysine
Met	methionine
µg	microgram(s)
µL	microliter(s)
µM	micromolar
M	molar
MDR	multi-drug resistant
mg	milligram(s)
$MgCl_2$	magnesium chloride
MGE	mobile genetic elements
MHA	mueller hinton agar
MHB	mueller hinton broth
MIC	minimum inhibitory concentration
min	minute(s)
mL	millilitre(s)
mM	millimolar
MoA	mechanism of action
MRSA	methicillin-resistant *Staphylococcus aureus*
MS	mass spectrometry
MW	molecular weight
OD	optical density
NaCl	sodium chloride
PCR	polymerase chain reaction
PDR	pandrug resistant
pI	isoelectric point
PBP	penicillin binding protein
Pro	proline
PTP	protein tyrosine phosphatase
RNA	ribonucleic acid
rpm	revolution per minute
RT	room temperature
s	second(s)
SEM	scanning electron microscopy
Ser	serine
STI	sexually transmitted infeciton
TBE	tris/borate/EDTA
TCS	two component system
TEM	transmission electron microscopy

Thr	threonine
T_m	melting temperature
TPP	thermal proteome profiling
Trp	tryptophan
Tris-HCl	tris-hydroxymethylaminomethane-hydrogen-chloride
TRITC	tetramethylrhodamine
TSB	tryptic soy broth
Tyr	tyrosine
UV	ultraviolet
VAN	vancomycin
VISA	vancomycin-intermediate *Staphylococcus aureus*
VSSA	vancomycin-susceptible *Staphylococcus aureus*
VRE	vancomycin-resistant Enterococci
XDR	extensive-drug resistant

Summary

Since the introduction of antibiotics into clinical use, bacteria have continued to evolve and acquire mechanisms of resistance. In a relatively short time period, this has rapidly escalated into a serious health crisis recognised by major governing/scientific bodies worldwide. The rate at which antibiotic resistance spreads now outpaces our current ability to discover and manufacture new antibiotics.

Steps taken to combat antibiotic resistance have had little impact in preventing the spread of relevant pathogens, especially within hospital settings. The current state of antibiotic development has only exacerbated these issues by severely limiting the arsenal of therapeutics available to treat problematic infections. Without sufficient incentives, large pharmaceutical companies have focused on developing financially 'safe' drugs to treat non-infectious related conditions, leaving the bulk of antibiotic research to smaller biotechnology companies and academia, often in collaboration together.

In this study, we have examined the clinical utility and mechanism of action (MoA) of BDM-I, which is a small synthetic molecule currently being developed by the Australian biotechnology company Opal Biosciences Limited. Importantly, BDM-I (3,4-methylenedioxy-β-nitropropene) appears to be a novel antimicrobial compound and has shown promising activity *in vitro* against clinically relevant pathogens, such as MRSA and VRE. In this regard, previous studies have shown that BDM-I does not inhibit common antimicrobial targets, and proposed that it binds to bacterial tyrosine phosphatases. While an antibiotic inhibiting a novel cellular target(s) is desirable, in this case the specific MoA (of BDM-I) and its physiological effect on bacterial cells is not known, thus limiting the potential for further development.

Therefore, due to this knowledge gap, we attempted to gain insight into the BDM-I MoA (including its binding partner) using an omics approach (i.e. whole genome sequencing and proteomics). Additionally, we also aimed to study the activity of BDM-I against the clinically relevant ESKAPE pathogens.

To study the activity of BDM-I, extensive MIC testing was completed using clinical isolates with varying degrees of multi-drug resistance. Initial tests using gram-negative isolates (*K. pneumoniae*, *P. aeruginosa* and *E. coli*) did not identify any antimicrobial activity at concentrations ≤128 μg/mL. However, studies using the gram-positive pathogens *S. aureus* and *E. faecium* revealed that BDM-I displayed good (and potentially clinically relevant) activity, particularly against *S. aureus*. Additional MIC testing was then completed using a large number of clinical MRSA and VRE isolates with varying degrees of vancomycin susceptibility. Interestingly, we identified that BDM-I is highly effective against vancomycin intermediate *S. aureus* (VISA) isolates, which prompted further investigation into possible synergy between BDM-I and vancomycin. Results from these studies identified that BDM-I exerts an additive/synergistic effect on vancomycin in the case of hVISA and VISA isolates, as well as *vanB* VRE isolates.

Induction experiments were then conducted using MRSA and VRE, in order to generate mutants with increased resistance to BDM-I. In this regard, MRSA was (in most cases) unable to develop increased resistance. However, in the case of VRE, significant MIC increases were observed within 10 days of BDM-I exposure, which continued steadily until the experiment was terminated. Importantly, the generation of mutant isolates

enabled us to utilise whole genome sequencing in an attempt to identify mutations driving the increased resistance and elucidate the BDM-I MoA.

Subsequently, analysis of the sequencing data revealed mutations within different genes of the ATP synthase operon for all sequenced VRE mutants, indicating that BDM-I may affect ATP synthesis. In comparison, analysis of the MRSA mutant data revealed mutations within the *walK* gene, which is part of the WalKR two component regulatory system (associated with cell wall homeostasis). Following whole genome sequencing, we then conducted proteomic analysis of proteins extracted from BDM-I treated MRSA and VRE cells, in order to identify global changes in expression levels. Interestingly, and consistent with the above observations, we identified the downregulation of ATP synthase subunits within both VRE and MRSA by ≥2-fold, as well as the downregulation of WalK within MRSA by ≥9-fold. Additionally, we also identified that proteins involved in lactic acid fermentation were upregulated within VRE, while proteins involved in UMP biosynthesis (pyrimidine metabolism) were significantly downregulated within both isolates.

In combination, whole genome sequencing and proteomic analysis revealed that ATP synthase is likely (negatively) affected as a result of the BDM-I MoA. Therefore, we utilised ATP assays to examine whether ATP synthesis was inhibited upon exposure to BDM-I. Subsequently, results identified significant reductions in intracellular ATP concentrations, suggesting that BDM-I does in fact affect the activity of ATP synthase. Additionally, we also examined the relationship between BDM-I and WalK by imaging (via transmission electron microscopy) BDM-I MRSA mutants, in order to identify changes in the cell wall phenotype. Interestingly, this revealed significant reductions in

cell wall thickness, which correlated with increased resistance to BDM-I and increased susceptibility to vancomycin and daptomycin.

Finally, we attempted to identify the BDM-I binding partner using novel methods, including the drug affinity response sensitivity assay (DARTS) and thermal proteome proteomics (TPP). Unfortunately, we were unable to identify a potential binding partner using DARTS, likely due to the limited sensitivity of the protocol and its reliance on gel-based separation techniques. However, preliminary results from TPP analysis identified several proteins that were thermostabilised following BDM-I treatment, one of which (adenylate cyclase) may be linked to the apparent MoA of BDM-I (i.e., negatively affecting ATP synthesis).

By completing this study, we were able to identify that BDM-I displays significant activity against MRSA and VRE isolates. Furthermore, we were able to identify a synergistic relationship between BDM-I and vancomycin, which highlights the potential use of both antibiotics in combination to treat complicated infections. Regarding the BDM-I MoA, we identified through whole genome sequencing, proteomics and ATP assays, that BDM-I affects ATP synthesis (via the oxidative phosphorylation pathway). In this regard, *E. faecium* has the ability to adapt to BDM-I (at least to some extent) by potentially switching to substrate level ATP synthesis via lactic acid fermentation, while *S. aureus* adapts to BDM-I by regulating cellular pathways/processes (such as cell wall synthesis) that require large quantities of ATP, and this is likely due to the essentiality of ATP synthase in *S. aureus*.

Declaration

This is to certify that to the best of my knowledge, the content of this thesis is my own work. The thesis has not been submitted for any degree or other purposes. I certify that the intellectual content of this thesis is the product of my own work and that all the assistance received in preparing this thesis and sources have been acknowledged.

Michael Radzieta

Acknowledgments

Firstly, I would like to state my utmost gratitude to my primary supervisor A/Prof Slade Jensen, for all of the support, guidance and knowledge he has provided me over the past 4 years of my candidature. I would also like to thank my fellow PhD student Grace Micali for being a constant source of support over the past few years, both inside and outside the lab. Additionally, I would like to thank my former co-supervisor Dr Björn Espedido for all of the skills he taught me at the beginning of my candidature, which were paramount in moving forward independently with my research.

I would also like to acknowledge the scientists who have collaborated with my project and helped me develop my skills in a wide variety of experimental techniques. My gratitude goes do Prof Stuart Cordwell and William Klare from Sydney University, Prof Jens Coorrsen and Dr Chandra Malladi from Western Sydney University and Murray Killingsworth from the South West Sydney Local Health District. I would also like to thank Julie Phillips from Opal Biosciences for the opportunity to study BDM-I, as well as for providing me with financial assistance to attend multiple conferences during my candidature.

Finally, I would like to thank my family for their support over the last 4 years while I completed my (seemingly) never ending studies. In particular, I would like to acknowledge my love and appreciation for my fiancée Jen, for always keeping me positive and motivated, especially towards the end of my candidature when times were stressful and I needed her support the most. I would also like to thank my father Ron and my sister Katie for their support and constant interest in my work.

Chapter 1

Introduction

1.1 Antibiotic Discovery

The term antibiotic was initially used by Waksman et al. (1942) to describe any substance produced by a microorganism that was antagonistic to the growth of another in high dilution. However, it is now used to more broadly describe antibacterial compounds, including those that are semi-synthetic and synthetic, such as sulphonamides. In any case, following the discovery of penicillin in 1928 by Alexander Fleming, there was a substantial increase into the research and development of antimicrobial compounds. In the following decades numerous antibiotics were discovered and implemented into clinical use. However, since the 1960s, the discovery rate of novel antimicrobials has dropped significantly, with only two new antibiotic classes being discovered and deployed clinically (*i.e,* oxazolidinones and lipopeptides, such as linezolid and daptomycin, respectively) (Fischbach and Walsh, 2009). Worryingly, the majority of antibiotics in clinical use today are derivatives of compounds which were discovered between the 1940s and 1960s. This trend in reduced antibiotic development/deployment now coincides with the continual emergence and spread of antibiotic resistant bacteria (Figure 1.1) (Lewis, 2013).

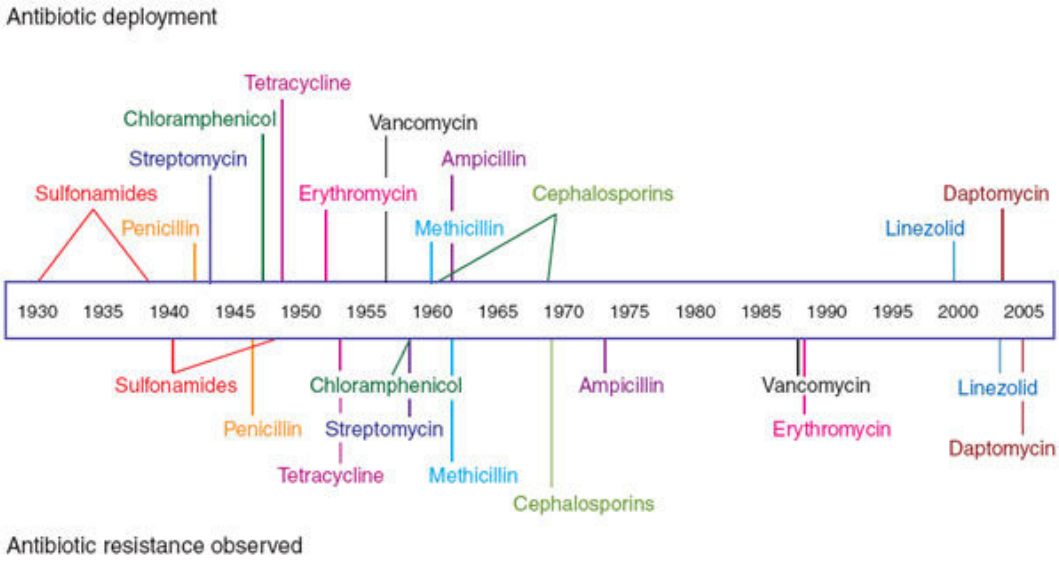

Figure 1.1: Timeline illustrating the date antibiotics were deployed (into clinical use) as well as the date resistance was first observed. Image adapted from Clatworthy et al. (Clatworthy et al., 2007)

Flemming's accidental discovery in 1928 was the catalyst that began the golden age of antibiotic discovery. His work, as well as that of Selman Waksman in the 1940s (developed the first method of high throughput screening of soil Streptomycetes) drove the discovery of antibiotics such as streptomycin, which was pivotal in treating once incurable diseases such as tuberculosis (Lewis, 2016). Over the next 20 years, using the "Waksman platform", most of the major classes of antibiotics that are currently used clinically were discovered and utilized with great effect to treat bacterial infections. However, in the 1960s the "Waksman platform" became obsolete, with no novel antimicrobials being discovered. This shifted antibiotic development towards synthetic compounds and the modification of existing natural compounds. Again, these methodologies were effective, with the development of the widely successful fluoroquinolones, as well as the production of analogues of naturally occurring

compounds (Lewis, 2016). Additionally, during this time pharmaceutical companies began moving away from antibiotic development due to the belief that infectious diseases were no longer a major concern. In the 1990s however, it became clear that this was not the case as the spread of resistance began to outpace the development of antimicrobials.

Modern methods of antibiotic discovery have been driven by advances in technology, particularly in genomics and computing which have enabled a 'genes-to-drugs' approach as the standard for therapeutic drug development (Brown and Wright, 2016). Whole genome sequencing coupled with high-throughput DNA manipulation techniques have driven the search for novel antibiotic targets (based on gene essentiality), that are insusceptible to known mechanisms of resistance. While these methods have been successful in identifying potential drug targets, screening methods have been unable to identify suitable compounds with the necessary pharmacodynamic profiles (Brown and Wright, 2016). Chemical screening of whole cells for growth inhibition has also been used in modern antimicrobial discovery, although this methodology is associated with its own drawbacks including the generation of extremely large datasets of active compounds, which are difficult to pursue due to a lack of prioritization tools (Brown and Wright, 2016).

Unfortunately, these modern approaches to drug discovery have been largely unsuccessful in identifying novel antimicrobial compounds to combat the increasing prevalence of antibiotic resistance, as only two new classes of antibiotics have been discovered since the 1960s (*i.e,* oxazolidinones and lipopeptides) (Fischbach and Walsh, 2009).

1.2 Major Antibiotic Classes

Antibiotics selectively inhibit essential cellular processes within prokaryotic organisms, and act to either kill (bactericidal) or inhibit their growth (bacteriostatic). The majority of antimicrobials currently used clinically target one of three main processes within a bacterial cell (Figure 1.2); cell wall synthesis, protein synthesis, and nucleic acid synthesis (Kohanski et al., 2010, Walsh, 2000).

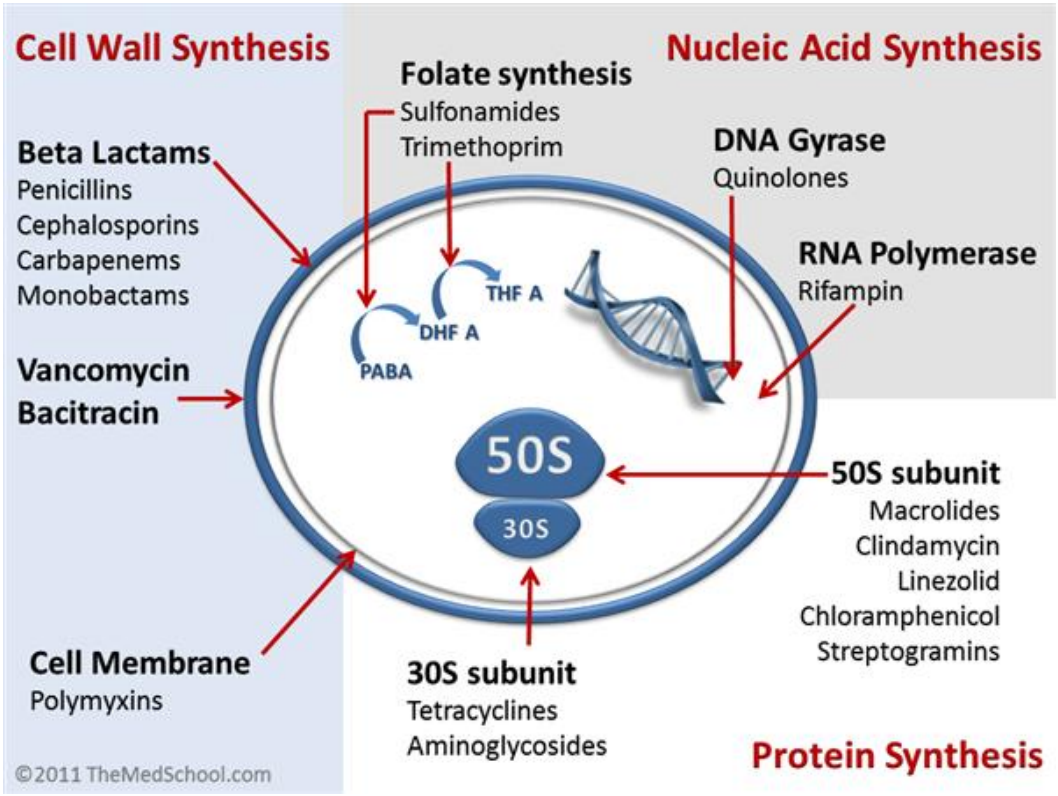

Figure 1.2: Cellular Targets of Antibiotics. Broadly speaking, antibiotics target one of three key cellular processes including cell wall synthesis, nucleic acid synthesis and protein synthesis. Image sourced online from https://www.orthobullets.com/basic-science/9059/antibiotic-classification-and-mechanism

1.2.1 Inhibitors of Cell Wall Synthesis

Most bacteria possess a cell wall making it an ideal target for antimicrobial compounds, due to its absence in mammalian cells, as well as its variation between different bacterial genera. The key component of the cell wall is a mucopolysaccharide called peptidoglycan, whose composition and location within the cell envelope differs between gram-positive and gram-negative bacteria. Peptidoglycan synthesis is a multi-step process with four key stages: the synthesis of peptidoglycan precursors in the cytoplasm; the transport of the newly formed lipid-anchored disaccharide-pentapeptide monomer subunit (lipid II) across the membrane; the insertion of glycan chains into the cell wall, and; transpeptidation linking and overall maturation (McDermott et al., 2003, Typas et al., 2011).

β-lactams (penicillins, carbapenems, cephalosporins) are the most widely used antibiotics possessing a broad spectrum of activity. They target the third stage of peptidoglycan synthesis by inhibiting the formation of peptide bonds which are catalysed by penicillin-binding proteins (PBPs). β-lactams contain a cyclic amide ring that competitively binds to the PBP binding site, which disables the enzyme and effectively blocks the PBP peptidoglycan cross-linking activity, resulting in the induction of cell stress responses and cell lysis (Kohanski et al., 2010). Another group of antibiotics targeting cell wall synthesis are the *Glycopeptides* (vancomycin, teicoplanin), which are large hetero-cyclic molecules with specific activity against gram-positive species. Unlike the β-lactams, glycopeptides bind to the cell wall directly instead of anabolic enzymes (PBPs). They function by binding to the D-Ala-D-Ala dipeptide terminus of peptidoglycan pentapeptide side chains and thus inhibit transglycosylase and PBP activity. As a consequence, this prevents the addition of new subunits to peptidoglycan which inhibits cell wall maturation and reduces

the overall mechanical strength of the cell (Kohanski et al., 2010, McDermott et al., 2003).

Additional antibiotics are available that inhibit peptidoglycan synthesis, such as fosfomycin and bacitracin, which inhibit the synthesis and transport of individual peptidoglycan units, respectively. Furthermore, cationic antimicrobial peptides (such as polymyxin B) and lipopeptide antibiotics such as daptomycin are also currently in use to treat infections caused by gram-positive organisms, although they target the cell membrane rather than peptidoglycan synthesis, and function by aggregating within the cell membrane and inducing rapid membrane depolarization resulting in cell death (Kohanski et al., 2010).

1.2.2 Inhibitors of Protein Synthesis

Protein synthesis is a complex process that is divided into three primary phases, initiation, elongation and termination. Synthesis is carried out within the ribosome, which is composed of two subunits (termed 50S and 30S), that complex with an mRNA transcript (tRNA) and initiation factors to translate linear protein from mRNA. Given the significant differences between prokaryotic and eukaryotic ribosomes and their essentiality in cellular metabolism, they present an ideal target for antibiotics.

Broadly speaking, protein synthesis inhibitors target either the 30S or 50S ribosomal subunits. Antibiotics that target the former include the tetracyclines, which block access of tRNA to the ribosome, and the aminocyclitols (spectinomycin, aminoglycosides). Spectinomycin and aminoglycoside antibiotics target the 16S rRNA segment of the 30S subunit, although they inhibit protein synthesis at this site using different mechanisms. Spectinomycin inhibits the elongation factor-catalysed translocation of peptidyl tRNA to

the ribosome, which reduces the binding stability of tRNA. In comparison, the aminoglycosides promote protein mistranslation by altering the complex formed between an mRNA codon and tRNA at the ribosome, promoting the addition of incorrect amino acids (Kohanski et al., 2010).

Antibiotics that target the 50S ribosomal subunit include the macrolides, lincosamides, streptogramins, amphenicols and oxazolidinones. The majority of these 50S ribosome inhibitors function by physically inhibiting the translocation of peptidyl tRNAs. In doing so, amino acids cannot be added to a growing peptide chain within the ribosome. An exception to this are the oxazolidinones, as they block the initiation of protein translation (Kohanski et al., 2010).

1.2.3 Inhibitors of Nucleic Acid Metabolism

Synthetic compounds including the quinolones (fluoroquinolones), sulphonamides and rifamycins are commonly used broad-spectrum antibiotics that target nucleotide synthesis (McDermott et al., 2003).

Sulphonamides such as trimethoprim are the oldest class of antimicrobials, and were the first to be introduced clinically in the 1930s. They are structurally similar to *p*-aminobenzoic acid (PABA), which is involved in the synthesis of purine and pyrimidine nucleotides, and function by competitively binding to the active site of the enzyme dihydropteroate synthetase and blocking the formation of nucleotide precursors (McDermott et al., 2003).

Quinolones inhibit the activity of topoisomerase enzymes which catalyze the supercoiling of DNA strands during cell division. Two enzymes can be targeted by quinolone

antibiotics depending on the gram-reaction of the target bacteria. Within gram-negatives, quinolone antibiotics will primarily target topoisomerase IV, while in gram-positives they will primarily target topoisomerase II (DNA Gyrase) (Kohanski et al., 2010, McDermott et al., 2003). The effect of quinolone binding to topoisomerase enzymes results in cell death due to the introduction of double-stranded DNA breaks, which are bound to and blocked by the topoisomerase-quinolone complex. This blockage inhibits DNA-replication machinery and stalls DNA synthesis, leading to bacteriostasis and eventually cell death (Kohanski et al., 2010).

The rifamycins are another class of antibiotics inhibiting nucleic acid synthesis and are used routinely to treat infections caused by *M. tuberculosis*. Rifamycin antibiotics such as rifampin target the β-subunit of an actively transcribing RNA polymerase, effectively inhibiting the initiation of bacterial transcription. This mechanism is bactericidal in gram-positive species and bacteriostatic in gram-negative species, which is attributed to differences in drug uptake associated with the physiologies of each cell type (Kohanski et al., 2010, McDermott et al., 2003).

1.3 Antibiotic Resistance

Antibiotic-like compounds have existed within nature long before their implementation into clinical settings. It is estimated that antibiotics and antibiotic resistance genes have existed for millions of years, dating back to the Cambrian period (Allen et al., 2010). The role of antibiotic-like compounds in microbial communities is not fully understood, with evidence suggesting they play a role in microbial signalling networks, in addition to cell inhibition. In this regard, it is believed that such compounds play essential roles in various aspects of microbial life, including; pathogenesis, community structure and biofilm

formation (Allen et al., 2010, Hall and Barlow, 2004, Ryan and Dow, 2008). Similarly, antibiotic resistance genes also appear to play important roles in microbial interactions, possibly functioning in the regulation of biosynthetic pathways (Allen et al., 2010).

While it is established that antibiotics predate their clinical implementation, it is due to heavy selective pressures associated with both clinical and industrial uses of antibiotics, that we are seeing an alarming increase in the generation of antibiotic resistant organisms. Arguably, the greatest misuse of antibiotics is seen within the agricultural industry. Antibiotics have been used in agriculture and aquaculture extensively since their discovery in the mid-1900s to treat disease, promote growth and enhance feed proficiency. The large-scale use of antibiotics in feed and water creates an ideal environment for the increased prevalence of antibiotic resistant organisms associated with farm animals, which can then be disseminated into the environment risking potential exposure to humans. For example, the emergence of vancomycin-resistant enterococci (VRE) in Europe in 1996 was attributed to the use of the related antibiotic avoparcin in animal feed, which eventually led to the ban of the compound from animal husbandry (Arias and Murray, 2012, Dantas and Sommer, 2014, Levy and Marshall, 2004, Silbergeld et al., 2008).

The misuse (or simply use) of antibiotics within a clinical setting is the second greatest contributor to the development of antibiotic resistance, especially within healthcare environments. Antibiotics are often prescribed for non-bacterial infections to demanding patients, who will often choose not to finish a course of antibiotics once their health improves. These practices facilitate the selection and proliferation of resistant strains which can potentially be spread within the community (Bush et al., 2011). Major concerns

surrounding the misuse of antibiotics are within the developing world, where antibiotics are available over the counter without prescriptions, which, when coupled with poor hygiene, results in a reservoir for the generation of multi-resistant superbugs.

1.3.1 Mechanisms of Resistance

Antibiotics can be classified by their primary cellular targets, as well as whether they are bacteriostatic or bactericidal. As stated previously, most antimicrobial compounds target one of three primary targets; nucleic acid synthesis, protein synthesis, or cell wall synthesis (Kohanski et al., 2010, Walsh, 2000). Similarly, there are three primary resistance mechanisms employed by bacteria to circumvent the inhibitory actions of antimicrobials. These methods include; the enzymatic inactivation of an antibiotic, the removal of the antibiotic from the cell and the modification of the antibiotic's target, as illustrated in Figure 1.3.

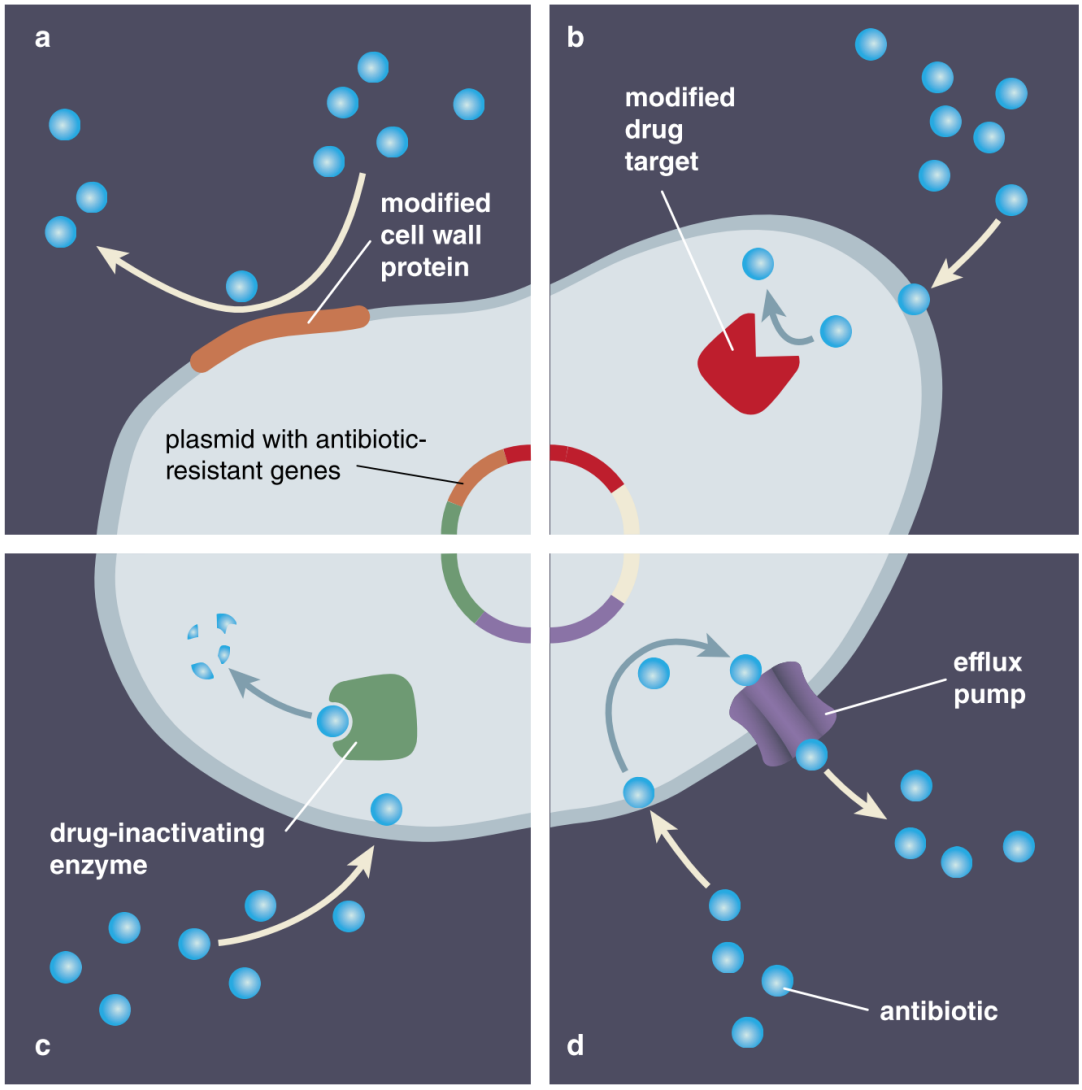

Figure 1.3: Bacterial Mechanisms of Antibiotic Resistance including; (a and b) modification of drug target through mutation, (c) enzymatic inactivation of the drug molecule and (d) the removal of the antibiotic by efflux pumps. Image adapted from Dantas and Sommer (Dantas and Sommer, 2014).

Antibiotic resistance in bacteria is either intrinsic, arises via genetic mutation, or is acquired through horizontal gene transfer (of resistance determinants), or a combination thereof. Intrinsic resistance is often genera specific and describes resistance against antibiotics which is due to the innate physiology of a specific bacterial species (Cox and Wright, 2013). It is most often associated with gram-negative bacteria due to the presence of an outer membrane that surrounds a relatively thin layer of peptidoglycan. The outer membrane is composed of lipid molecules bound to polysaccharide units, which, due to the tightly packed nature of the hydrocarbon chains and the large number of linked fatty acid chains, significantly reduce its permeability and thus the ability of antibiotics to cross into the cell (Arzanlou et al., 2017, Cox and Wright, 2013). To compensate for this reduced permeability, gram-negative species possess porins within the membrane that allow for the diffusion of molecules into the cell. However, porins also inhibit the entry of antibiotics into the cell via several mechanisms, including size limitation and charge repulsion (Cox and Wright, 2013).

Intrinsic resistance is also driven by multi-drug resistance efflux pumps (Figure 1.3d), which are present within both gram-positive and gram-negative bacterial species. Efflux pumps can be either substrate specific or target a broad range of molecules (such as classes of antibiotics), and function by actively exporting drug molecules out of a cell at a faster rate than they can enter by diffusion (Cox and Wright, 2013, Walsh, 2000). There are five main classes of efflux pumps within prokaryotes, the ATP binding cassette (ABC), the major facilitator (MF), the multidrug and toxic compound efflux (MATE), the small multidrug resistance (SMR) and the resistance-nodulation-division family (RND). The RND family are the main drivers of intrinsic resistance in gram-negative bacteria and have been identified in multiple species, including *P. aeruginosa* (MexAB-

OprM RND system) and *E. coli* (AcrAB-TolC RND system), and drive resistance against multiple antibiotics including β-lactams, fluoroquinolones, tetracycline and macrolides. While efflux pumps alone are not sufficient to produce high level resistance, it is due to a combination of both the outer membrane and constitutively expressed efflux pumps that some gram-negative species are intrinsically resistant to certain antibacterial compounds (Cox and Wright, 2013).

In addition to intrinsic resistance, bacteria are also capable of acquiring resistance to antibiotics through the horizontal gene transfer of resistance determinants (carried by plasmids, for example). Such determinants typically encode proteins involved in the enzymatic inactivation of a drug, the modification of a drug target, or even drug efflux as discussed above (Munita and Arias, 2016).

Of these, a common mechanism is the enzymatic alteration or complete degradation of an antibiotic (Figure 1.3c), which was first discovered in the 1950s for penicillin resistant bacteria. The chemical alteration of antibiotic compounds is common in both gram-positive and gram-negative bacteria, and typically occurs through the acetylation, phosphorylation or adenylation of a compound. These reactions result in steric hindrance and a significant decrease in a drugs affinity for its target (Munita and Arias, 2016, Walsh, 2000). Resistance driven by drug modification has been documented extensively in the case of aminoglycoside resistance. Multiple aminoglycoside modifying enzymes (AMEs) have been described and are the main contributors to aminoglycoside resistance worldwide. Genes encoding for AMEs are typically found on mobile genetic elements (MGEs) and covalently alter the hydroxyl or amino groups of aminoglycoside molecules. The AMEs present within bacterial populations tend to vary widely based on geographical

distribution. For example, the phosphotransferase family of enzymes is widely distributed amongst gram-negative and gram-positive bacteria and provides resistance against kanamycin and streptomycin, while the acetyltransferase family of enzymes is found predominantly in gram-negative species affecting most aminoglycoside antibiotics (Munita and Arias, 2016).

Alternatively, antibiotics may be enzymatically destroyed before they are able to reach their targets within the cell. In the context of penicillin resistance which has been observed since the 1950s, was the discovery of the β-lactamase enzymes which destroy β-lactam antibiotics by removing the amide of the β-lactam ring. To date, over 1000 β-lactamases have been discovered which illuminates a "prime example of antibiotic-driven bacterial evolution" (Munita and Arias, 2016). Multiple β-lactamases have been identified and are generally characterized into one of four groups based on their substrate specificity.

Group A β-lactamases contain a serine residue in their catalytic site and include a variety of different proteins with differing activities, including the penicillinases, extended spectrum β-lactamases (ESBLs) and carbapenemases. Unique to group A proteins is their sensitivity to clavulanic acid (β-lactamases inhibitor) and their activity against the monobactams, but not the cephamycins (Bush, 2013).

Group B β-lactamases are known as the metallo-β-lactamases due to the fact they utilize a metal ion as a cofactor when binding to the β-lactam ring. Originally, the genes encoding these enzymes were known to be located only on the chromosome, however in the 1990s a large number of gram-negative hospital pathogens were reported to carry genes encoding these enzymes, indicating that they were now being spread via horizontal gene

transfer (Munita and Arias, 2016, Queenan and Bush, 2007). A prominent member of the group B β-lactamases is the New Delhi Metallo β-lactamase (NDM-1), which was first isolated in 2008 from a Swedish patient who had been hospitalized in India. The bla_{NDM} gene is of particular concern due to its high rate of transmission between different gram-negative species, which has allowed for its rapid dissemination within several countries (Bush and Jacoby, 2010).

Group C β-lactamases are active against all penicillins and cephalosporins currently available. In terms of clinical importance, the group C enzyme AmpC remains the major facilitator of β-lactam resistance in several gram-negative species, most often located on the chromosome (although it has been identified on plasmids) of several bacteria including *E. aerogenes*, *M. morganii* and *P. aeruginosa*, among others (Jacoby, 2009).

The final class of β-lactamass (group D) are commonly known as the OXA class of enzymes and are characterized by their ability to degrade third generation cephalosporins and carbapenems. Many OXA enzymes have been described and are typically carried on a range of mobile genetic elements, most of which are capable of interspecies transmission. For example, OXA-48 is a common group D β-lactamase which is wide spread in *K. pneumoniae* and other Enterobacteriaceae (Bush and Jacoby, 2010, Evans and Amyes, 2014, Munita and Arias, 2016).

Another mechanism of acquired resistance involves the modification of a drug target to reduce its affinity for an antibiotic (Figure 1.3a-b). This mechanism typically occurs by either protecting the target site, or completely modifying the target site. A well-studied example of target protection is tetracycline resistance in *Streptococcus* spp, which is

mediated by the plasmid bound Tet(M) protein. Tet(M) acts as a homologue of elongation factors used in translation, and acts by releasing tetracycline which has bound to the ribosome. When releasing tetracycline, it also causes a conformational change within the ribosome which prevents tetracycline from rebinding to its target site (Munita and Arias, 2016).

Alternatively, bacteria may modify the target site of antibiotics either via the acquisition of mutations within the site, or via the activity of specialized enzymes. Numerous target site mutations have been identified which confer resistance to a variety of antibiotics, with one of the most well characterized being rifampin resistance. Rifampin acts by inhibiting the DNA-dependent RNA polymerase (*rpoB*) which blocks bacterial transcription. High level resistance to rifampin can arise due to single nucleotide polymorphisms (SNPs) within *rpoB* that cause an amino acid substitution. This alteration significantly reduces the affinity of rifampin to its target site. Other examples of mutational resistance include fluoroquinolone and oxazolidinone resistance, due to chromosomal mutations in genes encoding the target sites (Dantas and Sommer, 2014, Munita and Arias, 2016).

Bacteria can also develop resistance by enzymatically altering the target site. This mechanism has been observed within vancomycin resistant Enterococci (VRE), as well as within *S. aureus* strains resistant to erythromycin. Vancomycin resistance in Enterococci is mediated by the *vanHAX* genes, which encode several enzymes which produce peptidoglycan terminating with D-Ala-D-Lac rather than D-Ala-D-Ala, which has a 1000-fold decreased affinity to vancomycin (discussed further in section 1.4) (Walsh, 2000). Erythromycin resistance in *S. aureus* can be facilitated using a similar

strategy, involving the modification of the 23S RNA component of the ribosome by the enzyme Erm (a methyl transferase) (Walsh, 2000).

1.3.2 Spread of Resistance

In most cases, it is not long after an antibiotic is introduced clinically that significant resistance emerges (see Figure 1.1); which can occur on a timescale of months to years (Walsh, 2000). The ability of bacteria to rapidly acquire, and in turn disseminate genetic material conferring resistance, is an evolutionary mechanism that often outpaces our (current) ability to develop effective novel treatments. The mechanisms that facilitate the transfer of DNA between bacteria have been studied extensively, and typically occur in one of two ways (Figure 1.4); vertical transfer (*de novo* mutations that occur during replication are passed on to subsequent generations), or more importantly, horizontal gene transfer (Andersson and Hughes, 2010, Dantas and Sommer, 2014).

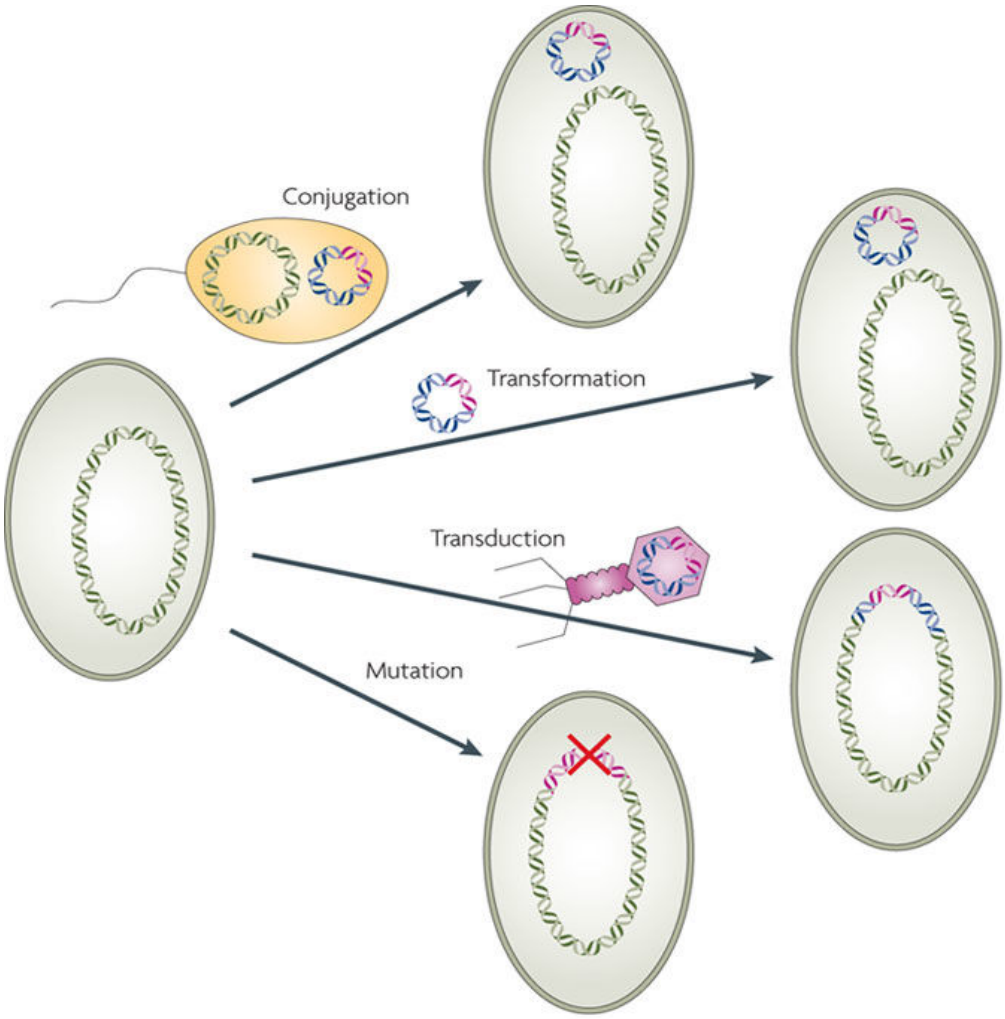

Figure 1.4: Mechanisms of spreading antibiotic resistance. Resistance spreads commonly through horizontal gene transfer, including conjugation (direct transfer of plasmid DNA from a donor to recipient cell), transformation (uptake of DNA from the environment by competent cells) and transduction (transfer of resistance genes via a bacteriophage vector). Also illustrated are de novo mutations which are passed to daughter cells following replication. Image adapted from Andersson et al (Andersson and Hughes, 2010).

The most common mechanism by which resistance genes spread throughout a bacterial population is via horizontal gene transfer, which involves the transfer of mobile genetic elements (MGEs), such as plasmids, transposons and insertion sequences between bacterial cells (Normark and Normark, 2002). Horizontal gene transfer can occur through three primary mechanisms known as transformation, conjugation, and transduction.

Transformation refers to the uptake, integration, and expression of extracellular DNA under natural growth conditions by physiologically competent bacteria. Transformation was first identified as a mechanism that can facilitate the spread of antibiotic resistance genes in 1951. In this case, penicillin and streptomycin resistance determinants were introduced into previously sensitive strains of *S. pneumoniae*, by exposing them to extracellular DNA derived from resistant strains (von Wintersdorff et al., 2016). In general, for transformation to take place a number of conditions must be met, including; extracellular DNA must be present within the environment, the recipient bacteria must be competent, and the transformed DNA must be stabilized either through genome integration or recircularization. Some bacterial genera, such as *Neisseria* are constitutively competent, while others need to be induced into a competent state, which is often mitigated by environmental stressor conditions. Interestingly, studies have shown that antibiotics can also induce competence in certain species, highlighting the issue of antibiotic use prompting the spread of resistance (von Wintersdorff et al., 2016). Despite this, transformation is not considered the main mechanism driving the spread of antibiotic resistance, but has been observed in the case of penicillin resistance within the important pathogen *Streptococcus pneumoniae*, as well as resistance to fluoroquinolones and β-lactams within *Neisseria gonorrhoeae* (Barlow, 2009).

Transduction is another mechanism of horizontal gene transfer which involves the transfer of genetic material between cells via a bacteriophage vector. DNA that can be transferred via transduction includes chromosomal DNA and MGEs such as plasmids and transposons. Transduction has been associated with the transmission of antibiotic resistance genes within/between multiple species; including erythromycin and tetracycline resistance in *S. pyogenes*, β-lactam resistance in *E. coli*, and the spread of resistance plasmids in MRSA (von Wintersdorff et al., 2016). The role of transduction in the dissemination of antibiotic resistance is significant, with recent research finding that bacteriophages isolated from different environments (wastewater, animal and human faecal samples, meat) often carry multiple resistance genes, elucidating their roles as significant reservoirs of antibiotic resistance (Colomer-Lluch et al., 2014, Colomer-Lluch et al., 2011, Shousha et al., 2015).

In comparison to the others, conjugation is probably the most important horizontal gene transfer mechanism driving the spread of antibiotic resistance. Conjugation is a multi-step process involving the direct transfer of genetic material from a donor cell to a recipient cell via surface pili or adhesins (Thomas and Nielsen, 2005, von Wintersdorff et al., 2016). Genes that encode conjugation systems are generally located on plasmids or within the chromosome on integrative conjugative elements (Cabezón et al., 2015).

Plasmids (small, circular DNA molecules which are extrachromosomal in nature and capable of independent replication) represent the most commonly transferred MGE via conjugation and are often capable of carrying other MGEs in addition to resistance genes. Plasmids may be conjugative (self-transmissable), or non-conjugative (not self-transmissible) but mobilizable; a plasmid may lack all of the gene/sequences required for

self-transfer and thus rely on 'helper' conjugative plasmids. In any case, plasmids play a major role in the rapid dissemination of antibiotic resistance (and other important phenotypes) within healthcare settings and of particular concern, a single plasmid may confer resistance to multiple, distinct antibiotic classes. Once multiple resistance genes have accumulated on a plasmid, resistance can then be rapidly spread between different strains, species or genera, and this has been documented in healthcare settings (von Wintersdorff et al., 2016). For example, the wide dissemination of the *bla*$_{\text{CTX-M}}$ ESBL genes between genera of the Enterobacteriaceae has been attributed to various broad and narrow host range plasmids.

In addition to plasmids, several other MGEs, such as transposons, insertion sequences and integrons, also play a major role in the transmission of resistance genes between bacteria. Transposons and insertion sequences (IS) are DNA elements that can excise themselves and associated DNA from one genome location (on a plasmid or chromosome) and randomly integrate at another. Alternatively, integrons use site-specific recombination to move genes between locations, however these MGEs can often be co-located and transferred in a single event via conjugation into a recipient cells genome (Partridge et al., 2018). For example, integrons are often located on transposons, which in turn are often located on plasmids (Partridge et al., 2018). This cooperative framework enables bacteria to rapidly evolve through the accretion of antibiotic resistance genes within a particular cell.

1.4 ESKAPE Pathogens

Although antibiotic resistance is common across a wide variety of bacterial species, there are six species that are of particular concern in healthcare settings: *Enterococcus faecium;*

Staphylococcus aureus; Klebsiella pneumoniae; Acinetobacter baumanii; Pseudomonas aeruginosa, and; *Enterobacter* species (Boucher et al., 2009). They are collectively known by the acronym 'ESKAPE', indicating that these important hospital pathogens are readily capable of "escaping" the inhibitory effects of antimicrobials through the development of resistance mechanisms.

1.4.1 *Enterococcus faecium*

Enterococci are gram-positive cocci that are resident within the bowels of humans and other animals, often making up a small proportion of the gut microbial population (Moellering, 1992). Under the right conditions however, enterococci are capable of causing infection, often as a result of broad spectrum antibiotic use which reduces microbial competition in the gastrointestinal tract (Arias and Murray, 2012). Most enterococcal infections are nosocomial in origin, with certain pathogenic strains of *E. faecalis* and *E. faecium* being able to spread in hospital settings due to their durability in hostile environments.

A study completed in 2004 by Wisplinghoff et al., identified *Enterococcus* species as being the third most common cause of bacteraemia in the United States (Wisplinghoff et al., 2004), while another study conducted in 2008 on antibiotic-resistant pathogens associated with healthcare-acquired infections, identified *Enterococcus* species as being the second greatest cause of central line-associated bloodstream infections (Hidron et al., 2008). As such, it is apparent that *Enterococcus* species are a major contributor to the incidence of hospital acquired infections in the United States and, of particular concern, the mortality rate associated with these infections is high (33.9%) (Wisplinghoff et al., 2004). In an Australian context, a study in 2013 identified that one third of enterococcal bacteraemias were caused by *E. faecium;* of these, 90% were ampicillin resistant and

36.5% were vancomycin non-susceptible, with the majority of infections being hospital-associated (Coombs et al., 2014).

Enterococci are intrinsically resistant to a number of antibiotic classes and retain the ability to acquire additional resistance, either via mutation or through the process of horizontal gene transfer (Arias and Murray, 2012). β-lactam antibiotics such as the penicillins (primarily ampicillin) are often used alone or in combination to treat enterococcal infections. However, their use is limited against *E. faecium* as 70-95% of clinical isolates now exhibit high level resistance due to mutations within the penicillin binding protein 5 (PBP5) (Cattoir and Giard, 2014). Although *E. faecalis* causes the majority of enterococcal infections, *E. faecium* is considerably more difficult to treat due to its multidrug resistance. In this regard, glycopeptide antibiotics, such as vancomycin or teicoplanin are commonly used to treat serious enterococcal infections, often in combination with aminoglycosides due to their synergistic activity.

However, resistance to vancomycin is now increasingly common, as 36.5% of hospital acquired *E. faecium* isolates are vancomycin non-susceptible in Australia (stated above), with similar statistics observed within the US (33%) and in Europe (1% - >30% varying between regions) (Cattoir and Giard, 2014). This resistance (to vancomycin) is due to the acquisition of genes encoding for proteins that alter the terminal residues of peptidoglycan amino acid chains from D-Ala-D-Ala to either D-Ala-D-Lac or D-Ala-D-Ser, which have significantly reduced affinity for vancomycin. The most common gene operons that drive such resistance are the *vanA* operon, which is common in North America and Europe, and the *vanB* operon which is common in Australia (Cattoir and Giard, 2014). In the case of vancomycin resistance, a last resort therapy used to treat multidrug resistant isolates of *E.*

faecium is the cyclic lipopeptide daptomycin, which exhibits potent bactericidal activity against gram-positive bacteria. Currently, resistance to daptomycin is relatively uncommon in enterococci, although there have been reported cases of therapy failure with the sudden onset of high-level resistance (Cattoir and Giard, 2014).

1.4.2 *Staphylococcus aureus*

Staphylococci are gram-positive cocci which asymptomatically colonise human epithelia and are generally non-pathogenic in healthy individuals. Approximately 20% of individuals are persistent carriers of *S. aureus* within their nasal passages or axillae (under-arms), while 60% of individuals are intermittent carriers, playing host to fluctuating populations of *S. aureus* strains (Pendleton et al., 2013). Staphylococci are however opportunistic pathogens, often causing both acute and chronic (upon formation of biofilms) infections within wounds. The capacity of *S. aureus* to cause infection is due to their ability to produce a variety of toxins and virulence factors (Gould et al., 2012, Stefani et al., 2012). Produced by nearly all strains are several extracellular proteins including; haemolysins, hyaluronidase, proteases and collagenase, which are all vital in breaking down host tissue for nutrients. Additionally, certain strains (often community acquired) are able to produce unique toxins which are particularly detrimental to host health, such as the exotoxin TSST-1, which is produced by approximately 25% of *S. aureus* strains and can lead to toxic shock syndrome (Pendleton et al., 2013).

In recent years infections caused by MRSA have arisen from within community settings, giving rise to community acquired MRSA (CA-MRSA). The majority of CA-MRSA (≈90%) infections affect skin and soft tissue, predominantly resulting in cellulitis or abscesses. Severe CA-MRSA infections can result in necrotising fasciitis or necrotising pneumonia, with substantially higher mortality rates of 20% and 75%, respectively (Skov

et al., 2012). Associated with CA-MRSA is an increase in the prevalence and severity of virulence factors, most notably Panton-Valentine leukocidin (PVL), which is present within the majority of CA-MRSA lineages.

Methicillin resistance within *S. aureus* was first reported in the 1960s, however it is only in the last two decades that MRSA has been considered a significant threat as a nosocomial and community acquired pathogen (Pendleton et al., 2013). MRSA strains are those which have developed resistance to β-lactam antibiotics through the acquisition of the Staphylococcal Cassette Chromosome *mec* (SCC*mec*), a mobile genetic element which encodes for a low affinity penicillin-binding protein (PBP 2a) (2009).

Presently, severe *S. aureus* and MRSA infections are treated with the glycopeptide antibiotic vancomycin, which has been the treatment of choice for such infections since it was introduced in 1958. Of clinical concern, intermediate-resistant strains have been observed, with the earliest report being in 1996 (Hiramatsu et al., 1997). In Australia, MRSA strains exhibiting vancomycin resistance fall under one of two categories; VISA (vancomycin intermediate *S. aureus* which typically have an MIC of 4-8 μg/mL) and hVISA (heterogeneous vancomycin intermediate *S. aureus* which possess subpopulations of cells with increased vancomycin MICs) (Gosbell, 2014). In a clinical setting, studies have identified that bacteraemias caused by MRSA with vancomycin MICs of 2 or 3 μg/mL, result in a much higher mortality rate of 27%, in comparison to 12.5% associated with MRSA strains with vancomycin MICs of <1.5 μg/mL (Gosbell, 2014).

Currently, high-level vancomycin resistance in *S. aureus* is relatively uncommon. In 2009, only 11 strains had been reported worldwide that displayed high-level resistance to

vancomycin through acquisition of the VanA operon (French, 2010). However, no such strains have been identified in Australia. Such data may indicate that the longevity of vancomycin as the treatment of choice is coming to an end, emphasizing the need for new antimicrobials to be developed.

1.4.3 *Klebsiella pneumoniae*

K. pneumoniae is a non-fastidious, gram-negative bacillus which belongs to the Enterobacteriaceae family, and is a common commensal organism within the human gut microbiome. Like *S. aureus* and *E. faecium*, *K. pneuemoniae* is an opportunistic pathogen which accounts for one third of all infections caused by gram-negative species, the majority of which are healthcare associated, including; urinary tract infections, pneumoniae, surgical wound infections and septicaemia. *K. pneumoniae* is also associated with community-acquired infections, including necrotizing pneumonia and pyogenic liver abscesses (Harris et al., 2015, Navon-Venezia et al., 2017).

K. pneumoniae is heavily associated with antibiotic resistance, both intrinsically in the case of ampicillin (due to the presence of the SHV-1 penicillinase within the chromosome), and via the acquisition of antibiotic resistance genes through horizontal gene transfer. Remarkably, *K. pneumoniae* isolates have been identified which possess numerous resistance determinants, resulting in pan drug-resistant (PDR) and extensive drug-resistant (XDR) clinical isolates (Wyres and Holt, 2018).

The resistome (collection of genes which confer antibiotic resistance) of *K. pneumoniae* is well characterized and is responsible for the observed resistance against the five major classes of antibiotics which are used to treat infections caused by the Enterobacteriaceae

family. These classes include the β-lactams, aminoglycosides, quinolones, tigecycline and polymyxins (Navon-Venezia et al., 2017).

Resistance to β-lactams in *K. pneumoniae* was first observed in the 1960s following the discovery of the β-lactamase genes $bla_{\text{SHV-1}}$ and $bla_{\text{TEM-1}}$. Subsequently, in the 1980s to 2000s the first extended spectrum β-lactamase (ESBL) gene ($bla_{\text{SHV-2}}$) was identified in *K. pneumoniae*, which conferred resistance to a broad range of β-lactams including third generation cephalosporins and monobactams. Multiple ESBL genes have been identified within *K. pneumoniae* including the plasmid/transposon mediated $bla_{\text{TEM-3}}$, $bla_{\text{CTX-M}}$, and bla_{OXA} genes. More recently in 2008, the NDM-1 metallo-beta-lactamase was detected and has now been identified in multiple plasmids present within the Enterobacteriaceae family. Worryingly, *K. pneumoniae* is now the major ESBL carrying pathogen worldwide and continues to increase in prevalence globally, and is considered epidemic in several countries (Navon-Venezia et al., 2017, Wyres and Holt, 2018).

Between the 1940s and 1980s, aminoglycosides were the treatment of choice against *K. pneumoniae*, before they were replaced by the third generation cephalosporins, carbapenems and fluoroquinolones. During this time *K. pneumoniae* developed significant resistance against aminoglycosides, primarily through the acquisition of drug alteration enzymes (carried on plasmids) which function in the acetylation, adenylation or phosphorylation of antimicrobial compounds. The major resistance determinant within *K. pneumoniae* is the 16S rRNA methylase, which confers broad spectrum resistance against all aminoglycosides as identified in 2003 (Navon-Venezia et al., 2017).

Quinolones have been used extensively since the 1960s to treat infections caused by *K. pneumoniae*. Since their introduction, multiple resistance mechanisms against quinolones have been identified including; modification of the target site, production of efflux pumps and production of drug modifying enzymes. These mechanisms are a combination of plasmid mediated and chromosomal routes of resistance, including sequence mutations of the cellular target (DNA gyrase and topoisomerase IV) and reduced cell permeability through the production of multidrug efflux pumps such as *acrAB* (Navon-Venezia et al., 2017).

Polymyxins such as colistin are a class of antibiotics often used in last resort cases against infections caused by MDR gram-negative bacteria, including *K. pneumoniae*. Resistance to colistin was first identified in the early 2000s and is chromosomally driven by the modification of the target site, which (in this case) is commonly referred to as the LPS modification system. This system modifies the structure of LPS by producing a phenotype with reduced anionic charge, which severely limits the binding affinity of polymyxins to the LPS structure (Navon-Venezia et al., 2017). In recent years, plasmid mediated resistance to polymyxins has emerged through the acquisition of the *mcr-1* gene, which was likely acquired via conjugation from a donor *E. coli* isolate (Liu et al., 2016).

The final antibiotic commonly used to treat infections caused by *K. pneumoniae* is Tigecycline, which belongs to the glycylcycline class of antimicrobials. Tigecycline has been used since 2005 as an effective alternative to circumvent resistance mechanisms against tetracyclines. However, resistance to tigecycline is now increasingly reported in *K. pneumoniae* isolates, driven by chromosomal mutations within the drug target (30S

and 16S ribosomal subunits) and the acquisition of genes which alter cell permeability (Navon-Venezia et al., 2017).

1.4.4 *Acinetobacter baumannii*

A. baumannii is a gram-negative, coccobacilli which is found almost exclusively within hospital environments, particularly intensive care units. *A. baumannii* is an opportunistic pathogen most often associated with skin/soft tissue infections, urinary tract infections, ventilator associated pneumonia and bloodstream infections, and is responsible for approximately 2-10% of all gram-negative nosocomial infections worldwide (Antunes et al., 2014). *A. baumannii* is particularly problematic in healthcare settings due to its persistence in non-favourable environments, as it remains viable in a range of pH levels, temperatures and nutrients levels, which facilitates colonization on inanimate surfaces for up to 5 months (Pendleton et al., 2013).

Like other gram-negative pathogens, *A. baumannii* is intrinsically resistant to several antibiotics due to its outer membrane, constitutively expressed efflux pumps and low expression of outer membrane porins, all of which result in a reduced permeability to antimicrobials (Pendleton et al., 2013). Unsurprisingly, *A. baumannii* is also capable of acquiring resistance through horizontal gene transfer from other gram-negative species, including *P. aeruginosa* and Enterobacteriaceae (Poirel et al., 2011). Resistance to antibiotics such as the quinolones/fluoroquinolones, aminoglycosides, polymyxins and β-lactams is driven by similar resistance mechanisms observed within *K. pneumoniae* (section 1.4.3), including target modification, drug modification and the removal of antimicrobials via efflux pumps (Poirel et al., 2011).

Multi-drug resistance within *A. baumannii* isolates has become increasingly common within the last two decades in certain regions. For example, in the USA the percentage of MDR *A. baumannii* isolates has increased from 32.1% in 1999 to 51% as reported in 2010 (Pogue et al., 2013). Unique to MDR *A. baumannii* are large genomic resistance islands capable of carrying tens of resistance genes against antimicrobials and antiseptic agents. The first resistance island (AbaR1) was identified in 2006 within the MDR isolate AYE. AbaR1 was identified as being 86-kb in length and contained 45 of the 52 resistance genes present within the AYE strain. Analysis of AbaR1 revealed its composition of mobile genetic elements, including 82 of its 88 open reading frames which originated from three different genera; *Pseudomonas*, *Salmonella* and *Escherichia* (Fournier et al., 2006).

A. baumannii remains a primary concern in healthcare settings, due primarily to its highly adaptable genome and rapid acquisition of resistance determinants from other bacteria, as well as the lack of novel antimicrobials currently available (or in development) for treating MDR *A. baumannii* infections.

1.4.5 *Pseudomonas aeruginosa*

P. aureginosa is a gram-negative rod-shaped bacterium which inhabits a wide range of environments including soil, aquatic, plant, and animal habitats. Due to its nutritional versatility, *P. aeruginosa* is one of the most common causes of nosocomial infections, especially within immunocompromised patients or those treated within ICUs. *P. aeruginosa* is most commonly associated with chronic lung infections in cystic fibrosis (CF) patients, which can often result in complete respiratory failure, lung transplantation or death (Folkesson et al., 2012, Pendleton et al., 2013).

Like other gram-negative species, *P. aeruginosa* is intrinsically resistant to a variety of antibiotics including aminoglycosides, fluoroquinolones and β-lactams, due to the low permeability of its outer membrane, as well as the increased production of efflux pumps and antibiotic modification enzymes. Unique to *P. aeruginosa* is the membrane porin OprF which imposes a strict exclusion limit of 500 Da on exogenous substances, severely limiting the number of antimicrobials capable of entering the cell. The combination of OprF and efflux pumps such as the resistance-nodulation-cell division systems MexAB-OprM and MexXY-OprM, as well as inducible AmpC (β-lactamase) result in *P. aeruginosa* exhibiting high levels of intrinsic resistance, which plays a significant role in associated poor clinical outcomes (Breidenstein et al., 2011, Pendleton et al., 2013).

P. aeruginosa is also capable of acquiring resistance determinants through horizontal gene transfer, predominantly those which confer resistance against aminoglycosides and β-lactams. Of greatest concern is the documented acquisition of plasmid mediated extended-spectrum β-lactamases (ESBLs) and metallo-β-lactamases (MBLs), resulting in high level resistance to penicillin/cephalosporins and carbapenems, respectively (Breidenstein et al., 2011). Point mutations are also a major contributor to the development of antibiotic resistance in *P. aeruginosa*. For example, mutations within the gene *mexZ* cause an overexpression of the efflux pump MexXY-OprM, resulting in multi-drug resistance against aminoglycosides, fluoroquinolones and cefepime.

Chronic infections caused by *P. aeruginosa* pose a unique challenge in treatment, owing to the ability of *P. aeruginosa* to form biofilms under different environmental conditions. Biofilms can form on inanimate surfaces such as medical equipment, as well as epithelia, such as the lungs of patients with cystic fibrosis (Breidenstein et al., 2011). Biofilms

consist of a community of bacterial cells encased in an extracellular polysaccharide (EPS) substance, which allows for adhesion to surfaces and severely limits the effectiveness of antimicrobial agents and disinfectants (Rasamiravaka et al., 2015). Increased resistance within cells growing in a biofilm is due to several factors. Firstly, cells within a biofilm possess a unique transcriptome profile that differs substantially from those observed within planktonic cells, which often results in the increased expression of efflux pumps and enzymes associated with antibiotic resistance. Secondly, cells towards the centre of a biofilm have reduced nutrient availability and therefore grow at a slower rate, which greatly limits the activity of antibiotics which act on growing cells such as β-lactams. Finally, the EPS provides not only a physical barrier for antibiotics, but also creates an environment for the accumulation of secreted enzymes such as β-lactamases (Breidenstein et al., 2011).

The combination of intrinsic resistance, biofilm formation, and the acquisition of resistance determinants makes *P. aeruginosa* a primary concern within healthcare settings.

1.4.6 *Enterobacter* Species

The *Enterobacter* species are non-fastidious, gram-negative rods which are commonly associated with urinary and respiratory tract infections, often within immunocompromised patients (Pendleton et al., 2013, Santajit and Indrawattana, 2016).

Like the other Enterobacteriaceae, resistance in the *Enterobacter* species is largely driven by plasmid encoded ESBLs and carbapenemases, including both metallo and non-metallo β-lactamses such as NDM-1 and KPC, respectively. While treatment options for MDR

Enterobacter species vary depending on the isolate, there are often few antibiotics currently available besides colistin and tigecycline (Esposito and De Simone, 2017, Pendleton et al., 2013).

1.5 Glycopeptide Resistance in *E. faecium* and *S. aureus*

Glycopeptide antibiotics are tricyclic or tetracyclic compounds of microbial origin with a narrow spectrum of activity against gram-positive bacteria. There are two glycopeptide antibiotics that are currently used clinically, namely vancomycin and teicoplanin, as well as several semisynthetic derivatives of these compounds, including telavancin and oritavancin (derived from vancomycin) as well as dalbavancin (derived from teicoplanin) (Figure 1.5) (Henson et al., 2015, Kang and Park, 2015).

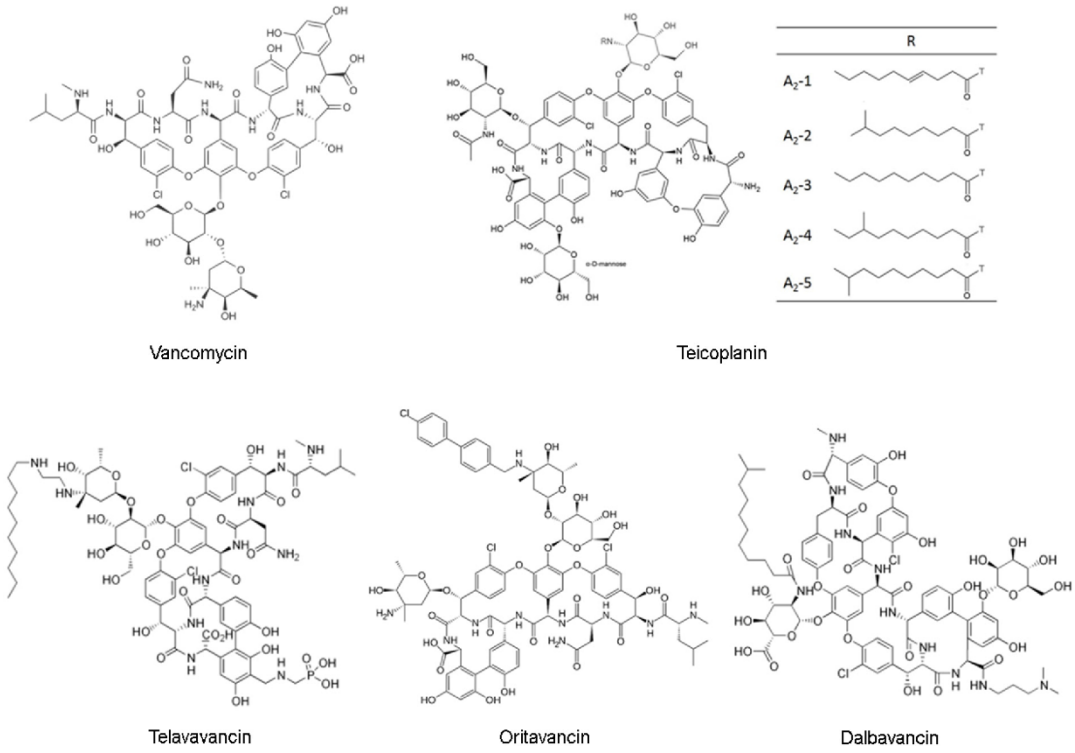

Figure 1.5: Chemical structure of Glycopeptide antibiotics. Vancomycin and Teicoplanin are natural products while Telavancin and Oritavancin are second generation derivatives of vancomycin, and Dalbavancin is a derivative of Teicoplanin. Image adapted from Kang et al (Kang and Park, 2015).

Vancomycin and teicoplanin share a similar mechanism of action, and act by inhibiting peptidoglycan synthesis in dividing bacteria. Inhibition is achieved by forming a noncovalent complex with the C-terminal D-Ala-D-Ala of the murein monomer amino acid chain, which subsequently blocks glycosyltransferase and the incorporation of precursor molecules to growing peptidoglycan. This action prevents further transpeptidation and subsequently results in the interruption of cell wall synthesis.

The mechanism of action of the lipoglycopeptides differ slightly, due to the addition of a lipophilic side chain. Telavancin is unique as it exhibits a dual mechanism of action by inhibiting peptidoglycan synthesis and affecting membrane polarization. Telavancin binds to a peptidoglycan precursor called lipid (undecaprenyl)-linked *N*-acetylglucosamine-*N*-muramylpentapeptide at the D-Ala-D-Ala residues, which inhibits both the transglycosylation and transpeptidation steps of peptidoglycan synthesis. Additionally, the decylaminoethyl hydrophobic side chain interacts with the cell membrane which results in an increased affinity for the target site, as well as a concentration-dependent reduction in the cell membrane potential and integrity (Kang and Park, 2015).

Oritavancin and Dalbavancin exhibit a similar mechanism of action to Vancomycin and Teicoplanin, in that they both bind to the D-Ala-D-Ala terminus of a stem pentapeptide and inhibit transglycosylation and transpeptidation. However, they differ due to their ability to dimerize and anchor to the cell membrane which increases their stability and binding affinity for the target site (Kang and Park, 2015).

Vancomycin was the first glycopeptide antibiotic discovered in the 1950s and was recognised as a potent inhibitor of gram-positive pathogens, notably *S. aureus* and problematic enterococci (*E. faecalis* and E. *faecium*). Initially, it was not used extensively due to its poor toxicity profile and the concurrent release of safer β-lactam antibiotics such as methicillin. However, due to the well documented difficulty in treating enterococci due to their high tolerance to β-lactams and widespread resistance to aminoglycosides, vancomycin (for a time) was the most reliable option for treating enterococcal infections (Cetinkaya et al., 2000). The regular use of vancomycin against Enterococci eventually led to the emergence of vancomycin-resistant Enterococci in 1988, which have continued to spread to endemic levels worldwide (Table 1.1). As of 2013, the percentage of Enterococci exhibiting resistance to vancomycin within each region ranged from 4% in Europe to 35.5% in the United States. Worryingly, the percentage of *E. faecium* isolates which are vancomycin resistant are significantly higher, reaching upwards of 79.4% in the United States (Cetinkaya et al., 2000, O'Driscoll and Crank, 2015). Vancomycin was not regularly used to treat infections caused by *S. aureus* until the late 1980s, and was generally limited for use against complicated infections caused by multi-drug resistant isolates such as MRSA (Henson et al., 2015). Unsurprisingly, it was only several years later the first vancomycin-resistant *S. aureus* (VRSA) strain was isolated in 2002 (McGuinness et al., 2017).

Table 1.1: Percentage of enterococci exhibiting Vancomycin resistance based on region. Table adapted from O'Driscoll *et al* (O'Driscoll and Crank, 2015)

Species	Europe 2013	USA 2009-2010	Canada 2007-2012	Asia-Pacific 2007-2008	Latin America 2007-2008	Worldwide 2007-2012
E. faecium	8.8	79.4	22.4	14.1	48.1	-
E. faecalis	1	8.5	0.1	0.01	3.1	10.3
All enterococci	4	35.5	6	11.0	12.9	-

1.5.1 Vancomycin Resistance in VRE and VRSA

As stated in section 1.3.1, vancomycin resistance is driven by one of several VanX operons encoded on the transposon Tn*1546*, which originated from a VRE conjugative plasmid. Seven VanX operons have been identified (*vanA*, *vanB*, *vanD*, *vanE*, *vanG* and *vanL*), of which *vanA* and remains the most significant in terms of the degree of resistance conferred and its prevalence worldwide (Henson et al., 2015, McGuinness et al., 2017). The VanA operon is comprised of several genes including *vanA*, *vanX*, *vanS*, *vanR*, *vanY* and *vanZ*, and is controlled by a two-component regulatory system encoded by *vanS* and *vanR*, which sense vancomycin and induce expression of the operon respectively. The mechanism of VanA resistance involves altering the C-terminal D-Ala-D-Ala of murein monomers to D-Ala-D-Lac, which has a lower binding affinity to vancomycin by 1000-fold. Resistance to vancomycin in *S. aureus* is driven solely by the acquisition of the VanA operon via conjugation with VRE isolates. In order for vancomycin resistance to be maintained, an original copy of the enterococcal operon must be retained, or TN1546 must be incorporated into a resident staphylococcal plasmid via transposition (McGuinness et al., 2017). The VanA cluster confers high levels of resistance to all available glycopeptide antibiotics including vancomycin, teicoplanin, dalbavancin and telavancin, with only oritavancin retaining efficacy against *vanA* VRE. The VanB cluster is the second most common VanX operon behind VanA, and generally confers resistance to vancomycin and (less frequently) teicoplanin, while remaining susceptible to other glycopeptides (Henson et al., 2015).

1.5.2 Vancomycin Intermediate Resistance in *S. aureus*

While VRSA is still relatively uncommon worldwide, the prevalence of vancomycin intermediate resistant *S. aureus* (VISA) is on the rise. As stated previously (section 1.4.2),

VISA isolates are characterized by having a vancomycin MIC of 4-8 μg/mL, and are typically associated with persistent infections and prolonged exposure to vancomycin (McGuinness et al., 2017). VISA resistance develops in a stepwise manner and is generally preceded by the development of a hVISA resistance (see section 1.4.2). There are several characteristics associated with the VISA phenotype including; increased cell wall thickness, reduced cross-linking of peptidoglycan, decreased autolytic activity, altered surface protein profile and disruption of the *agr* system (McGuinness et al., 2017). The genetic basis of the VISA phenotype has been studied extensively, with several genes/mutations emerging as being key in the development of VISA resistance. The most significant appear to be mutations within genes encoding two-component regulatory systems such as *walKR* and *graRS*, as well as mutations within the gene *rpoB* which encodes for a DNA-dependent RNA polymerase β-subunit (McGuinness et al., 2017). Cell wall thickening is the most common phenotypic characteristic of VISA isolates, conferring resistance by reducing the ability of vancomycin to access its active site (C terminal D-Ala-D-Ala) and sequestering the molecule within the cell wall (Henson et al., 2015).

The rapid emergence and continued spread of VRE, VRSA and VISA isolates have illuminated major concerns in the reliance on glycopeptide antibiotics as last resort antibiotics to treat complicated infections. Alternative, novel compounds are desperately needed to combat multi-drug resistant pathogens in the antibiotic resistant era.

1.5 Approaches to Combating Antimicrobial Resistance

The reality of antibiotic resistance and its toll on human health has resulted in calls for drastic changes in antibiotic stewardship on a global scale. Bacteria developing resistance to antibiotics is Darwinian in nature, illustrating the fast- tracked evolution of bacteria to adapt to hostile environments. While antibiotic resistance genes and associated mobile genetic elements are not new, the intense selective pressures applied to bacteria in both healthcare and the environment are. As discussed previously, environments with significant anthropogenic pressure such as medical facilities, agriculture/aquiculture facilities and wastewater systems are key reservoirs of antibiotic resistant genes due to high bacterial load and sub-therapeutic antibiotic use (Berendonk et al., 2015).

A number of methods have been proposed to combat the emergence and spread of antibiotic resistance. Firstly, significantly more research (and funding) is required to understand the factors involved in the dissemination of antibiotic resistance genes throughout bacterial populations, as well as understanding the factors that promote the selection and movement of resistant strains from the environment and animals to human populations (Bush et al., 2011). Understanding this will allow for the development of appropriate methods to monitor, diagnose and intervene against the spread of antibiotic resistance. Secondly, the education of the public must be made a priority to raise awareness of the dangers associated with antibiotic resistance, the incorrect use of antibiotics and its role in selecting for bacterial strains with increased resistance. Thirdly, greater attention should be given to developing nations where a number of factors such as high population densities, uncontrolled antibiotic use and lack of effective hygiene create environments ideal for the proliferation of antibiotic resistance. Interventions need

to be made at a governmental level to promote the infrastructure required to combat these issues. Fourthly, non-therapeutic antibiotic use such as the addition of antibiotics to animal feed as growth promoters should be restricted and monitored on a global scale. Finally, and most importantly, significantly more resources should be allocated to developing new antibiotics to keep up with the generation of resistant strains (Bush et al., 2011).

Research and development of novel antibiotics has been a longstanding issue in the past number of decades. The World Health Organization (WHO) has regularly reported on the ever-growing concern surrounding both the lack of innovation in antimicrobial development, as well as the sparse number of antibiotics which are developed each year. Most recently in 2017, a report by WHO outlined the lack of antibiotics in development capable of effectively combatting antibiotic resistance, identifying that of 51 new antibiotics in development, only 8 exhibited a novel mechanism of action, with the remainder being derivatives of already available compounds (Kmietowicz, 2017). As of 2015, 30 new antibiotics and 2 new β-lactam/β-lactamase inhibitor combinations have been introduced clinically worldwide. Of the 30 newly introduced antibiotics, all but 5 were derivatives of already available compounds, and all 5 of the first in class antibiotics (linezolid, daptomycin, retapamulin, fidaxomicin and bedaquiline) exhibited activity against gram-positive bacteria only. Additionally, the number of pharmaceutical companies with antibiotic divisions has declined significantly since the 1990s, decreasing from 18 in 1990 to only 4 as of 2015 (Butler et al., 2016).

The lack of innovation in the context of antimicrobial development has also resulted in a growing trend towards alternative methods for treating bacterial infections. ‘Non-

compound' approaches including the use of antibodies, bacteriophages, vaccines, antimicrobial peptides and lysins have been explored to certain degrees in recent years (Czaplewski et al., 2016). It is likely that a combination of these approaches must be adopted on a global scale to combat antibiotic resistance.

1.6 BDM-I

BDM-I (3,4-methylenedioxy-β-nitropropene; Figure 1.6) is a novel anti-infective compound that is currently being developed by the Australian biotechnology company Opal Biosciences (Melbourne AUS). It is a yellow crystalline solid that is insoluble in water, but soluble in organic solvents such as dimethylsulfoxide (DMSO). BDM-I belongs to a class of benzyl nitroalkenes that have been studied since the 1950s for a number of therapeutic properties, including as broad-spectrum antibiotics and anti-cancer drugs. BDM-I has displayed effectiveness *in vitro* against a broad range of microorganisms including bacteria, fungi and protozoa, and has been tested against a wide range of pathogenic organisms, including important clinical strains of bacteria such as MRSA and VRE (White et al., 2014).

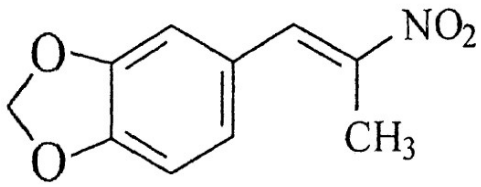

Figure 1.6: Molecular structure of BDM-I

Over 31 BDM-I derivative compounds have been developed and assayed against a range of bacterial and fungal species; results from these tests concluded that BDM-I itself was the most broadly active agent. However, certain derivatives were highly effective against a narrow spectrum of organisms such as gram-negative bacteria. Tests on BDM-I have also indicated that it has very low toxicity to mammals, with studies conducted on mice showing that BDM-I has a high lethal dose (2000 mg/kg), and that a 7-day repeat course of the compound (300 mg/kg) resulted in no observable antagonistic effects (White et al., 2014). Although these findings indicate that the BDM-I target is highly specific to microbial organisms, the mechanism of action (MoA) of BDM-I is not fully understood.

In 2014, White et al conducted a study on the BDM-I MoA, which subsequently confirmed its classification as a novel compound. Specifically, a series of experiments were conducted to examine whether BDM-I had any effect on the most common cellular targets for antibiotics including the cell wall and membrane, protein synthesis and RNA synthesis. Interestingly, White et al discovered that BDM-I acts intracellularly, most likely by inhibiting microbial protein tyrosine phosphatases (PTPs) (White et al., 2014).

Furthermore, a previous study on the mechanism of action of the structurally similar benzyl nitrostyrene compounds identified their mechanisms of actions as being inhibitors of protein tyrosine phosphatases (Park and Pei, 2004). Additionally, via this study they identified that these compounds were inhibited by thiols which are present within eukaryotic cells, possibly explaining the specificity of compounds like BDM-I to microbial cells. However, this mechanism of action is yet to be shown in the case of BDM-I.

1.7 Protein Phosphorylation in Bacteria

Post-translational modification of proteins by phosphorylation has been studied extensively within eukaryotes over the past century. However, it has only been since the 1980s that prokaryotic organisms were also shown to utilise phosphorylation as a regulatory mechanism (Chao et al., 2014). The most frequently observed phosphorylated residues in eukaryotes are Serine (pSer), Threonine (pThr) and Tyrosine (pTyr), with an approximate distribution of 86.4%, 11.8% and 1.8% respectively (Cain et al., 2014). Initially, protein phosphorylation in bacteria was thought to be limited to histidine and aspartate residues as part of two-component regulatory systems. However, in the last number of decades, studies have shown that Ser, Thr and Tyr phosphorylation occurs in bacteria at a similar distribution to eukaryotes (Cain et al., 2014, Chao et al., 2014). In recent years, multiple studies have been published using novel analytical methods to identify the phosphoproteome of several bacterial species, including; *E. coli* (Lin et al., 2015), *B. subtilis* (Macek et al., 2007), *L. lactis* (Soufi et al., 2008), *M. tuberculosis* (Prisic et al., 2010) and *S. pneumoniae* (Sun et al., 2010). Data from these studies indicate that phosphorylation occurs on numerous proteins involved in a broad range of cellular processes. In-depth analysis of the *E. coli* phosphoproteome identified that 30% of the proteins encoded by essential genes were phosphorylated, and are involved in a variety of cellular functions including central carbon metabolism, DNA metabolism, transcription and translation (Lin et al., 2015).

Phosphorylation of tyrosine residues occurs at a significantly lower rate in comparison to serine and threonine, typically making up ≤15% of the total phosphoproteome in bacteria. Tyrosine phosphorylation has been shown to direct a range of cellular processes which appear to be species specific. These processes include; capsule production, growth,

proliferation, migration, flagellin export, stress adaptation and synthesis of secondary metabolites (Whitmore and Lamont, 2012).

Tyrosine phosphorylation is carried out by the bacterial tyrosine (BY) kinase family, composed of a transmembrane domain which functions as a sensor and anchor, as well as an intracellular catalytic domain. The catalytic domains of BY kinases contain Walker A (P-loop) and B motifs, differing from typical motifs present within eukaryotic tyrosine kinases (Whitmore and Lamont, 2012). Initially, BY kinases were thought to be solely autophosphorylating enzymes controlling exopolysaccharide production. However, recent studies have identified multiple protein substrates which are phosphorylated by BY kinases, elucidating additional roles in regulating bacterial physiology (Grangeasse et al., 2007). The first proteins identified to be phosphorylated by BY kinases were UDP-sugar dehydrogenases and glycosyltransferases, which stimulated the formation of polysaccharide precursors. Interestingly, some proteins such as UDP-glucose dehydrogenases are involved in several metabolic pathways such as Teichuronic acid biosynthesis in *B. subtilis,* which is a key component of peptidoglycan (Soldo et al., 1999). Additional proteins identified to be phosphorylated by BY kinases include the heat-shock sigma factor (σ^{32}) and antisigma factor (σ^{E}) of *E. coli*, and single-stranded DNA binding proteins of *B. subtilis*. These findings indicate that tyrosine phosphorylation is directly involved in regulating gene expression in bacteria (Grangeasse et al., 2007).

Conserved sequence motifs encoding for tyrosine phosphatases have also been identified in bacteria, which function in the removal of a phosphate molecule resulting in the dissemination or inhibition of phospo-mediated signalling (Cain et al., 2014). Bacterial tyrosine phosphatases are characterized into three groups; eukaryotic like phosphatases

(PTPs) which also dephosphorylate serine and threonine sites, low molecular weight protein tyrosine phosphatases (LMW-PTPs) which are also found in eukaryotic cells, and polymerase-histidinol phosphatases (PHP) which are commonly found in gram-positive bacteria (Whitmore and Lamont, 2012). Eukaryotic like PTPs typically function as secreted effector proteins to alter host cells during infection, highlighting their primary role in bacterial virulence. However, LMW-PTPs and PHPs have been shown to function in regulating the phosphorylation state of bacterial proteins, primarily acting against BY kinases encoded upstream of phosphatase genes (Grangeasse et al., 2007). Bacterial tyrosine phosphatases have been shown to function in several cellular processes, with significant evidence illuminating their roles in polysaccharide production and biofilm formation, as well as secreted effector proteins to manipulate host cells during infection (Whitmore and Lamont, 2012).

It is important to note that studies on post-translational modifications in bacteria, specifically tyrosine phosphorylation, is a relatively new area of research. Therefore, it is difficult to hypothesize the effects of the proposed MoA of BDM-I as a (potential) tyrosine phosphatase inhibitor on the physiology of bacterial cells.

1.8 Scope of Thesis

Antibiotic resistance continues to be one of the most significant global threats facing modern medicine. While major pharmaceutical companies continue to focus on developing more financially “safe” drugs for chronic illnesses with long term treatment needs, all of the most clinically relevant bacterial pathogens continue to develop and spread resistance to (in some cases) every antibiotic which is currently available.

BDM-I has been identified as a novel antimicrobial with activity *in vitro* against several clinically important microorganisms. Understanding the pharmacodynamics of novel drugs is a major step in its development and is vital to developing appropriate treatment regimens in clinical settings. While BDM-I has been studied previously, the MoA remains elusive, with evidence suggesting that BDM-I may inhibit tyrosine phosphatases (White et al., 2014). Therefore, the aim of the studies presented in this thesis was to gain a deeper understanding of the BDM-I MoA, while also investigating the efficacy of BDM-I against clinical isolates associated with nosocomial infections.

Previous MoA studies focused on confirming that BDM-I did not affect cellular targets typically inhibited by antibiotics (section 1.2), while also relying on predicted targets to identify potential binding partners (White et al., 2014). By utilizing an omics approach (whole genome sequencing and proteomics), significant pathways and individual proteins were identified which are affected by BDM-I. Utilizing this top down approach, pathways and proteins of interest can then be studied further to identify how they are affected by BDM-I, providing valuable insight into the BDM-I MoA.

Previous efficacy studies with BDM-I have been limited to testing laboratory strains of common bacterial species. However, no in-depth studies have been undertaken which examine the utility of BDM-I against clinical bacterial isolates associated with persistent infections and antibiotic resistance. To address this lack of data, MIC studies were conducted on a range of bacterial isolates (ESKAPE pathogens) to assess the useability of BDM-I against clinical bacterial pathogens.

In combination, the results of these studies have contributed to identifying the BDM-I MoA as an inhibitor of ATP Synthesis via the oxidative phosphorylation pathway. Furthermore, MIC studies have confirmed that BDM-I is a viable treatment option against MRSA both in monotherapy and (potentially) combination therapy with vancomycin.

Chapter 2

Materials and Methods

2.1 Chemicals, Reagents and Oligonucleotides

Lysostaphin, lysozyme, ethidium bromide, Triton X-100, dimethylsulfoxide (DMSO), pronase, cOmplete™ Mini EDTA-free Protease Inhibitor Cocktail, 4',6-diamidino-2-phenylindole (DAPI), SYTOX Green, FM-464, vancomycin, chloramphenicol, daptomycin, erythromycin and flucloxacillin were purchased from Sigma. 3,4-methylenedioxy-β-nitropropene (BDM-I) was supplied by BioDiem. All other chemicals were purchased through commercial sources and were of analytical grade. Oligonucleotides were designed in CLC Genomics Workbench and purchased from Sigma.

Table 2.1: Buffers and Reagents

Buffer	Composition
Lysis buffer (Genomic Extractions)	20 mM Tris-Cl 2 mM EDTA 1% Triton X-100 pH 8
Electrophoresis running buffer	45 mM Tris(hydroxymethyl)aminomethane 45 mM Boric Acid 1 mM EDTA
Anode running buffer (10x)	200 mM Tris-Cl pH 8.9
Cathode running buffer (10x)	100 mM Tris 100mM Tricine 0.1% SDS (w/v)
Comassie brilliant blue stain	0.125% Comassie blue R250 (w/v) 30% Methanol (v/v) 10% Acetic Acid (v/v)
Comassie destain solution	30% Methanol (v/v) 10% Acetic Acid (v/v)
SDS-PAGE loading buffer (5x)	300 mM Tris-Cl (pH 6.8) 10% SDS (w/v) 50% Glycerol (v/v) 25% 2-mercaptoethanol 5g/L bromophenol blue
SDS-PAGE Running Buffer (10x)	25 mM Tris 192 mM Glycine 0.1% SDS (w/v) pH 8.3

2.2 Bacterial Strains

Bacterial strains used in this study are listed in Table 2.2, along with their relevant genetic characteristics and antibiotic phenotype. Clinical strains used are listed in Tables 2.3 to 2.7 along with relevant clinical information and resistance phenotypes.

2.3 Bacterial media, growth conditions and storage

Media used for bacterial growth as well as their constituent reagents are listed in Table 2.8. Prior to use, all growth media was sterilised by autoclaving at 121°C and 103 KPa for approximately 30 minutes. Solutions which contained heat labile substances were filter sterilized using a 0.20 μm pore size Minisart syringe-driven filter unit (Sartorius, Goettingen GER). Unless stated otherwise, liquid cultures were grown in Luria-Bertani (LB) broth at 37°C with shaking at 250 rpm in a MaxQ 6000 incubator shaker (Thermo Scientific, Waltham USA), or an Orbital Mixer Incubator (Ratek, Victoria AUS) for 16-24 h under aerobic conditions. Growth on solid media was prepared by incubating LB Agar (unless stated otherwise) at 37°C for approximately 16-24 h under aerobic conditions. Bacterial growth was measured spectrophotometrically by measuring the optical density of liquid cultures at 600nm (OD_{600}) using a SpectraMax M2^e Plate Reader. For long term storage, 1 mL of an overnight culture inoculated from a single colony was mixed with 1 mL of sterile 20% glycerol in LB broth (v/v). Alternatively, colonies were stored directly from solid media by inoculating 1 mL of 10% glycerol in LB broth (v/v) with a sterile swab before being stored at -80°C.

Table 2.2: Bacterial Strains used in this study

Strain	Isolate Number	Features	Source/Reference
E. coli	IM08B	Chloramphenicol Sensitive	(Monk et al., 2015)
S. aureus	RN4220	Restrictionless derivative of NCTC 8325-4	(Kreiswirth et al., 1983)
S. aureus	Sa375	MRSA, VISA	Liverpool Hospital
S. aureus	Sa0057	MRSA, VSSA	Liverpool Hospital
E. faecium	Efm0003	VRE, VanB	Royal Prince Alfred Hospital
E. faecium	Efm0008	VRE, VanA	Royal Prince Alfred Hospital

Table 2.3: Clinical Gram-Negative Isolates Selected for MIC Testing

P. aeruginosa		***E. coli***		***K. pneumoniae***	
Isolate No.	**Hospital**	**Isolate No.**	**Hospital**	**Isolate No.**	**Hospital**
Pa0001	RPA	**Ec0002**	-	**Kp0001**	Bankstown
Pa0005	RPA	**Ec0003**	-	**Kp0002**	Bankstown
Pa0010	RPA	**Ec0004**	BH	**Kp0003**	RPA
Pa0015	RPA	**Ec0005**	-	**Kp0004**	BH
Pa0020	RPA	**Ec0006**	-	**Kp0005**	BH
Pa0025	RPA	**Ec0007**	-	**Kp0007**	Liverpool
Pa0030	RPA	**Ec0008**	-	-	-
Pa0035	RPA	**Ec0009**	-	-	-

Table 2.4: Clinical MRSA Isogenic Isolate Series Selected for MIC Testing

Series	Isolate Number	Isolate Type	Phenotype
A	Sa0048	Initial	VSSA
	Sa0049	Persistent	VSSA
	Sa0050	Persistent	hVISA
B	Sa0016	Initial	hVISA
	Sa0018	Recurrent	hVISA
	Sa0067	Recurrent	hVISA
	Sa0020	Persistent	hVISA
	Sa0070	Recurrent	hVISA
	Sa0054	Recurrent	hVISA
C	Sa0057	Initial	VSSA
	Sa0058	Persistent	hVISA
	Sa0059	Persistent	VISA
	Sa0060	Persistent	hVISA
	Sa0378	Persistent	VISA
	Sa0375	Persistent	VISA

Table 2.5: Clinical MRSA Isogenic Isolate Pairs Selected for MIC Testing

Pair	Isolate Number	Isolate Type	Phenotype
A	Sa0040	Initial	hVISA
	Sa0012	Recurrent	hVISA
B	Sa0227	Initial	VSSA
	Sa0328	Recurrent	VSSA
C	Sa0307	Initial	VSSA
	Sa0365	Persistent	VSSA
D	Sa0243	Initial	VSSA
	Sa0194	Persistent	VSSA
E	Sa0138	Initial	VSSA
	Sa0116	Persistent	VSSA
F	Sa0015	Initial	hVISA
	Sa0019	Recurrent	hVISA
G	Sa0309	Initial	VSSA
	Sa0238	Persistent	VSSA
H	Sa0283	Initial	VSSA
	Sa0284	Persistent	VSSA
I	Sa0212	Initial	VSSA
	Sa0214	Recurrent	VSSA
J	Sa0158	Initial	VSSA
	Sa0160	Persistent	VSSA
K	Sa0343	Initial	VSSA
	Sa0191	Recurrent	VSSA
L	Sa0037	Initial	hVISA
	Sa0044	Recurrent	hVISA
M	Sa0237	Initial	VSSA
	Sa0285	Persistent	VSSA
N	Sa0051	Initial	hVISA
	Sa0052	Persistent	hVISA
O	Sa0331	Initial	VSSA
	Sa0332	Persistent	VSSA
P	Sa0255	Initial	VSSA
	Sa0256	Persistent	VSSA
Q	Sa0294	Initial	VSSA
	Sa0192	Persistent	VSSA
R	Sa0014	Initial	VSSA
	Sa0017	Recurrent	VISA
S	Sa0228	Initial	VSSA
	Sa0265	Persistent	VSSA
T	Sa0055	Initial	VSSA
	Sa0056	Recurrent	hVISA
U	Sa0091	Initial	VSSA
	Sa0162	Persistent	VSSA
V	Sa0304	Initial	VSSA
	Sa0305	Persistent	VSSA
W	Sa0006	Initial	VSSA
	Sa0011	Recurrent	hVISA
X	Sa0068	Initial	hVISA
	Sa0047	Persistent	VSSA
Y	Sa0329	Initial	VSSA
	Sa0330	Persistent	VSSA
Z	Sa0322	Initial	VSSA
	Sa0324	Persistent	VSSA

Table 2.6: Clinical VRE Isolates Selected for MIC Testing

Isolate Number	Hospital	Phenotype
Efm0092	RPA	VSE
Efm0093	RPA	VSE
Efm0097	RPA	VSE
Efm0100	RPA	VSE
Efm0103	RPA	VSE
Efm0136	RPA	VSE
Efm0138	RPA	VSE
Efm0200	RPA	VSE
Efm0219	RPA	VSE
Efm0222	RPA	VSE
Efm0174	RPA	VanB
Efm0209	RPA	VanB
Efm0202	RPA	VanB
Efm0151	RPA	VanB
Efm0180	RPA	VanB
Efm0218	RPA	VanB
Efm0217	RPA	VanB
Efm0160	RPA	VanB
Efm0128	RPA	VanB
Efm0125	RPA	VanB
Efm0067	QLD	VanA
Efm0072	MH	VanA
Efm0076	MH	VanA
Efm0081	AH	VanA
Efm0087	AH	VanA
Efm0234	Wollongong	VanA
Efm0236	Wollongong	VanA
Efm0315	St George	VanA
SVH193	RPA	VanA
SVH228	RPA	VanA

Table 2.7: Clinical VRE Isogenic Isolate Series Selected for MIC Testing

Series	Isolate Number	Isolate Type
A	Efm0006	Initial
	Efm0007	Persistent
	Efm0010	Persistent
	Efm0027	Persistent
	Efm0028	Persistent
	Efm0029	Persistent
	Efm0030	Persistent
	Efm0031	Persistent

Table 2.8: Media used for Culturing Bacteria

Media	Composition	Reference
Luria-Bertani Broth	171 mM NaCl 63.5 mM Tryptone 0.5 % Yeast Extract	(Willetts and Finnegan, 1970)
LB Agar	171 mM NaCl 63.5 mM Tryptone 0.5 % Yeast Extract 1.2 % Agar	(Willetts and Finnegan, 1970)
Mueller Hinton Broth	2% Beef Extract 17.5% Casein Hydrolysate 1.5% Starch	Becton Dickinson (California, USA)
Mueller Hinton Agar	2% Beef Extract 17.5% Casein Hydrolysate 1.5 % Starch 1.7% Agar	Becton Dickinson (California, USA)
Brain Heart Infusion Agar	0.77% Calf Brains 0.98% Beef Heart 1% Proteose Peptone 0.2% Dextrose 0.5% Sodium Chloride 0.25% Disodium Phosphate 1.5% Agar	Becton Dickinson (California, USA)
B2 Broth	1% Casein Hydrolysate 27.8 mM Glucose 5.7 mM di-Potassium bis orthophosphate 428 mM NaCl 2.5% Yeast Extract	(Schenk and Laddaga, 1992)
Tryptic Soy Broth	13.9 mM Glucose 1.7% Peptone 0.3% Peptone (Soy) 14.3 mM di-Potassium bis orthophosphate 85.5 mM NaCl	-

Table 2.9: Stock Concentration and Solvent used for Antibiotics

Antibiotic	Stock Concentration (µg/mL)/Solvent
BDM-I	10/DMSO
Vancomycin	10/H_2O
Daptomycin	10/H_2O
Chloramphenicol	10/Methanol
Ceftaroline dihydrochloride	10/DMSO
Flucloxacillin	10/H_2O
Erythromycin	10/H_2O

2.4 Transformation of *E. coli*

2.4.1 Preparation of Chemically Competent *E. coli*

Overnight cultures of the strain of interest were grown from a single, well isolated colony in LBB. 200 µL of the O/N culture was then inoculated into 10 mL of sterile LBB and grown until an OD_{600} of 0.5 was reached. Cells were then harvested at 5000 x g for 8 min at 4°C, then resusupended in 5 mL of ice-cold 100 mM $MgCl_2$. Cells were then harvested again and resuspended in 1 mL of ice-cold 100mM $CaCl_2$ and allowed to sit on ice. Glycerol was then added to a final concentration of 16% (v/v) before the cells were separated into 100 µL aliquots and stored at -80°C.

2.4.2 Transformation of Chemically Competent *E. coli*

100 µL aliquots of chemically competent cells (section 2.4.1) were thawed on ice prior to use. Typically, 5 µL of purified plasmid DNA (section 2.5.2) equating to approximately 1 µg of DNA was added to a 100 µL aliquot and mixed by pipetting before being incubated on ice for 30 min. The cells were then heat-shocked by rapidly heating them to 42°C for 1 min, then allowing them to recover on ice for 10 min. 1 mL of LBB was then added to the transformed cells, which were then incubated for 1 h at 37°C with shaking. The transformed cells were then plated onto solid LB agar supplemented by an appropriate antibiotic, before being incubated at 37 °C for 16-24 h. Single, well isolated colonies were then screened for successful transformation using PCR (section 2.6.1) or restriction endonuclease digestion (section 2.6.2).

2.5 Routine DNA Procedures

2.5.1 Isolation of Genomic DNA for Sequencing and Cloning

Genomic DNA used for sequencing and cloning reactions was isolated using the ISOLATE II Genomic DNA Kit (Bioline) as per the manufacturer's instructions. For hard to lyse bacteria, additional steps were required for cell lysis. Briefly, a single isolated colony of the strain of interest was inoculated into 10 mL of LBB and incubated overnight at 37°C with shaking. The cells were then harvested from a 1 mL aliquot of the overnight culture (5000 x g / 8 min / RT) and resuspended in pre-prepared lysis buffer (20 mM Tris/HCl; 2 mM EDTA; 1% Triton X-100; pH 8) supplemented with lysozyme (20 mg/mL) or lysostaphin (0.2 mg/mL) before being incubated for 45 min at 37°C. 25 µL of Proteinase K (20 mg/mL) was then added and the suspension was incubated at 56°C for a further 30 min. Subsequent steps were then completed as per the manufacturer's instructions, with isolated DNA being eluted in 70-100 µL of sterile Milli-Q water. Isolated DNA was quantified using either a Nanodrop (ThermoFisher) or Qubit 2.0 Fluorometer (ThermoFisher).

2.5.2 Isolation of Plasmid DNA for Cloning, Screening and Sequencing

Plasmid DNA used for downstream molecular reactions was isolated from *E. coli* using the ISOLATE II Plasmid Mini Kit (Bioline) as per the manufacturer's instructions. For isolation of plasmid DNA from *S. aureus*, a pre-incubation step was required for efficient cell lysis. Briefly, a single isolated colony of the strain of interest was inoculated into 10 mL of LBB supplemented with the appropriate antibiotic, before being incubated for 16h at 37°C with shaking. The cells were then harvested with centrifugation (5000x g / 8 min / RT) and resuspended in 250 µL of Resuspension Buffer P1 supplemented with

lysostaphin (0.2 mg/mL) and incubated for 45 min at 37°C. Subsequent steps were then completed as per the manufacturer's instructions, with isolated DNA being eluted in 50 µL of sterile Milli-Q water.

2.5.3 Agarose Gel Electrophoresis

DNA fragments were separated using electrophoresis through horizontal agarose gels following standard biological methods. Typically, 1.5% agarose gels were used to resolve DNA fragments ranging in size from 0.2 to 10 Kb using the HyperLadder™ 1Kb molecular weight marker (Bioline). Agarose was dissolved in 0.5X TBE Buffer (45 mM Tris(hydroxymethyl)aminomethane; 45 mM Boric Acid; 1 mM EDTA) prior to casting. 5X DNA loading buffer (Bioline) was then mixed with samples at a ratio of 1:5 before the samples were loaded into the gel. Electrophoresis was carried out at 200 V until the dye front had reached the final quarter of the length of the gel. Staining was completed by immersing the gel in Ethidium bromide (1 mg/L) for approximately 30 min, followed by visualization and imaging using a GelDoc-It TS Imaging System (UVP).

2.6 Recombinant DNA Methods

2.6.1 Polymerase Chain Reaction

Polymerase chain reactions (PCRs) were carried out in 50 µL reactions containing approximately 200 ng of DNA, using either Accuzyme™ DNA Polymerase (Bioline) or the 2X MyTaq™ Mix (Bioline). In the case of the former, DNA was combined with 1 U Accuzyme, 0.1 mM dNTP mix and 20 µM of each primer. For the latter, DNA was mixed with the 2X MyTaq Mix and 20 µM of each primer. Reactions were carried out in 0.2 mL PCR tubes using a C1000 Thermal Cycler (Bio-Rad). Standard cycling conditions

included a 5 min denaturation at 95°C, a 30 sec annealing step at 55 to 65°C (depending on primers used), and 45 sec extension step which were repeated 35 times, before a final extension step for 5 min. PCR products were visualised using Agarose gel electrophoresis (section 2.5.3) and purified using the ISOLATE II PCR and Gel Kit (Bioline) as per the manufacturer's instructions.

Table 2.10 Primer Names and Nucleotide Sequence

Name[a]	Nucleotide sequence (5'-3')	Target
VRE mutant sequencing primers		
atpD-F	CACCTTTCCCAGAAGATG	Upstream of *atpD* gene in *E. faecium*
atpD-R	GATACTTCAGATCCAGCTTGAG	Downstream of *atpD* gene in *E. faecium*
atpD-F2	CATTTGGATGCGACAACC	Upstream of *atpD* gene in *E. faecium*
atpC-R	GCTGCATGGTGATCATAGAC	Downstream of *atpC* in *E.faecium*
atpA-F	GACCGTAAAACAGGGAAAACT	Upstream of *atpA* gene in *E. faecium*
murA2-R	TGACGTCCTTTCTAACGATTG	Downstream of *murA2* gene in *E. faecium*
***walK* cloning primers**		
walK(Bam)-F	ATAGGATCCACAACAAGTTGAACGTGAGCG	Upstream of G560S mutation in *walK*
walK(Xho)-R	ATACTCGAGCGCATTCATGTTCAGTACTTGG	Downstream of G560S mutation in *walK*

[a]Oligonucleotides are grouped under experimental subheadings.

2.6.2 Restriction Endonuclease Digestion and Ligation

Restriction endonuclease enzymes and associated buffers were acquired from New England Biolabs and used according to the manufacturer's instructions. Double digests were completed using the recommended double digest buffer for both enzymes used. Following digestion, reactions were purified using the ISOLATE II PCR and Gel Kit before ligation experiments. Purified DNA fragments were diluted to a vector:insert ratio of 1:7 in a 20 µL volume containing 1 U of T4 DNA Ligase (New England Biolabs) and

1X T4 DNA ligase reaction buffer. Ligation reactions were incubated overnight at 4°C overnight in a C1000 thermal cycler then heat deactivated at 70°C for 10 min.

2.7 Minimum Inhibitory Concentration (MIC) Determination

2..7.1 Broth Microdilution Method

Determination of MICs was completed according to the guidelines outlined by the Clinical and Laboratory Standards Institute Broth Microdilution Method (CLSI M07-A9, 2012). Initially the inoculum was prepared using the direct-colony suspension method and diluted to obtain a final concentration of $5x10^5$ colony forming units (Cfu/mL) for each organism. A series of BDM-I dilutions were then prepared (10-1 μg/mL) in MHB and 100 μL was pipetted into a single column of a sterile 96 well plate. Following this, 10 μL of each bacterial suspension was inoculated in duplicate into the respective rows of the 96-well plate and incubated at 37°C for 16-24 h. Results were obtained upon visual inspection for growth, and the MIC determined as the concentration of BDM-I at which growth was first inhibited.

2..7.2 Agar Dilution Method

Additional MIC tests were performed using the Agar dilution Method according to the Clinical and Laboratory Standards Institute (CLSI M07-A9, 2012). MHA agar plates were prepared and supplemented with a range of BDM-I concentrations (5-1 μg/mL). The bacterial inoculum was then prepared as described in section 2.7.1, differing in that the final concentration required was $1x10^7$ CFU/mL. 2 μL of each inoculum was then pippeted onto three isolated areas of agar in triplicate, for each concentration of BDM-I as well as MHA with no BDM-I. The plates were then incubated for 16-24 h at 37°C,

with MICs being determined as the lowest concentration of BDM-I which inhibited growth.

2.8 Synergy Studies using Checkerboard Assays

BDM-I synergism was determined using the checkerboard method as described by the literature (Orhan et al., 2005, Sopirala et al., 2010). Antibiotic dilutions were prepared in MHB at double the desired concentration and combined in equal volumes (50 µL) into a single well of a sterile 96-well plate. The final concentration range for each antibiotic was as follows; 5-0.25 µg/mL BDM-I, and two-fold dilutions of vancomycin from 16-0.0625 µg/mL. 10 µL of the prepared bacterial suspension (diluted to $1x10^5$ Cfu) was then inoculated into each well, and the plate then incubated at 37°C for 16-24 h overnight. MIC values were then determined as described by the CLSI for broth microdilution testing. Determination of the fractional inhibitory concentration index (FICI) was calculated with the equation: FICI = FIC A + FIC B, where FIC A is the MIC of drug A in combination divided by the MIC of drug A alone, and FIC B is the same for drug B. FICI values were then determined as follows: FICI of ≤0.5 indicates synergy, FICI of >0.5 to ≤1 indicates additivity, FICI of >1 to ≤4 indicates no interaction and FICI of >4 indicates antagonism (Sopirala et al., 2010).

2.9 BDM-I Resistance Induction

BDM-I resistance induction experiments were completed on two MRSA isolates, Sa057 (VSSA) and Sa375 (VISA) and two VRE isolates, Efm003 (VanB) and Efm008 (VanA) in triplicate series over a period of approximately 70-110 days. Isolates were passaged daily in 10 mL Luria Bertani broth (LBB) supplemented with sub inhibitory

concentrations of BDM-I, which was gradually increased as growth was observed. During this time, isolates were stored at -80°C and subjected to additional MIC testing in order to confirm changes in BDM-I MICs.

2.10 Whole Genome Sequencing of Mutant Isolates

2.10.1 Library Preparation

DNA libraries were constructed using 1 μg of purified genomic DNA (section 2.5.1) extracted from mutant isolates. Using the NEBNext Fast DNA Fragmentation & Library Prep Set for Ion Torrent (New England Biolabs) and the Ion Xpress Plus fragment library kit (Life Technologies), 400 bp barcoded libraries were generated as per the manufacturer's instructions. The barcoded libraries were then amplified using a thermal cycler and subsequently purified using the Agencourt AMPure XP Reagent (Beckman Coulter). The purified libraries were then combined and bound to Ion Sphere™ Particles for enrichment and clonal amplification using an Ion OneTouch™ 2 System (Life Technologies) as per the manufacturer's instructions. Quantification of the amplified library was completed using a Qubit 2.0 Fluorometer (Life Technologies). The DNA samples were loaded onto an Ion 318™ v2 chip (Life Technologies) and sequenced according to the manufacturer's instructions.

2.10.2 Analysis of Sequencing Reads and Confirmation of Mutations

Whole genome sequencing reads were analysed using CLC Genomics Workbench ver.7.0.3 (CLCbio). Briefly, mutant reads were mapped to a reference genome (AUS004 or JKD6008) before variant detection was completed using a minimum coverage of 10 and a minimum variant frequency of 95%. Detected variants were then filtered to identify

mutations which caused changes to the amino acid sequence. Confirmation of significant mutations was carried out through Sanger Sequencing (Macrogen) of PCR fragments which amplified regions of interest (section 2.6.1).

2.11 Allelic Exchange of *S. aureus* Mutant G560S

Allelic exchange experiments were completed using mutant Sa375 isolates produced in section 2.9 and sequenced in section 2.11. Allelic exchange was completed using the system outlined by Monk et al with the vector pIMAY-Z (Figure 2.1) (Monk et al., 2015). pIMAY-Z and the *E. coli* strain IM08B were supplied by Dr Ian Monk from the Doherty Institute in Melbourne, Australia.

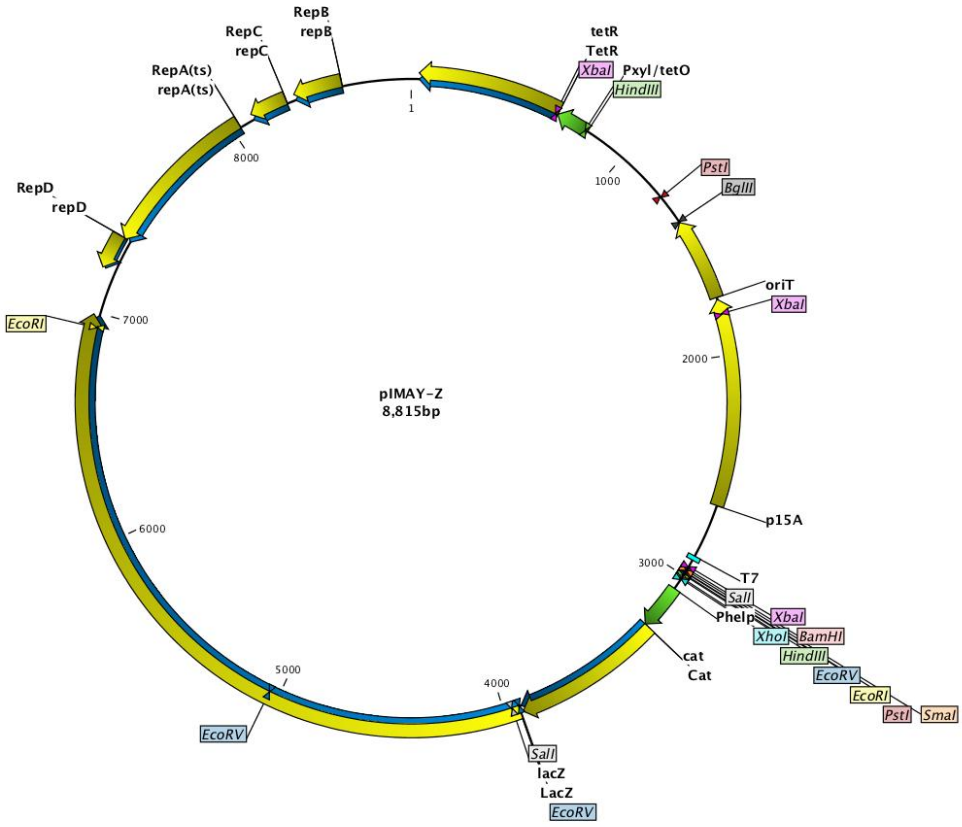

Figure 2.1: Plasmid Map of pIMAY-Z

2.11.1 Plasmid Vector and PCR Insert Isolation

Due to the low copy number of pIMAY-Z, 3x cultures of IM08B cells containing pIMAY-Z were incubated overnight in LBB supplemented with chloramphenicol (10 μg/mL). The cells were harvested at 5000xg for 8 min, and pIMAY-Z was then extracted using the ISOLATE II Plasmid Mini Kit (section 2.5.2) and stored at 4°C.

Genomic DNA was extracted from a mutant Sa375 isolate using the Isolate II Genomic DNA extraction kit (section 2.5.1). PCR was then performed (section 2.6.1) using the primers described in Table 2.9 to amplify the region containing the mutation of interest.

2.11.2 Cloning of Insert into pIMAY-Z

Cloning was performed by digesting 1 μg of pIMAY-Z and PCR product using BamHI and XhoI according to the manufacturer's instructions (section 2.6.2). Ligation was then performed (section 2.6.2) prior to the ligation mixture being transformed into chemically competent IM08B cells (section 2.4), then plated onto LBA (CML10; XGAL20) and incubated overnight at 37°C. Successful plasmid constructs were confirmed using colony PCR, restriction digests of isolated plasmid, and sanger sequencing performed by the Australian Genome Research Facility (Sydney AUS).

2.11.3 Electroporation of Constructs into the Progenitor Sa375 Isolate

Electrocompetent cells were prepared from the progenitor Sa375 isolate as described by Monk et al (Monk et al., 2012). Briefly, a 10 mL overnight culture of Sa375 was diluted to an OD_{600} of 0.5 into 25 mL of pre-warmed TSB, and incubated at 37°C with shaking (250rpm) for 30 min. The culture was then placed on ice for 10 min before the cells were harvested at 5000xg for 8 min at 4°C. The cells were then washed twice with ice cold, sterile Milli-Q water (20 mL then 15 mL), followed by three washes with ice cold, sterile

10% glycerol (10 mL, 5 mL then 2 mL). Following the final wash, the cells were resuspended in 1 mL of ice cold 10% glycerol and separated into 50 µL aliquots, before being stored at -80°C.

Electrocompetent Sa375 cells were thawed before electroporation, harvested at 5000xg for 5 min then resuspended in 50 µL of electroporation buffer (10% glycerol, 200 mM sucrose). Up to 20 µL of plasmid construct was then mixed with the cells, before the total volume was transferred to a 0.1 cm Gene Pulser Electroporation Cuvette (Bio-Rad). Electroporation was then carried out using a Gene Pulser Xcell (Bio-Rad) at 21 kV/cm, 100 Ω, 25 µF. Immediately after electroporation, 750 µL of pre-warmed (28°C) recovery media (TSB with 200 mM sucrose) was added to the cells, then transferred to a 1.5 mL Eppendorf tube and incubated for 1 h at 28°C. The cells were then plated on BHIA (CML10) and incubated for 48 h at 28°C.

2.11.4 Selection of Recombinant Colonies

A single colony was then resuspended in 200 µL of TSB, and serial diluted to 10^{-3} before being plated onto BHIA (CML10 XGAL100) and then incubated overnight at 37°C. Blue colonies were then streaked onto fresh BHIA (CML10 XGAL100) and incubated overnight at 37°C. 10mL of TSB was then inoculated with a single blue colony and grown overnight at 28°C without antibiotic to promote plasmid loss. Serial dilutions of the overnight culture were then prepared to a final value of 10^{-6} before being plated onto BHIA (XGAL100) and then incubated overnight at 37°C. White colonies were then patched onto duplicate plates of BHIA (XGAL100) and BHIA (CML10 XGAL100) and incubated overnight at 37°C. White, chloramphenicol sensitive colonies were then

selected as potential integrants. Confirmation of the successful integration of G560S into the progenitor Sa375 *walK* gene was carried out by sanger sequencing (Macrogen)

2.12 Transmission Electron Microscopy (Analysis of Cell Wall Thickness)

Transmission electron microscopy (TEM) was completed on Sa375 mutants following whole genome sequencing. Overnight cultures of each mutant Sa375 isolate as well as the progenitor Sa375 and Sa057 isolates were centrifuged and re-suspended in a 2.5% Glutaraldehyde solution in 0.1M cacodylate buffer (pH 7.4). Following fixation for at least 4 h, the buffer was exchanged with 2% Osmium tetroxide and rinsed with Sodium acetate, and finally stained with Uranyl acetate for 60 min. The samples were then dehydrated in alcohol then infiltrated with Spurr resin in acetone (1:1) for 30 min, then again in 6:1 resin for 22 h. Polymerisation of samples was then allowed to carry out for 15 h at 70°C before being cut and imaged using a Morgagni 268D transmission electron microscope (FEI, Eindhoven, The Netherlands) at 80 kV and fitted with a Soft Imaging Systems MegaView III CCD camera (Munster, Germany). Images were analysed using the Olympus Soft Imaging Systems AnalySIS software (Olympus) by measuring the thickness of 10 separate cells a total of 10 times. The average thickness and standard deviation were then determined for each isolate.

2.13 Proteomic (2D-Gel) Analysis of BDM-I Treated *E. faecium*

Initially, 2-D Gel Electrophoresis coupled with mass spectrometry was used to examine changes to the proteome in BDM-I treated and mutant VRE isolates. All experimental work was carried out in collaboration with Professor Jens Coorssen at the Proteomics Research Group at Western Sydney University (School of Medicine, WSU).

2.13.1 Sample Preparation

An overnight culture (LBB) was used to inoculate 500 mL of fresh LBB and incubated until an OD_{600} of approximately 0.45 was obtained. The cell pellets were then harvested at 16000 x *g* for 10 min at 4°C. Harvested cells were washed with PBS then homogenised using a Mikro-Dismembrator (Sartorius) at 2000 rpm for 90 s and cooled in liquid N_2, the samples were then stored at -80°C until required. Samples were prepared for protein extraction via treatment with 3x volume of 20 mM HEPES (lysis buffer) and 2x cold PBS. Subsequently, ultracentrifugation was performed at 124, 436 *g* for 3 h at 4°C in a Beckman Coulter Optima L-100 XP ultracentrifuge. Following centrifugation, the supernatant (containing soluble proteins) was collected and snap frozen before being stored at -80°C until required. The remaining pellet was washed with cold 20 mM HEPES buffer, resuspended and centrifuged at 124, 436 *g* for 30 min. The supernatant was discarded, and the pellet resuspended in 500 µL of total protein extraction buffer (8 M urea, 2 M thiourea, 4% CHAPS, 1x protease inhibitors). Samples were then centrifuged at 1000 rpm in a bench top centrifuge at 4°C for 2-5 min. The supernatant was then collected (containing membrane proteins) and stored at -80°C. Protein estimation was then performed using the fluorescent dye method with BSA as a standard.

2.13.2 1st and 2nd Dimension Separation

Protein samples were diluted to a maximum concentration of 100 µg/mL in preparation for isoelectric focusing using 7 cm IPG strips (pH 3-10, Bio-Rad). Initially, diluted protein samples were mixed with 58.8 µL total protein extraction buffer, then a further 58 µL of protein extraction buffer containing 2% ampholytes. Disulfide reduction of protein samples using 2.3 µL TBP/DTT disulfide reduction buffer (2.3 mM tributyl phosphine and 45 mM DTT) was completed prior to alkylation. Alkylation was

performed using 5.1 µL of alkylation buffer (230 mM acrylamide monomer). Each reaction was performed at 25°C for 60 min. 125 µL of protein sample was then pipetted into a clean rehydration tray (Bio-Rad) before a 7 cm IPG strip was placed over the top and subsequently left for 16 h at room temperature (RT). Isoelectric focusing was then conducted at 17°C within a Protean IEF Cell (Bio-Rad). Initially, 250 V of current was applied for 15 min, which was subsequently increased to 4000 V at 50 µA/gel over the course of 2 h, with electrode wicks being changed when the current decreased. IEF was then continued at 4000 V for 9 h.

Upon completion of IEF, IPG strips were equilibrated by soaking in 2 mL of equilibration buffer #1 (2% DTT) for 10 min at RT, then in 2 mL of equilibration buffer #2 (350 mM acrylamide monomer) for 10 min at RT. Equilibrated IPG strips were then transferred to a 2nd dimension, 12.5% SDS-PAGE stacking gel (1 mm thick), and overlaid with 0.5% agarose containing 0.1% SDS and 375 mM Tris (pH 8.8). Electrophoresis was performed at 90 V overnight at 4°C for complete separation. Gels were subsequently washed and stained with Sypro Ruby (Bio-Rad) in preparation for imaging and analysis with the program Delta2D (Decodon, Greifswald, GER).

2.14 Proteomic (shotgun) Analysis of BDM-I Treated *E. faecium* and *S. aureus*

Shotgun proteomics was completed in collaboration with Professor Stuart Cordwell's Laboratory (School of Life and Environmental Sciences, USYD) on BDM-I treated Sa057 and Efm008 isolates.

2.14.1 Sample Preparation and Peptide Enrichment

Overnight cultures of each isolate (LBB) were used to inoculate 10 mL of fresh LBB to an OD_{600} of 0.05. The cultures were then treated with BDM-I at MIC_{50} (1.5 μg/mL for Sa057, 4 μg/mL for Efm008) or DMSO (vehicle control) and incubated for approximately 2.5 h until an OD_{600} of ≈0.45-0.5 was reached, indicating the cells were in the mid-exponential phase. The cells were then harvested at 5000xg at 4°C and washed 2x with ice cold PBS, before the pellets were frozen at -80°C. Frozen, washed bacterial cell pellets were then lyophilised overnight and kept at -80C until required. Pellets were resuspended in tissue lysis buffer containing 150mM Tris-HCl, 125mM NaCl and 0.1mm acid-washed glass beads (Sigma). The cells were lysed by four rounds of bead-beating (4 m/s, 1 min) with 1 min rest periods on ice. Cell debris was removed by centrifugation for 15 min at 4°C at 16 000 x *g*. 250 μL of sample was mixed with ice-cold water/methanol/chloroform in a ratio of 3:4:1 to precipitate proteins. Proteins were resuspended in 6 M urea, 2 M thiourea and reduced with dithioerythritol (DTT; 10mM) at 37°C for 1 h followed by alkylation with iodoacetamide (IAA; 20mM) for 1 h at room temperature in the dark. Samples were then diluted 10-fold in 100mM triethylammoniumbicarbonate (TEAB) and quantified using the Qubit protocol (Life Technologies). Samples were digested with trypsin in a ratio of 1:50 enzyme/sample for 16 h at 37°C. Lipids were precipitated using formic acid (FA) to a final concentration of 2% and pellets removed by centrifugation at 16 000 x *g* for 15 min at 4°C.

Supernatants were acidified with trifluoroacetic acid (TFA) to a final concentration of 0.1%, and peptide purification was performed using 60 cm^3 hydrophilic lipophilic balance (HLB) cartridges (Waters Corp., Bedford, MA). Cartridges were activated with 100% methanol (1 volume), followed by 100% acetonitrile (1 volume) and 70% acetonitrile /

0.1% TFA (1 volume). The cartridges were equilibrated with 0.1% TFA (2 volumes) and loaded with peptide sample. Samples were reapplied three times to ensure sufficient binding, washed with 0.1% TFA, and eluted with 70% acetonitrile / 0.1% TFA (1 volume). Samples were then lyophilised, resuspended in 90% ACN / 0.1% TFA, then 1 µg was aliquoted and dried in a vacuum centrifuge prior to LC-MS/MS.

2.14.2 LC-MS/MS of Enriched Peptides

Peptides were resuspended in 0.1% formic acid and separated on a Dionex 3500RS coupled to a Q-Exactive Plus with Tune v2.4.1824 in positive polarity mode. Peptides were separated using an in-house packed 75 m 55 cm pulled column (1.9 m particle size, C18AQ; Dr Maisch, Germany) with a gradient of 2–30% MeCN containing 0.1% formic acid over 120 min at 250 nl/min at 55 °C. An MS1 scan was acquired from 350 –1550 m/z (70,000 resolution, 3e6 AGC1, 100 ms injection time) followed by MS/MS data-dependent acquisition of the 20 most intense ions with higher collision dissociation (HCD) (17,500 resolution, 1e5 AGC, 60 ms injection time, 27 normalized collision energy (NCE), 1.2 m/z isolation width). The top 20 most abundant ions were selected for MS/MS by higher energy collisional dissociation (HCD). A total of n=3 replicates were performed for each treatment group.

2.14.3 Analysis of Proteome Data

Total proteome data from bacteria were identified and quantified separately with MaxQuant (1.6.0.16) against the Uniprot *Staphylococcus aureus* subsp. *aureus* str. JKD6008 proteome (4/2/17, 2652 proteins) and Uniprot *Enterococcus faecium* (strain Aus0004) proteome (4/2/17, 2826 proteins) with default settings of 20 and 4.5 ppm for first and main search precursor tolerance, respectively. The peptides were searched using

the MaxQuant LFQ algorithm for normalisation allowing for two full missed tryptic cleavages. Oxidation of methionine, protein N-terminal acetylation, carbamidomethylation of cysteine were set as variable modifications. The requantify option was enabled with a minimum of two unique + razor peptides used for protein quantification. All data were searched with both peptide spectral match and protein false discovery rate (FDR) set to 1%. Proteins were included for analysis if they contained ≥2 peptides mapping. Proteins only occurring in only one replicate in either group were discarded, and missing values for remaining proteins were imputed from a normal distribution using Perseus (v 1.6.07). Multiple t-tests were performed on $\log_2$ transformed LFQ intensities, with a FDR cutoff of p_{adj} <0.05. A $\log_2$ difference of ≥2-fold was considered differentially expressed between groups for statistically significant results.

2.15 DARTS Analysis of BDM-I Treated Cell Supernatant

Drug Affinity Responsive Target Stability (DARTS) has previously been described as a viable method for the identification of small molecule targets. The methodology used was adapted from that described by Pai et al for target identification in yeast (Pai et al., 2015).

2.15.1 Cell Lysate Preparation and Drug Treatment

An overnight culture of Sa057 was diluted into 500 mL of pre-warmed LBB to an OD_{600} of 0.05, which was then incubated for approximately 2.5 h at 37°C with shaking (250 rpm). The cells were then harvested at 5000xg for 10 min at 4°C, then washed twice with 25 mL of sterile, ice-cold PBS. The cells were then resuspended in 2 mL of lysis buffer (20mM Tris-HCl, 2mM EDTA, 1% Triton X-100, pH 8) supplemented with lysostaphin and 1X cOmplete protease inhibitors (Roche) before being incubated at 37°C for 45 min

in a water bath. The cells were then sonicated using a Q55 Probe Sonicator (Qsonica) at an amplitude of 50 in 3x3 sec bursts. The suspension was then centrifuged for 20 min at 21 000xg at 4°C, before the lysate was transferred to a 1.5 mL Eppendorf and kept on ice. The protein lysate was then quantified using the Pierce BCA Protein Assay Kit (ThermoFisher), before the lysate was stored at -20°C.

The protein lysate was diluted to a concentration of 4 mg/mL in 1X TNC buffer (100 mM Tris-HCl, 500 mM NaCl, 100 mM CaCl, pH 8.0), before 99 µL aliquots were prepared in 3x separate Eppendorf tubes. In the first tube, 1 µL of DMSO was added as a control, and 1 µL of BDM-I at MICx1 and MICx5 were added to the two remaining aliquots, which were then incubated at 25°C for 30 min with shaking (250 rpm). Pronase (Sigma-Aldrich) stocks were prepared at protein:pronase concentrations of 1:50, 1:100, 1:250 and 1:500 in 1X TNC buffer and kept on ice. Following incubation, each sample was separated into 4 x 20 µL aliquots and inoculated with 2 µL of each pronase solution, then incubated for exactly 30 min at 25°C. Following incubation, protein digestion was stopped with the addition of 1.6 µL of 25X protease inhibitors (Roche) followed by incubation on ice for 10 min.

2.15.2 SDS-PAGE Electrophoresis and Staining

5X SDS-PAGE buffer was then added to each sample and incubated at 70°C for 10 min. 13 µL of each sample was then loaded onto a 4-15% Mini-Protean (Bio-Rad) gel and run at 100 V for 90 min at RT. The gels were then incubated for 30 min in a fixing solution (40% Methanol, 10% Acetic Acid), followed by 40 min in a staining solution (0.025% Coomassie Brilliant Blue, 10% Acetic Acid), and finally 15 min (x3) in a wash solution (10% Acetic Acid). The gels were then imaged with white light using a GelDoc-It TS

Imaging System (UVP) and analyzed for the presence of additional bands within drug treated samples.

2.16 Thermal Proteome Profiling of Whole Cells

Thermal proteome profiling was completed in collaboration with Professor Stuart Cordwell's Laboratory (School of Life and Environmental Sciences, USYD) as described by Mateus et al (Mateus et al., 2018).

2.16.1 Sample Preparation

Four 10 mL cultures of LBB were prepared from an overnight broth of Sa057, which was diluted to an OD_{600} of 0.05 and incubated at 37°C for 150 min. Drug (3 μg/mL) or vehicle control (DMSO) was then added to 2x cultures and incubated for a further 10 min. Each culture was then harvested at 5000 xg for 8 min at RT and washed with sterile PBS (containing drug or DMSO). Cells were then resuspended in PBS to an OD_{600} of 10 and heated to 63°C for 3 min, followed by a 3 min incubation at RT. The cells were then snap frozen in liquid nitrogen and stored at -80°C until use.

2.16.2 Peptide Preparation

Frozen, washed bacterial cell pellets were lyophilised overnight and kept at -80C until required. Cell pellets were prepared as in Mateus et al (2018) with the following modifications. Solubilized, filtered proteins were resuspended in 6 M urea, 2 M thiourea and reduced with dithioerythritol (DTT; 10mM) at 37°C for 1 h followed by alkylation with iodoacetamide (IAA; 20mM) for 1 h at room temperature in the dark. Samples were then diluted 10-fold in 100mM triethylammoniumbicarbonate (TEAB) and quantified

using the Qubit protocol (Life Technologies, Carlsbad, CA). Samples were digested with trypsin in a ratio of 1:50 enzyme/sample for 16 h at 37°C. Lipids were precipitated using formic acid (FA) to a final concentration of 2% and pellets removed by centrifugation at 16 000xg for 15 min at 4°C.

Supernatants were acidified with trifluoroacetic acid (TFA) to a final concentration of 0.1%, and peptide purification was performed using 60 cm3 hydrophilic lipophilic balance (HLB) cartridges (Waters Corp., Bedford, MA). Cartridges were activated with 100% methanol (1 volume), followed by 100% acetonitrile (1 volume) and 70% acetonitrile / 0.1% TFA (1 volume). The cartridges were equilibrated with 0.1% TFA (2 volumes) and loaded with peptide sample. Samples were reapplied three times to ensure sufficient binding, washed with 0.1% TFA, and eluted with 70% acetonitrile / 0.1% TFA (1 volume).

10 µg of each sample of peptides (n=5 each condition) were aliquoted, lyophilised and resuspended in 100mM TEAB and labelled with Tandem Mass TagsTM 10-plex (TMT10plex) according to the manufacturer's protocol (Thermo Fisher Scientific, MA). Samples were combined and diluted to 1mL in 0.1% TFA and purified by HLB as described above. Labelled samples were lyophilized and stored at -80°C until required.

2.16.3 LC-MS/MS of Peptides

8 µg of TMT-labelled peptides were separated into 8 fractions by hydrophilic interaction liquid chromatography (HILIC) using an Agilent 1100 chromatography system. Fractionation was performed using a 20 cm, 320 µm i.d column packed with TSK-Amide 80 HILIC resin, 3 µm particles size. Samples were resuspended in buffer B (90%

acetonitrile / 0.1% TFA) and separated using a linear gradient: sample loading for 10 min with 100% buffer B at 12 µL/min, sample elution from 90 - 60% B at 6 µL/min for 40 min. Peptide elution was monitored by an absorbance detector at 280 ± 4. Fractionated samples were lyophilised and stored at -20°C until analysis with mass spectrometry.

Fractionated labelled peptides were resuspended in 0.1% formic acid and separated on a Thermo Easy-nLC coupled to a Q-Exactive HF-X with Tune v2.4.1824 in positive polarity mode. Peptides were separated using an in-house packed 75 m 50 cm pulled column (1.9 m particle size, C18AQ; Dr Maisch, Germany). Peptides were eluted with a gradient of 2-30% MeCN containing 0.1% formic acid over 150 min at 300 nl/min at 60°C. An MS1 scan was acquired from 350 –1650 m/z (60,000 resolution, 3e6 AGC1, 50 ms injection time) followed by MS/MS data-dependent acquisition of the 15 most intense ions with higher collision dissociation (HCD) (60,000 resolution, 1e5 AGC, 75 ms injection time, 29 normalised collision energy (NCE), 0.7 m/z isolation width).

2.16.4 Proteomic Data Analysis

Total proteome data from bacteria were identified and quantified separately with MaxQuant (1.6.0.16) against the Uniprot Staphylococcus aureus subsp. aureus str. JKD6008 proteome (4/2/17, 2652 proteins) with default settings of 20 and 4.5 ppm for first and main search precursor tolerance, respectively. Oxidation of methionine, and carbamidomethylation of were set as variable modifications, with a maximum of five modified amino acids and allowing for two full missed tryptic cleavages. All data were searched with both peptide spectral match and protein false discovery rate (FDR) set to 1%. HCD MS/MS were deisotoped and searched with a tolerance of 0.002 Da for all fragment ions and peptides were searched with 10-plex TMT multiplicity. Total reporter

ion intensity for each protein was calculated at the protein level, normalised against the summed reporter ion intensity for all proteins including contaminants present in that channel.

2.17 ATP Assays

ATP assays were conducted on MRSA and VRE isolates following the observation that ATP synthase appears to be affected by BDM-I. Assays were completed on two isolates; Sa057 and Efm008 in triplicate using the ATP Bioluminescence Assay Kit HS II (Sigma-Aldrich). Briefly, growth curves were generated for each isolate plotting OD_{600} values against Cfu/mL to be used as standards to determine culture Cfu/mL. Overnight cultures of each isolate were diluted to an OD_{600} of 0.05 in 2x10 mL LBB and incubated at 37°C with shaking (250 rpm) for 30 min. Following incubation, one broth was inoculated with BDM-I (MIC_{50}) and the other with an identical volume of the vehicle control (DMSO), before being incubated for a further 2 h at 37°C with shaking (250 rpm). Following incubation, the OD_{600} was determined for each culture, then cell lysates were prepared according to the manufacturer's instructions and kept on ice until used. 50 µL aliquots were then pipetted in triplicate into individual wells of a Nunclon™ Delta Surface opaque 96-well plate (Thermo Scientific) and mixed with 50 µL of luciferase reagent. Immediately after mixing, luminescence was determined in RLU on a SpectraMax M2^e Plate Reader (Molecular Devices) at 562 nm. ATP concentrations were determined in nmoles using a standard curve and normalized to 10^5 Cfu for both BDM-I treated and control samples.

2.18 Plasmid Stability Assays

Stability assays were completed using a mini replicon plasmid (pJEG001) to determine the effect of BDM-I on plasmid stability. Assays were completed in triplicate using pJEG001, pJEG001 BDM-$I_{MIC0.75}$, pJEG001 BDM-I MIC_{75} and a known control pJEG005. 10 mL overnight cultures were prepared in LBB containing erythromycin (10 μg/mL) and incubated at 37°C with shaking for 16-24 h. 1 mL of overnight culture was then added to 9 mL of fresh LBB containing erythromycin and incubated at 37°C for 4 h with shaking. After incubation, serial dilutions were prepared from 10^{-1} to 10^{-6} and spread plate onto LB agar. 10 μL was then taken from the 10^{-1} dilution and inoculated into fresh LBB containing appropriate concentrations of BDM-I, and incubated for 16-24 h at 37°C with shaking. The following day patch plates were prepared using an overnight spread plate with at least 100 counted colonies. Using a new toothpick for each colony, 100 colonies were patched onto LB agar and LB agar containing erythromycin, before being incubated for 16-24 h. Simultaneously, serial dilutions were prepared from each overnight broth as described previously, with fresh broths being incubated from the 10^{-1} dilution. This process was repeated daily until 0 patched colonies of pJEG5 were cultured on LBA containing erythromycin.

Chapter 3

Assessing the Clinical Utility of BDM-I Against ESKAPE Pathogens

3.1 Introduction

As discussed in Chapter 1, the current state of antibiotic development is very concerning when considering both the number of new antimicrobials in clinical trials, as well as the fact that no new antimicrobials currently in development display significant activity against gram-negative pathogens. Previous BDM-I studies have identified that it displays a broad spectrum of activity *in vitro* against bacteria, fungi and some protozoa. However, preliminary MIC testing has indicated that BDM-I displays a greater range of activity against gram-positive species than gram-negative ones, with only *H. influenzae*, *P. multocida* and *N. gonorrhoeae* exhibiting MIC values of ≤5 μg/mL (White, 2008). Understanding the full range of antimicrobial activity for a novel compound is vital during its development, therefore we aimed to assess the potential clinical utility of BDM-I in more detail. Using the broth microdilution method (BMD), we aimed to determine the MIC of BDM-I against a number of clinical isolates from the previously mentioned ESKAPE pathogens, including the gram-negative species *P. aeruginosa*, *E. coli* and *K. pneumoniae*, as well as the gram-positive species *S. aureus* and *E. faecium*. Additionally, MIC testing was also performed using the Agar Dilution Method to test the useability of this method with BDM-I, given that the BMD method is not a suitable method for MIC determination of several bacterial species (for example, *N. gonorrhoea*).

Furthermore, induction experiments were performed using select MRSA and VRE isolates, in order to determine the useability of BDM-I for extended periods. Specifically,

these experiments allowed us to assess the ability of each isolate to generate resistance in vitro to BDM-I.

3.2 Assessing the Efficacy of BDM-I Against Gram-Negative Isolates

Based on difficulty in obtaining clinical gram-negative isolates, only 22 were selected across three species representing the most common causes of nosocomial infections (8 *P. aeruginosa*, 8 *E. coli* and 6 *K. pneumoniae*). Due to solubility issues with BDM-I at higher concentrations (generally >128 μg/mL), a BDM-I range of 128-0.25 μg/mL was selected for BMD testing. The MICs were determined in duplicate for each isolate, with the average MICs determined shown in Table 3.1. The MIC data generated reflects similar results from previous studies (White, 2008), with BDM-I not exhibiting any activity against the gram-negative isolates tested, confirming the limitations of BDM-I against these important pathogen types.

Table 3.1 Average BDM-I MICs Determined for Selected Gram-Negative Isolates

P. aeruginosa		***E. coli***		***K. pneumoniae***	
Isolate No.	**Mean MIC (μg/mL)[a]**	**Isolate No.**	**Mean MIC (μg/mL)[a]**	**Isolate No.**	**Mean MIC (μg/mL)[a]**
Pa0001	>128	**Ec0002**	>128	**Kp0001**	>128
Pa0005	>128	**Ec0003**	>128	**Kp0002**	>128
Pa0010	>128	**Ec0004**	>128	**Kp0003**	>128
Pa0015	>128	**Ec0005**	>128	**Kp0004**	>128
Pa0020	>128	**Ec0006**	>128	**Kp0005**	>128
Pa0025	>128	**Ec0007**	>128	**Kp0007**	>128
Pa0030	>128	**Ec0008**	>128	-	-
Pa0035	>128	**Ec0009**	>128	-	-

[a]MIC testing was completed in duplicate for each isolate and values were determined based on visual inspection for growth in a 96-well plate.

3.3 BDM-I has Antimicrobial Activity against *S. aureus and E. faecium* Clinical Isolates

MIC tests were then completed on a range of *S. aureus* and *E. faecium* clinical isolates, in order to examine the efficacy of BDM-I against clinically important gram-positive pathogens. Testing was initially completed using a similar BDM-I range as described in section 3.2 (128-0.25 μg/mL), however the results indicated that a lower range was needed due to the increased activity of BDM-I against these isolates (<10 μg/mL). Therefore, MIC testing was repeated using a range of 10-1 μg/mL, which formed the basis for testing all clinical isolates listed in Tables 2.2 and 2.4-2.7 (section 2.1).

The MICs of 26 MRSA isogenic pairs were initially determined as outlined in Table 2.5, with each pair consisting of an isolate obtained at the initial stage of infection, and another obtained following persistent bacteraemia (and vancomycin therapy, in most cases). Studying isogenic pairs allowed us to determine the efficacy of BDM-I against clinical isolates associated with persistent infections and treatment failure. The mean MIC was determined for each isolate based on duplicate data sets, and is shown in Table 3.2. As seen, there were no significant differences in MICs observed between initial and recurrent/persistent isolate types, with most MICs being in the range of 3-4 μg/mL.

Further MIC testing was then performed on three clinical MRSA isogenic isolate series, with the average MIC values shown in Table 3.3. Examining changes in MIC within a persistent series of isolates with previously observed development of vancomycin resistance, allows us to identify potential cross-resistance between the two compounds. As seen in the case of series A and B, the BDM-I MIC remained unchanged at 5 μg/mL

and 3 μg/mL respectively during the course of infection. However, within series C we observed a gradual decrease in BDM-I MIC over time, which coincided with a gradual increase in vancomycin resistance as observed by the isolate's vancomycin phenotype. This observation is possibly indicative of a "seesaw" effect between BDM-I and vancomycin which is discussed in section 3.4.

Additional MIC tests were also performed using the Agar Dilution method to evaluate whether BDM-I was capable of diffusing through Agar. Testing was completed using four clinical MRSA isolates with known BDM-I MICs (identified through broth microdilution testing). Table 3.4 shows the determined MICs for each isolate comparing the Agar and Broth Microdilution methods. As seen, there was no difference in the BDM-I MICs when comparing the two methods, indicating that MIC testing can be performed using Agar dilution as an alternative method.

Table 3.2 Average BDM-I MICs for MRSA Isogenic Isolate Pairs

Pair	Isolate Number	Isolate Type	Mean MIC (µg/mL)[a]
A	Sa0040	Initial	4
	Sa0012	Recurrent	4
B	Sa0227	Initial	5
	Sa0328	Recurrent	4.5
C	Sa0307	Initial	4
	Sa0365	Persistent	4
D	Sa0243	Initial	4
	Sa0194	Persistent	4
E	Sa0138	Initial	4
	Sa0116	Persistent	4
F	Sa0015	Initial	4
	Sa0019	Recurrent	3
G	Sa0309	Initial	3
	Sa0238	Persistent	3
H	Sa0283	Initial	3
	Sa0284	Persistent	3
I	Sa0212	Initial	3
	Sa0214	Recurrent	3
J	Sa0158	Initial	3
	Sa0160	Persistent	3.5
K	Sa0343	Initial	3
	Sa0191	Recurrent	3
L	Sa0037	Initial	3
	Sa0044	Recurrent	3
M	Sa0237	Initial	3
	Sa0285	Persistent	3
N	Sa0051	Initial	3
	Sa0052	Persistent	3
O	Sa0331	Initial	3
	Sa0332	Persistent	3
P	Sa0255	Initial	3
	Sa0256	Persistent	3
Q	Sa0294	Initial	4
	Sa0192	Persistent	4
R	Sa0014	Initial	3
	Sa0017	Recurrent	2
S	Sa0228	Initial	3
	Sa0265	Persistent	3
T	Sa0055	Initial	3
	Sa0056	Recurrent	3
U	Sa0091	Initial	3
	Sa0162	Persistent	3
V	Sa0304	Initial	3
	Sa0305	Persistent	3
W	Sa0006	Initial	4
	Sa0011	Recurrent	4
X	Sa0068	Initial	3
	Sa0047	Persistent	4
Y	Sa0329	Initial	3
	Sa0330	Persistent	3
Z	Sa0322	Initial	3
	Sa0324	Persistent	3

[a]MIC testing was completed in duplicate for each isolate

Table 3.3 Average BDM-I MICs for Clinical MRSA Isogenic Isolate Series

Series	Isolate Number	Isolate Type	Vancomycin Phenotype	Mean MIC (μg/mL)[a]
A	Sa0048	Initial	VSSA	5
	Sa0049	Persistent	VSSA	5
	Sa0050	Persistent	hVISA	5
B	Sa0016	Initial	hVISA	3
	Sa0018	Recurrent	hVISA	3
	Sa0067	Recurrent	hVISA	3
	Sa0020	Persistent	hVISA	3
	Sa0070	Recurrent	hVISA	3
	Sa0054	Recurrent	hVISA	3
C	Sa0057	Initial	VSSA	4
	Sa0058	Persistent	hVISA	3
	Sa0059	Persistent	VISA	3
	Sa0060	Persistent	hVISA	3
	Sa0378	Persistent	VISA	3
	Sa0375	Persistent	VISA	2

[a]MIC testing was completed in duplicate for each isolate. No changes in MIC were observed within series A and B. However, series C exhibited a gradual decrease in BDM-I MIC in an inverse relationship to the generation of vancomycin resistance.

Table 3.4 Comparison of MICs Determined using the Agar and BMD Methods

Isolate	Phenotype	Agar MIC (μg/mL)	BMD MIC (μg/mL)
Sa040	VSSA	4	4
Sa057	VSSA	4	4
Sa060	hVISA	3	3
Sa375	VISA	2	2

In general, the above analysis revealed that BDM-I retains clinical activity and displays increased efficacy against MRSA clinical isolates with varying degrees of vancomycin susceptibility. Following this, we conducted further MIC studies using 30 clinical *E. faecium* isolates and a single VRE isogenic isolate series, with the determined MICs shown in Table 3.5 and 3.6, respectively. Ten isolates were selected representing different vancomycin phenotypes, including vancomycin susceptible enterococci (VSE) and vancomycin resistant enterococci (VanB and VanA phenotypes). Similar MICs were observed between these phenotypes, with most isolates exhibiting a BDM-I MIC between 6 and 8 μg/mL. Interestingly, a few isolates displayed an increased sensitivity to BDM-I,

notably Efm0174, Efm0002, Efm0072 (Table 3.5) and Efm0007 (Table 3.6), which all had an MIC of 3-3.5 μg/mL.

Table 3.5 Average BDM-I MICs for Clinical *E. faecium* Isolates

Isolate Number	Hospital	Phenotype	Mean MIC (μg/mL)
Efm0092	RPA	VSE	9
Efm0093	RPA	VSE	7
Efm0097	RPA	VSE	8
Efm0100	RPA	VSE	7
Efm0103	RPA	VSE	8
Efm0136	RPA	VSE	8
Efm0138	RPA	VSE	8
Efm0200	RPA	VSE	8
Efm0219	RPA	VSE	8
Efm0222	RPA	VSE	5
Efm0174[a]	RPA	VanB	3
Efm0002[a]	Liverpool	VanB	3.5
Efm0202	RPA	VanB	7
Efm0151	RPA	VanB	6
Efm0180	RPA	VanB	6
Efm0218	RPA	VanB	6
Efm0217	RPA	VanB	6
Efm0160	RPA	VanB	7
Efm0128	RPA	VanB	8
Efm0125	RPA	VanB	8
Efm0067	QLD	VanA	6
Efm0072[a]	MH	VanA	3
Efm0076	MH	VanA	7
Efm0081	AH	VanA	6
Efm0087	AH	VanA	8
Efm0234	Wollongong	VanA	6
Efm0236	Wollongong	VanA	7
Efm0315	St George	VanA	5
SVH193	Westmead	VanA	7
SVH228	Westmead	VanA	7

[a]Isolates with an atypical *E. faecium* MIC of 3 μg/mL

Table 3.6 Average BDM-I MICs of a Single VRE Isogenic Isolate Series

Series	Isolate Number	Isolate Type	Mean MIC (μg/mL)
A	Efm0006	Initial	6-7
	Efm0007[a]	*Persistent*	3
	Efm0010	Persistent	6
	Efm0027	Persistent	5
	Efm0028	Persistent	7
	Efm0029	Persistent	7
	Efm0030	Persistent	6
	Efm0031	Persistent	6

[a]Isolates with an atypical *E. faecium* MIC of 3 μg/mL

3.4 The Relationship between BDM-I and Vancomycin MICs for MRSA and VRE

MIC data for MRSA isolates (section 3.3) suggested a potential "seesaw" effect and possible synergism between BDM-I and vancomycin. To explore this further, MIC tests were completed on additional MRSA clinical isolates possessing varying degrees of vancomycin susceptibility, in order to obtain a large data set for statistical analysis. In total, 43 VSSA isolates, 54 hVISA isolates and 6 VISA isolates were subjected to MIC testing, with the average MICs determined for each phenotype being 3.42 µg/mL, 3.28 µg/mL and 2.5 µg/mL, respectively (Table 3.7). Following statistical analysis, a "see-saw" effect was confirmed as BDM-I MICs are inversely correlated to vancomycin MICs (Rho = -0.24; $P = 0.0154$). This can be observed in Table 3.7, where VSSA isolates have a higher average BDM-I MIC when compared to VISA isolates.

Table 3.7 Average BDM-I and Vancomycin MICs for 103 Clinical MRSA Isolates

Isolate Vancomycin Phenotype	BDM-I MIC (µg/mL)	Vancomycin MIC (µg/mL)
VSSA (n=43)	3.42	1.16
hVISA (n=54)	3.28	1.92
VISA (n=6)	2.5	2.2

This confirmed see-saw effect indicated a potential synergistic relationship between BDM-I and vancomycin, which was subsequently explored. In this regard, checkerboard assays were conducted using three MRSA isolates and three VRE isolates with various vancomycin phenotypes, in order to identify potential synergism between the two compounds. The isolates selected included Sa057 (VSSA), Sa060 (hVISA), Sa375 (VISA), Efm201 (*vanB* located on the chromosome), Efm123 (*vanB* located on a plasmid) and Efm008 (*vanA* located on a plasmid). The calculated FICI values for each MRSA isolate were determined as 1.42 (SD = 0.28) for Sa057, 1.29 (SD = 0.26) for Sa060 and

1.14 (SD = 0.09) for Sa375. According to the guidelines described in section 2.3, these FICI values indicate there is no *in vitro* interaction between BDM-I and vancomycin when tested in combination against MRSA. However, the raw data showed a significant decrease in vancomycin MIC for Sa375 from 4 μg/mL to 0.583 μg/mL (SD = 0.38), when combined with BDM-I at MIC_{50} (1 μg/mL). A similar result was observed for Sa060, where at sub-inhibitory BDM-I concentrations the vancomycin MIC decreased from 4 μg/mL to 0.75 μg/mL (SD = 0.43).

Similar results were observed with the VRE isolates, with the FICI values being calculated as 1.06 (SD = 0.2) for Efm008, 0.62 (SD = 0.15) for Efm123 and 0.62 (SD = 0.01) for Efm201. This data indicates that BDM-I exerts a definite additive effect in combination with vancomycin for VRE isolates possessing *vanB* vancomycin resistance. In the case of Efm008, an FICI value of 1.06 places the data in the "no interaction" range, however, considering the calculated standard deviation, we are unable to conclude with certainty that using BDM-I in combination with vancomycin has no effect on the efficacy of vancomycin against VRE possessing *vanA* resistance.

Additional checkerboard assays were completed using other cell wall active antibiotics including flucloxacillin and ceftaroline dihydrochloride combined with BDM-I. However, there were no synergistic or additive relationships observed, indicating the additive activity observed above is specific to BDM-I and vancomycin.

3.5 *In vitro* Generation of Mutants with Increased BDM-I MICs

In section 3.3, we identified that there were no observable differences in BDM-I MICs between initial and persistent isolates derived from a single patient who had failed

antimicrobial therapy, indicating that cross-resistance (to BDM-I) does not emerge in the context of extended vancomycin exposure. In order to further explore the clinical utility of BDM-I, we then determined if BDM-I MICs increased for MRSA or VRE following prolonged periods of exposure against clinically relevant bacteria, in order to identify the potential of select isolates to develop increased resistance to BDM-I.

This was achieved through induction experiments as explained in section 2.5, which were conducted using four clinical isolates: two MRSA isolates, Sa057 (VSSA) and Sa375 (VISA), and; two VRE isolates, Efm003 (*vanB* resistance) and Efm008 (*vanA* resistance). Induction experiments were completed in triplicate for each isolate, and their initial BDM-I MICs are shown in Table 3.8.

Table 3.8: Test Isolates Selected for Induction Experiments and Additional MoA Studies

Isolate	Phenotype	Mean MIC (µg/mL)
***S.aureus* Sa375**	MRSA, VISA	2
***S.aureus* Sa0057**	MRSA, VSSA	4
***E.faecium* Efm0003**	VRE, *VanB*	7
***E.faecium* Efm0008**	VRE, *VanA*	7

3.5.1 MRSA Isolates do not Develop BDM-I Resistance Readily *in vitro*

MRSA isolates were subcultured for approximately 100 days in triplicate and subjected to additional BMD at different time points to identify changes in MICs. Figure 3.1 illustrates changes in BDM-I MICs for Sa057 (a) and Sa375 (b), determined as an average of each triplicate series. Sa057 displayed little ability to adapt to BDM-I, with no significant changes in MIC being observed within the 100-day time-period. Interestingly, an increased resistance to BDM-I was observed for Sa375 approximately 15 days into the experiment, however these changes in MIC were not stable and fluctuated significantly until the final days of exposure. Following approximately 100 days of exposure, the

Sa375 series developed a stable phenotype with BDM-I MICs of 5 μg/mL which was higher than that of the progenitor (2 μg/mL).

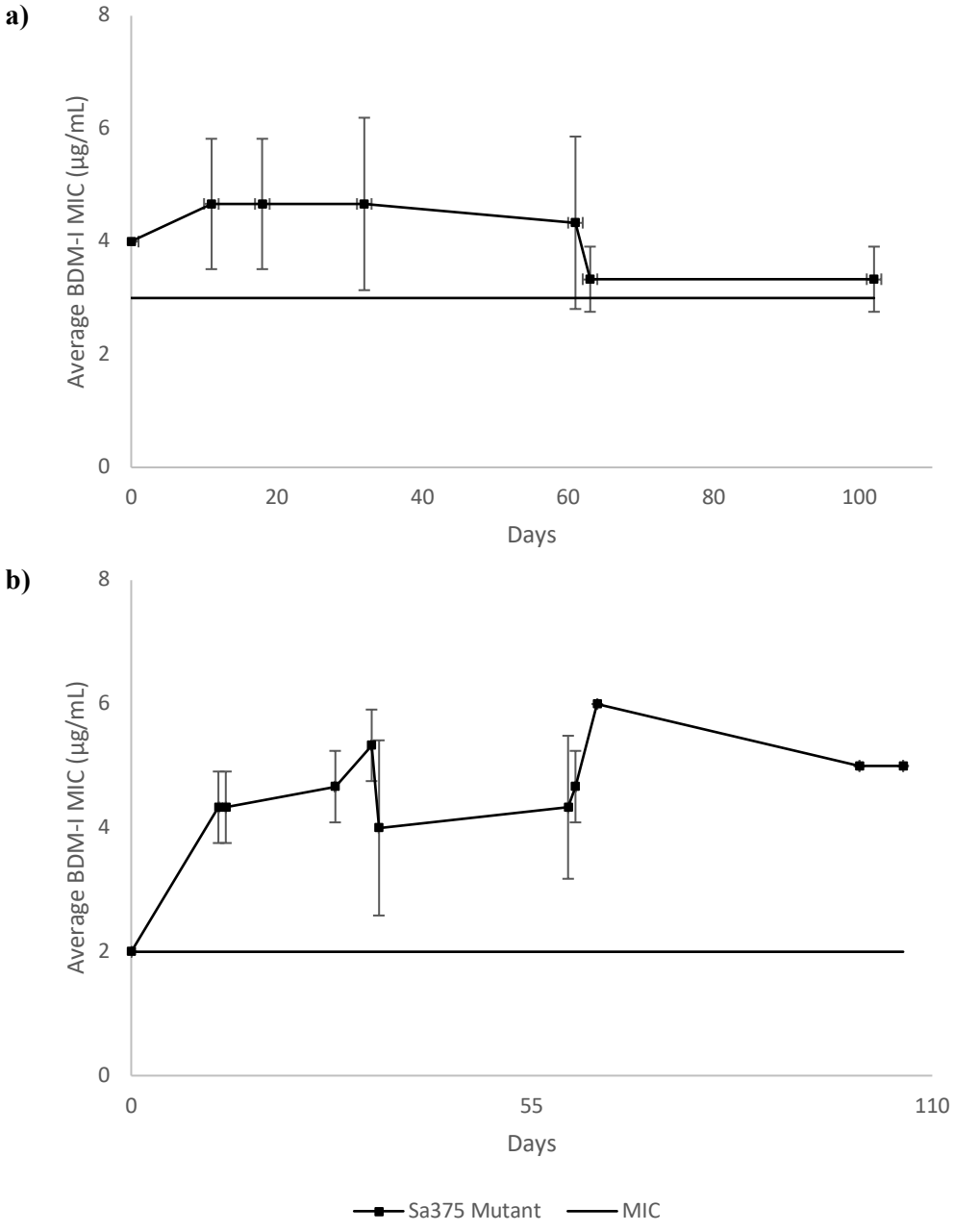

Figure 3.1 Changes in BDM-I MIC observed for MRSA isolates Sa057 (a) and Sa375 (b) following 100 and 110 days of continuous exposure, respectively. Each isolate was subcultured in triplicate, and the average MICs for each isolate determined following BMD testing at different time points. The horizontal line indicates the MIC of the progenitor isolates.

3.5.2 VRE Readily Develops Increased Resistance to BDM-I *in vitro*

In contrast to the results observed in section 3.5.1, both VRE isolates were readily capable of developing increased resistance to BDM-I. Significant increases in MICs were observed over an 80-day period for both Efm003 (a) and Efm008 (b) as shown in Figure 3.2. Sharp increases in MICs were observed around day 10 for both isolates, increasing to approximately 12 μg/mL, which continued to rise until the final time point. As shown in Figure 3.2, both strains developed mutants with final MICs more than double that of the progenitor strains, indicating that VRE are readily capable of developing increased resistance to BDM-I following prolonged periods of exposure.

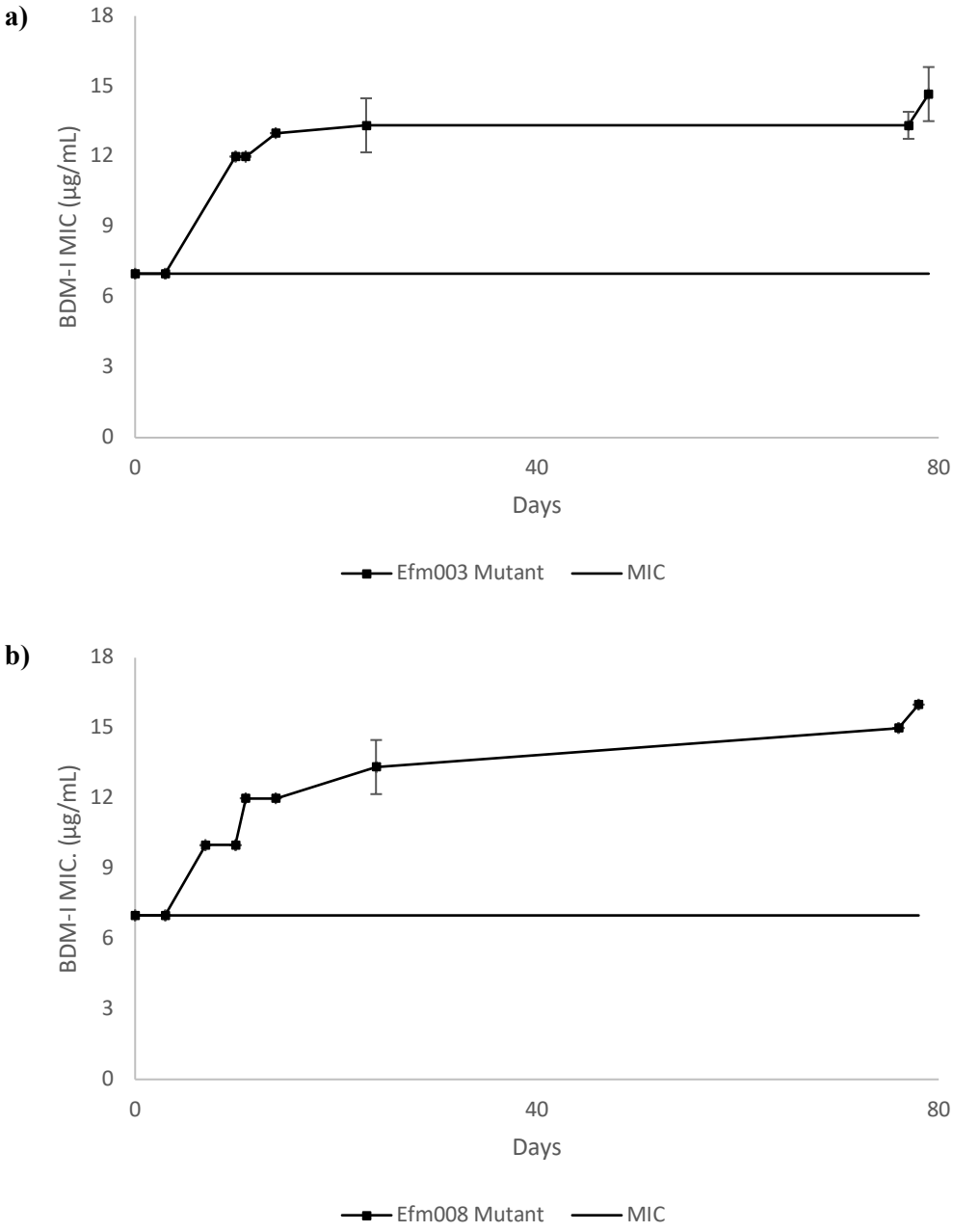

Figure 3.2 Changes in BDM-I MIC observed for VRE isolates Efm003 (a) and Efm008 (b) following 80 days of continuous exposure. Each isolate was subcultured in triplicate, and the average MICs for each isolate determined using BMD testing at different time points. The horizontal line indicates the progenitor isolates MICs.

3.6 Discussion

It is important to examine the clinical utility of novel compounds against common bacterial pathogens, especially those classified as clinically important such as the ESKAPE pathogens. In Chapter 3 we examined the activity of BDM-I against a range of bacteria including gram negative (*E. coli, K. pneumoniae* and *P. aeruginosa*) and gram positive (*S. aureus* and *E. faecium*) clinical isolates, as well as the activity of BDM-I in combination with several antibiotics, particularly the front-line therapeutic vancomycin (sections 3.2 to 3.4). In addition, we also examined the ability of *S. aureus* and *E. faecium* isolates to develop increased resistance to BDM-I following prolonged periods of exposure (section 3.5).

Previous work on BDM-I revealed that it is mainly active against gram-positive bacteria (White, 2008). Regardless, it was important to conduct further MIC testing with BDM-I on common gram-negative pathogens to confirm its spectrum of antimicrobial activity. In this regard, several clinical isolates were selected for MIC testing using two-fold dilutions of BDM-I with a range of 128-0.5 μg/mL. As expected, BDM-I did not inhibit any of the tested isolates tested, confirming that its activity is limited to gram-positive pathogens. However, additional MIC testing should be conducted on other gram-negative pathogens of interest such as *N. gonorrhoeae*.

In any case, MIC tests completed on the gram-positive pathogens *S. aureus* and *E. faecium* (section 3.3) yielded promising results, with BDM-I displaying the best activity against MRSA, particularly for clinical isolates with increased resistance to vancomycin (i.e., hVISA and VISA). Overall, MRSA is more sensitive to BDM-I with average MICs

of 3.42, 3.28 and 2.5 μg/mL for VSSA. hVISA and VISA isolates, respectively, compared to average MICs of 7-8 μg/mL for VRE isolates. Furthermore, MIC analysis also identified a see-saw effect between BDM-I and vancomycin for MRSA, which formed the basis for doing checkerboard assays to identify any potential synergism between the two compounds. Checkerboard assays were conducted using MRSA and VRE isolates with varying vancomycin phenotypes (section 3.4), with the data acquired suggesting that BDM-I does exert an additive effect in combination with vancomycin, primarily for hVISA and VISA MRSA isolates as well as VanB VRE.

Extended exposure to an antibiotic in a clinical setting is often associated with the emergence of resistance *in vivo* (van Hal et al., 2013). Therefore, after determining the utility of BDM-I against MRSA and VRE, we then aimed to explore the capability of these bacteria to develop resistance to BDM-I following prolonged periods of exposure (section 3.5). Interestingly, neither of the MRSA isolates tested displayed any significant capability to develop increased resistance to BDM-I, with Sa375 developing marginally increased resistance with final MICs similar to that of VSSA isolates. Conversely, both VRE isolates rapidly developed increased resistance to BDM-I following only several days of exposure (section 3.5.2).

In summary, the data outlined in Chapter 3 has illuminated the utility of BDM-I against *S. aureus in vitro*, as both a single compound and in combination with the front-line antibiotic vancomycin. Furthermore, the data suggests that the risk of *S. aureus* developing resistance to BDM-I is relatively low, identifying the potential for its use in the treatment of chronic infections. While MIC analysis revealed that *E. faecium* isolates

are susceptible to BDM-I at concentrations <10 μg/mL, the rate at which VRE developed resistance to BDM-I suggests it is unlikely to be useful in clinical applications.

Chapter 4

Investigating the Genotype and Phenotype of Mutants with Increased Resistance to BDM-I

4.1 Introduction

Determining an antimicrobials mechanism of action (MoA) is often difficult. Traditionally, methods utilising radioactively labelled precursors (macromolecular synthesis) were used to explore which bacterial synthetic pathway(s) (i.e., synthesis of protein, DNA, RNA, lipid or peptidoglycan) was targeted by an antimicrobial compound. While this method is still commonly used by the pharmaceutical industry, its application in broader settings is limited due to a number of drawbacks, including its ability to only identify a narrow range of MoAs. Transcriptional profiling is a commonly used molecular method in the research environment and has also been effective in determining the MoA of antibiotics (Freiberg et al., 2005, Hutter et al., 2004).

Previous work studying the BDM-I MoA has utilised various molecular techniques, such as microarray analysis and targeted assays to study the effect of BDM-I on different cellular processes (White et al., 2014). Whole genome sequencing of *in vitro* or *in vivo* derived resistant mutants has been shown to be a viable method for studying the MoA of novel antibiotics. Ioerger et al identified resistance-associated mutations within *M. tuberculosis* against eight novel compounds selected through high throughput screening (HTS). Analysis of these mutations identified four likely drug targets and thus such an approach represents an unbiased method for target identification that does not rely on target-based approaches, which are only effective in a limited number of cases (Ioerger

et al., 2013). Similarly, through the sequencing of mutant cell lines with resistance against the anti-cancer drug Bortezomib, Wacker et al were able to identify single-point mutations within the gene that encodes for the (known) drug targets gene (Wacker et al., 2012). These studies highlight resistance mutant sequencing as a viable approach to identifying a novel drug's cellular target. The identification of single-point mutation(s) associated with increased resistance can give insight into potential resistance mechanisms, and by extension may reveal a drugs cellular target and/or MoA.

To date, no mutant isolates with increased BDM-I MICs have been successfully generated, which imposes a severe limitation for studying the BDM-I MoA using next-generation sequencing technologies. However, as part of this study (Chapter 3, section 3.5), we have successfully generated of *E. faecium* and *S. aureus* mutants *in vitro* with increased BDM-I resistance. Utilising these mutant isolates, we therefore conducted whole genome sequencing analysis in order to identify any mutations that may contribute to our understanding of the BDM-I MoA.

4.2 Whole Genome Sequencing of VRE Mutants

As described in section 3.5, the greatest increase in BDM-I MICs were observed for the enterococcal isolates Efm008 and Efm003 (section 3.5.2). Significant increases in MICs occurred within 10 days of the initial inoculation for each isolate, which gradually increased until the termination of the experiment following approximately 80 days of exposure, at which point the final MIC was more than double that of the progenitor isolate (final MIC of 16 μg/mL). The capacity for *E. faecium* to readily develop increased resistance to BDM-I makes it an ideal candidate for whole genome sequencing analysis.

As such, BDM-I resistance mutants (in addition to the isogenic parents) were selected for sequencing from the day 10 and day 60 exposure time-points. In total, 3 colonies were selected for sequencing from each of the three replicate series, giving a total of nine data sets from each time point (not including the final day Efm003 mutants). Subsequently, variant analysis was performed comparing the *in vitro* derived resistance mutants to the Efm003 and Efm008 progenitor isolates. Interestingly, this revealed that the mutants analysed commonly had mutations within the coding region of ATP Synthase genes, as summarised in Tables 4.1 and 4.2.

Table 4.1 Mutations Identified within day 10 Efm008 BDM-I mutants

Series	Colony	Region	Gene	Mutation	AA Change	Product
1	1	2088169	*atpE*	INS	-	ATP synthase, F_0 complex, c-subunit
	2	2085214	*atpG*	INS	-	ATP synthase, F_1 complex, γ-subunit
	3	2083071	*atpD*	DEL	Ile456fs	ATP synthase, F_1 complex, β-subunit
2	1	2087896	*atpF*	DEL	-	ATP synthase, F_0 complex, b-subunit
	2	2083526	*atpD*	SNP	Tyr304*	ATP synthase, F_1 complex, β-subunit
	3	2087739	*atpF*	INS	-	ATP synthase, F_0 complex, b-subunit
3	1	2088230	*atpE*	INS	-	ATP synthase, F_0 complex, c-subunit
	2	2083847	*atpD*	SNP	Tyr107*	ATP synthase, F_1 complex, β-subunit
	3	2088813	*atpB*	INS	-	ATP synthase, c-subunit

Table 4.2 Common mutations identified within day 60 Efm003 and Efm008 BDM-I mutants

Isolate	Series[a]	Region	Gene(s)	Mutation	AA Change	Product
Efm003[b]	3	2088755	*atpB*	SNP	Thr111Lys	ATP synthase, c-subunit
Efm008	1	2083906	*atpD*	SNP	Gly178Cys	ATP synthase, F_1 complex, β-subunit
	2	2083213	*atpD*	SNP	Gln409Lys	ATP synthase, F_1 complex, β-subunit
	3	2082315-2086186	*atpD, atpA, atpC, atpG*	IS*1256*-mediated deletion	-	ATP synthase, F_1 complex, β-, α-, ε- and γ-subunits

[a]Mutant colonies within a series had the same *atp* gene mutation
[b]Conamination present within series 1 and 2

Mutations identified within the day 10 Efm008 mutants varied between the series and colonies sequenced, both in terms of the mutation type identified as well as the ATP Synthase gene affected. IS*1256*-like insertions in different genes, including *atpE*, *atpG*, *atpF* and *atpB*, were identified for 5 of the 9 mutant colonies. Additional deletions and single nucleotide polymorphisms (SNPs) were also identified in *atpD* and *atpF* for the remaining 4 colonies. Similar trends were observed for the day 60 Efm008 mutants, with the identification of SNPs (resulting in amino acid changes) within *atpD* for series 1 and 2 (Gly178Cys and Gln409Lys, respectively). In the case of series 3, an IS*1256*-like insertion caused the partial deletion of *atpA*, and the complete deletion of *atpC*, *atpD* and *atpG*, all of which encode for constitutive protein subunits of the ATP Synthase F_1 complex.

In the case of Efm003 (and similar to the above), SNPs were identified within the *atpB* gene for the series 3 day 60 mutants. However, there were no mutations identified within any ATP synthase genes for the day 10 mutants. Variant analysis did however identify SNPs for 6 of the 9 mutant colonies within the gene EFAU004_00165, which encodes for an M-protein Trans-acting positive regulator.

While mutations within the ATP synthase operon were present within the majority of the mutant Efm003 and Efm008 series mutants, additional mutations were identified in individual colonies or series as outlined in Supplementary Tables 1 to 4. In summary, mutations identified within Efm003 day 10 isolates mutants appear to affect genes functioning in nucleotide and protein synthesis, including *guaB* and EFAU004_00965, which encode for proteins involved in the metabolism of purine and pyrimidine

nucleotides, respectively. Interestingly, mutations present within Efm008, day 10 isolates are present almost exclusively within genes encoding for subunits of ATP synthase.

Variant analysis also identified a further 8 SNPs within the day 10 mutant series of Efm003. 2 SNPs are present within the gene *fur,* encoding for the Fur family of transcriptional regulators responsible for regulating the uptake of ferric iron and defence against reactive oxygen species (ROS). Additional SNPs were identified within the genes *relA* (guanosine pentaphosphate synthesis), *apt* (AMP synthesis), *ylov* (glycerol metabolism), EFAU004_01802 (branched chain amino acid synthesis) and EFAU004_02036 (phospholipid synthesis).

In addition to SNPs within *atpD*, additional mutations were identified within the day 60 Efm008 mutant isolates, several of which are present within 2 of the 3 series. Interestingly, SNPs were identified within the gene EFAU004_02425 encoding a PAS domain sensory box histidine kinase within series 1 and 3 (Asp49Tyr and Asp99Tyr respectively). EFAU004_02425 is homologous to similar histidine kinases such as *walK* and *vicK* which are essential for maintaining cell wall homeostasis in gram-positive bacteria (Dubrac et al., 2007). Similar to Efm003, SNPs were also identified within *relA* in series 1 and 2.

The majority of the mutations summarised in Supplementary Tables 1 to 4 are specific to a single series or colony, and therefore were considered less likely to be important to the observed increases in BDM-I MICs. Emphasis has been placed on mutations within the ATP synthase operon, as they have been identified in all mutant series except day 10

Efm003 mutants. However, further analysis of additional mutations may be required in the future.

4.3 Whole Genome Sequencing of MRSA BDM-I Mutants

As outlined in Chapter 3, the MRSA isolates (Sa057 and Sa375) struggled, at least in part, to develop increased resistance to BDM-I during the induction experiments, particularly Sa057 which showed no significant changes in MIC after 110 days of continuous exposure. Interestingly, the greatest increase in BDM-I MICs was observed for the Sa375 *in vitro* derived mutants, which increased by >2-fold from 2 to 5 μg/mL in all three replicate series following 60 days of exposure. Therefore, whole genome sequencing and variant analysis was initially completed using Sa375 BDM-I mutants and the progenitor Sa375 VISA isolate. Somewhat unexpectedly, common mutations (amongst the mutants) were identified within the *walK* gene, which encodes a sensor protein kinase. In this regards, SNPs resulting in amino acid changes were present in all three-mutant series within two domains of WalK, as illustrated in Figure 4.4; the extracellular PAS Domain (series 1 and 3) and the Histidine Kinase-like ATPase domain (series 2).

Figure 4.1 Structure of WalK showing protein domains and the position of mutations identified within Sa375 BDM-I mutants. Image adapted from Howden et al (Howden et al., 2011).

The *walK* gene encodes part of the essential WalKR two-component regulatory system which regulates a diverse range of cellular processes, with the most widely studied being cell wall homeostasis (see section 4.6.1). Several other mutations were also variously identified within genes that play a role in cell wall synthesis. These included SNPs within *murA* and *atl* (series 2), and *mvaA* (series 1), which encode for UDP-GlcNAc enolpyruvyl transferase (responsible for the synthesis of UDP-N-acetylmuramic acid during the first stage of peptidoglycan synthesis (Blake et al., 2009)), the bifunctional enzyme N-acetylmuramoyl-L-alanine amidase/endo-beta-N-acetylglucosaminidase (which is the major peptidoglycan hydrolase within *S. aureus* and is essential for maintaining cell wall turnover (Grilo et al., 2014)) and 3-hydroxy-3-methylglutaryl coenzyme A reductase (plays an indirect role in peptidoglycan synthesis through the production of a lipid carrier known as unedecaprenyl pyrophosphate, via the mevalonate pathway (Balibar et al., 2009)), respectively.

A significant number of SNPs (n=21) were identified within the Sa375 mutant series 2, compared to those of series 1 and 3, which only contained a total of 3 SNPs each (Supplementary Table 5). The pathways affected by these mutations were diverse, and included nucleotide synthesis (*rpbB* and *yukA*), nutrient transport (*potD*, SAA6008_00647, SAA6008_01966 and *nrgA*) and capsule synthesis (*Cap5A*). Considering these mutations are unique to series 2, they were considered unlikely to be important regarding the BDM-I MoA but may warrant further investigation in the future.

In contrast to the above, Sa057 struggled to develop increased resistance to BDM-I, however some colonies (n=4) from the final day mutants series displayed marginally higher BDM-I MICs of 1-2 μg/mL (one colony from series 1 and three colonies from series 3) following additional MIC testing. Sequencing and variant analysis of these colonies revealed several mutations as outlined in Table 4.3, including SNP mutations within SAA6008_00679, which encodes a putative phosphate uptake regulator, in all sequenced colonies. Series 1 and series 3, colony 1 mutants have an identical amino acid change at position 99 (Met99Ile), while colonies 2 and 3 from series 3 possess two amino acid changes at positions 166 (Ser166Arg) and 172 (Thr172Ser). SNP mutations were also identified within the genes *murC* and *fmtC,* which encode for UDP-N-acetylmuramic acid (peptidoglycan synthesis) and Phosphatidylglycerol lysltransferase (cell membrane synthesis), respectively (series 1 and colony 1 from series 3), Additional SNPs were identified within *rpoC*, *whiA* and SA6008_01663 (series 3, colonies 2 and 3), which function in RNA synthesis, cell division and amino acid transport and metabolism, respectively.

Table 4.3 Mutations identified within *in vitro* derived Sa057 BDM-I Mutants

Isolate	Gene	Mutation	AA Change	Product
1/1	SAA6008_00679	SNP	Met99Ile	Putative phosphate uptake regulator
	fmtC	SNP	Arg784Pro	Phosphatidylglycerol lysltransferase
	murC	SNP	Ser144Arg	UDP-N-acetylmuramate-L-alanine-ligase
3/1	SAA6008_00679	SNP	Met99Ile	Putative phosphate uptake regulator
	fmtC	SNP	Arg784Pro	Phosphatidylglycerol lysltransferase
	murC	SNP	Ser144Arg	UDP-N-acetylmuramate-L-alanine-ligase
3/2	SAA6008_00679	SNP	Ser166Arg	Putative phosphate uptake regulator
	SAA6008_00679	SNP	Thr172Ser	Putative phosphate uptake regulator
	rpoC	SNP	Leu984Ile	DNA directed RNA polymerase beta chain protein
	whiA	SNP	Asp214Tyr	Sporulation regulator
	SA6008_01663	SNP	Ser151Phe	Amino acid transport and metabolism
3/3	SAA6008_00679	SNP	Ser166Arg	Putative phosphate uptake regulator
	SAA6008_00679	SNP	Thr172Ser	Putative phosphate uptake regulator
	rpoC	SNP	Leu984Ile	DNA directed RNA polymerase beta chain protein
	whiA	SNP	Asp214Tyr	Sporulation regulator
	SA6008_01663	SNP	Ser151Phe	Amino acid transport and metabolism

4.4 Exploring the Relationship between BDM-I and ATP Synthase

4.4.1 Bacterial ATP Synthase

Adenosine triphosphate (ATP) is the universal 'energy currency' within all living organisms, ranging from prokaryotes to higher order eukaryotes. ATP is hydrolysed to form adenosine diphosphate (ADP) and an inorganic phosphate molecule (P_i), and can be utilized as an energy source for various endergonic metabolic processes (Weber, 2010). The primary mechanism by which ATP is synthesized, is during oxidative phosphorylation by the F_1F_0 – ATP synthase complex.

The F_0F_1 – ATP synthase is a membrane bound protein comprised of two segments; the membrane bound F_0 complex and the F_1 'rotor stalk' portion (Senior et al., 2002). Within these two segments are a total of eight subunits; three within the F_0 segment with a stoichiometry of $ab_2c_{10\text{-}15}$, and five within the F_1 segment with a stoichiometry of $a_3\beta_3\gamma\delta\varepsilon$ (Figure 4.2) (Deckers-Hebestreit and Altendorf, 1996). ATP synthase utilizes a unique rotary mechanism powered by electrochemical energy, which is produced by a proton gradient across the F_0 segment. Proton flow causes the rotation of the $\gamma\varepsilon c_{10\text{-}15}$ assembly, which in turn alters the catalytic sites within the β-subunits, to synthesize ATP from ADP and Pi. Alternatively, under certain conditions bacteria are capable of hydrolysing ATP, in order to generate a transmembrane proton gradient that is required for processes such as locomotion (Weber, 2010).

In recent years, ATP synthase has been studied as a potential antimicrobial target. The first antimicrobial shown to inhibit ATP synthase was a diarylquinoline compound which exhibited potent activity against the pathogen *Mycobacterium tuberculosis* (Andries et

al., 2005). More recently in 2012, Balemans et al identified several compounds that interacted with subunit c of ATP synthase, and these were shown to have bactericidal activity against *S. aureus* and *S. pneumoniae* (Balemans et al., 2012). These studies have elucidated ATP synthase as a potential target for novel antimicrobial compounds.

In this study, we have identified that ATP synthase is likely affected by BDM-I. In section 4.2, we identified that all mutant *E. faecium* isolates (with increased resistance to BDM-I) possess mutations within the ATP synthase operon, most commonly in the form of SNPs within the *atpD* gene. Based on these results, we hypothesized that BDM-I may be inhibiting ATP synthase either directly or indirectly. To explore this, we conducted ATP assays on BDM-I treated (MIC_{50}) *E. faecium* and *S. aureus* isolates, to identify potential changes in intracellular ATP concentrations.

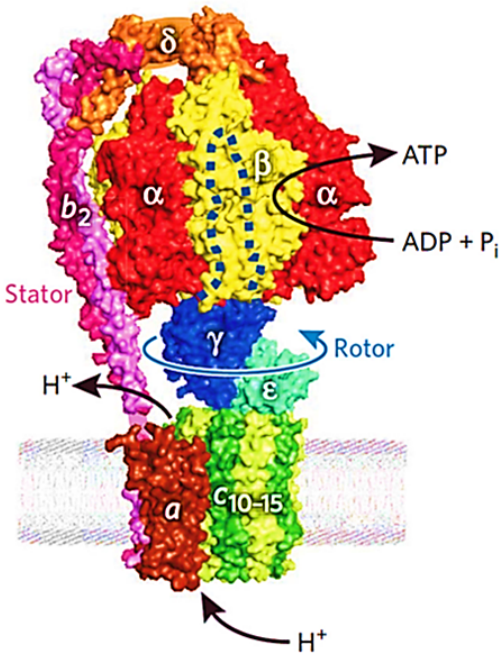

Figure 4.2 Structure of the bacterial ATP synthase machinery. Illustrated are the locations of each protein subunit within the F_0 (membrane bound) and F_1 segments (intracellular). Image obtained from Weber (Weber, 2010).

4.4.2 ATP Assays Utilized to Examine the Effect of BDM-I on ATP Synthase

ATP assays were performed using the Roche HS II ATP bioluminescence kit with Efm008 and Sa057 isolates, treated with sub-inhibitory BDM-I concentrations (MIC_{50}). Prior to performing the assay, standard curves were generated for each isolate comparing OD_{600} values and Cfu/mL, which enabled us to normalise intracellular ATP concentrations to a desired number of cells (10^5 Cfu). Cell cultures and ATP readings were prepared in triplicate for each isolate and treatment.

Following normalisation of wild type and treated isolates, we identified significant decreases in intracellular ATP concentrations within both Efm008 and Sa057. A 2-fold change in ATP concentration was observed following BDM-I treatment of Efm008; decreased from 2.00 nmols/10^5 Cfu to 1.03 nmols/10^5 Cfu, as shown in Figure 4.3. A significant decrease was also observed for Sa057; from 1.32 nmols/10^5 Cfu to 0.86 nmols/10^5 Cfu. In any case, this data suggests that BDM-I is likely inhibiting ATP synthesis, although it does not elucidate whether this is by direct or indirect inhibition of the ATP synthase enzyme. Interestingly, a previous study reported that BDM-I did not inhibit ATP synthesis within *B. cereus* and *S. aureus* (White et al., 2014). Differences in the results are likely due to the methodologies used, as the kits and growth conditions were dissimilar between each study. As such, this is the first observation of ATP synthesis inhibition due to BDM-I treatment.

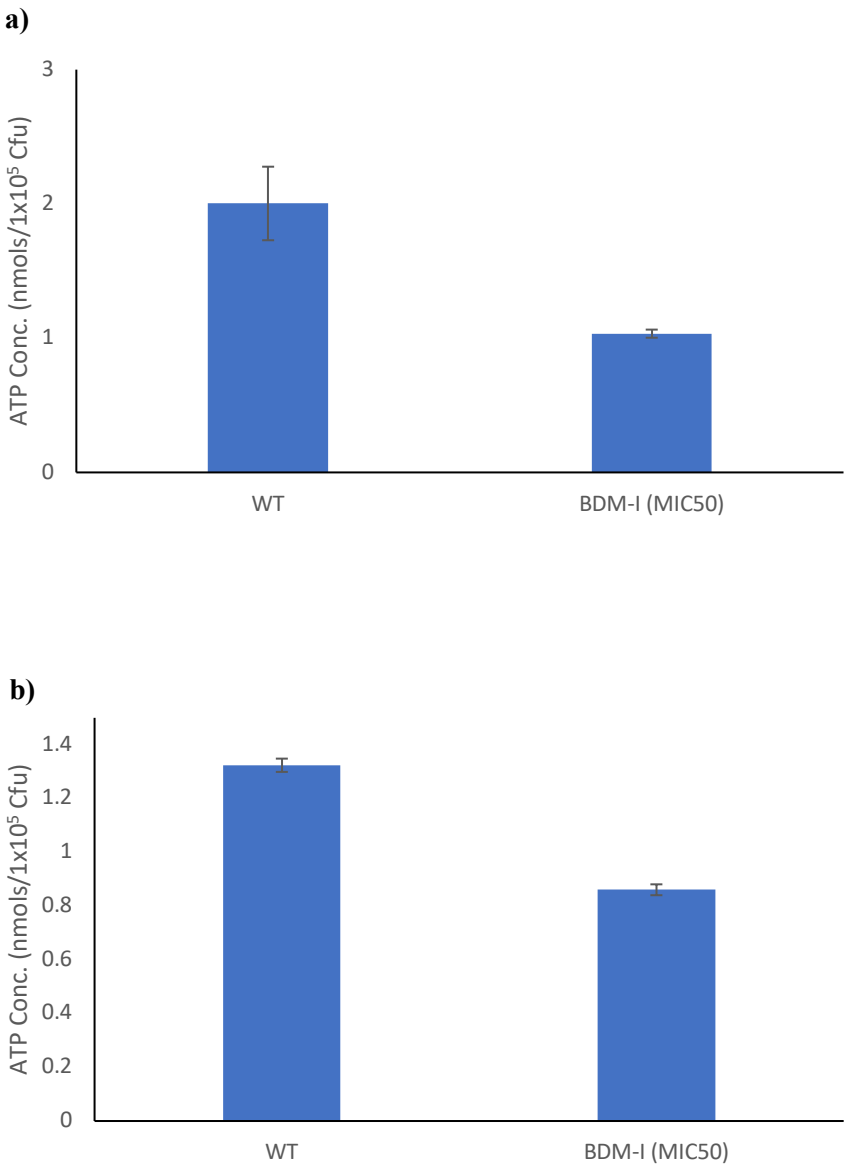

Figure 4.3 Reduced intracellular ATP concentrations observed within BDM-I treated VRE (a) and MRSA (b). Each isolate was treated with BDM-I (MIC50) and incubated for 2 h, prior to the intracellular ATP concentrations being quantified using the Roche HS II ATP bioluminescence kit. Unknown ATP concentrations were determined using a standard curve, and bacterial Cfu were determined based on the OD600 at the time of cell lysis using a standard curve. ATP concentrations (nmols) were then normalised to 105 Cfu. Analysis revealed a 2-fold decrease in intracellular ATP concentrations within Efm008 (a), as well as a significant reduction within Sa057 (b) from 1.32 nmols/105 Cfu to 0.86 nmols/105 Cfu. Each experiment was completed in triplicate.

4.4.3 Examining Synergism between BDM-I and Polymixin B

Cationic antimicrobial peptides (CAMPs) are amphipathic antimicrobials which interact with the cell membrane, causing the disruption of membrane integrity and cell death. The activity of CAMPs (such as polymyxin B) is generally limited to gram-negative bacteria, as gram-positive species such as *S. aureus* are intrinsically resistant (Vestergaard et al., 2017). In the context of *S. aureus*, intrinsic resistance is driven by the reduction of the cell surface charge by the incorporation of D-alanine on teichoic acids, or by the incorporation of L-lysine to membrane phosphatidylglycerols (Peschel et al., 2001, Peschel et al., 1999). Interestingly, Vestergaard et al identified that the inhibition of ATP synthase in *S. aureus* results in hyperpolarization of the membrane, and consequently increased sensitivity to polymyxin B (Vestergaard et al., 2017) .

Considering the observed effects of BDM-I on ATP synthase (sections 4.2 and 4.4.2), checkerboard assays were utilized to identify changes in polymyxin B sensitivity within Sa057, when used in combination with BDM-I. Interestingly, we observed a significant increase in the sensitivity of Sa057 to polymyxin B. When used in combination with BDM-I at MIC_{50} (2 μg/mL), the polymyxin B MIC decreased from 256 μg/mL to 64 μg/mL. The FICI calculated for this interaction (FICI = 0.75) indicates that BDM-I exerts an additive effect on polymyxin B, likely through the inhibition of ATP synthase activity and the hyperpolarization of the cell membrane.

4.5 Examining Phenotypic Changes within BDM-I VISA Mutants

4.5.1 Two-component Regulatory Systems in *S. aureus*

Two-component systems (TCS) are regulatory mechanisms employed by bacteria to sense and respond to an array of signal types. These systems are comprised of a membrane bound histidine kinase with an extracellular sensing loops capable of autophosphorylation, and a response regulator protein that functions as a transcriptional regulator (Dubrac et al., 2008). In recent years, several TCS have been identified in bacteria as being essential for cell viability. These include the CenKR TCS within *Caulobacter crescentus*, the MtrBA TCS within *Mycobacterium tuberculosis*, and the WalKR TCS, which is commonly found in firmicutes (Dubrac et al., 2008).

Vancomycin intermediate *Staphylococcus aureus* (VISA) are characterized by a higher vancomycin MIC within the range of 4-8 μg/mL (section 1.5). The genetic basis of vancomycin resistance within such strains has been linked to mutations within genes functioning in cell wall homeostasis, such as *walK* and *clpP* (Cui et al., 2003, Shoji et al., 2011). A previous study by van Hal et al, identified a missense mutation (Q369R) in WalK within the progenitor Sa375 isolate, which was likely driving the observed intermediate resistance to vancomycin (van Hal et al., 2013). VISA isolates possessing mutations within *walK* are often associated with thickened cell walls, which increase resistance to vancomycin by reducing cell wall permeability (Cui et al., 2003, Shoji et al., 2011).

As discussed in section 4.3, mutations were identified within the *walk* gene for all Sa375 mutant isolates. Further analysis revealed that each mutant also retained the previously

identified mutation within Sa375 (Q369R), which had been shown to produce a phenotype of thickened cell walls (van Hal et al., 2013). Based on the primary function of WalK in cell wall homeostasis, and the observed inverse relationship between BDM-I and vancomycin MICs, we hypothesized that the newly identified mutations within the mutant isolates may be compensatory and result in cell wall thinning. Furthermore, as the mutations within *walK* were consistently observed in all sequenced isolates, it is likely they are the primary driver of the observed increases in BDM-I MICs. Previous studies have shown that BDM-I does not affect the bacterial cell wall directly (White et al., 2014). However, based on our observations it was important to examine potential changes to the cell wall phenotype in our mutant isolates.

4.5.2 TEM Used to Identify Changes in Cell Wall Thickness

Transmission electron microscopy was used to examine the cell wall of Sa375 BDM-I mutants (1 colony from each of the 3 series), as well as the progenitor Sa375 isolate (VISA control) and Sa057 (VSSA control). The average cell wall thickness was determined by examining ten cells from each isolate and is displayed in Figure 4.4. As expected, Sa375 was found to have a significantly thicker cell walls compared to Sa057, which were measured at 30.1 nm (±2.42) and 21.8 nm (±2.14), respectively. This is consistent with previous studies that examined the effect of mutations within *walK* (Cui et al., 2003, Howden et al., 2011, Shoji et al., 2011, van Hal et al., 2013). Interestingly, a significant reduction in cell wall thickness was observed in all BDM-I mutants from 30.1 nm (Sa375 progenitor) to 18.93 nm (±0.72) for Sa375-L37F, 18.37 nm (±1.02) for Sa375-G560S, and 21.77 nm (±1.26) for Sa375-G30W.

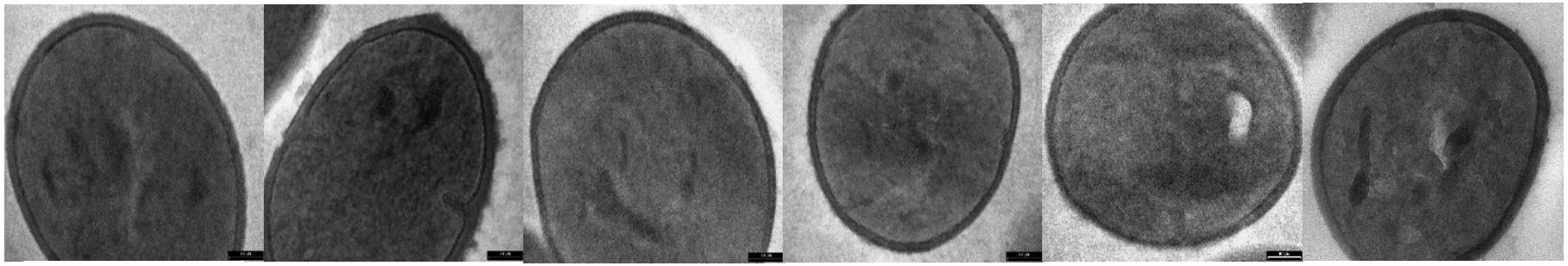

[a]Sa375 carries a previously identified *walK* mutation (Q369R) which is also present within each of the BDM-I mutant series
[b]Vancomycin
[c]Daptomycin

Figure 4.4 TEM images identifying changes in the cell wall phenotype within Sa057 (VSSA), Sa375 (progenitor VISA isolate), Sa375 BDM-I mutants and Sa375 with an introduced *walK* mutation (iG560S). Sa057 and Sa375 are derived from the same clinical series associated with chronic bacteraemia and the generation of vancomycin intermediate resistance. A mutation within *walK* (Q369R) is attributed to the thickened cell walls observed in the case of Sa375 (30.17 nm) compared to Sa057 (21.8 nm), as well as the increase in vancomycin resistance (4 µg/mL from 2 µg/mL respectively). TEM and MIC analysis of BDM-I mutants with novel *walK* mutations, revealed a significant decrease in cell wall thickness compared to Sa375 (18-21 nm) as well as increased susceptibility to vancomycin (4 µg/mL to 0.5-1 µg/mL) and daptomycin (4 µg/mL to 0.5-1 µg/mL). The novel mutation G560S was also introduced to the progenitor Sa375 strain (Sa375-iG560S) using allelic exchange, which was shown through TEM and MIC analysis to produce a phenotype with thinner walls (24.48 nm) and increased vancomycin susceptibility (1 µg/mL).

4.5.3 Changes in Vancomycin and Daptomycin Sensitivity in Sa375 Mutants

As stated previously, an increase in cell wall thickness is commonly associated with intermediate vancomycin resistance in *S. aureus*. In section 4.5.2, we observed a significant decrease in cell wall thickness for all mutant Sa375 isolates, identified to possess novel mutations within *walK*. Following this, we explored changes in vancomycin MICs for these mutants due changes in their cell wall phenotype. In this regard, additional BMD MIC tests were completed on isolates from section 4.5.2 using vancomycin and daptomycin as described previously.

MIC testing identified significant decreases in vancomycin MICs for all mutant isolates, in comparison to the progenitor Sa375. Mutant vancomycin MICs were determined to be 0.5 μg/mL for Sa375-L37F and Sa375-G560S, and 1 μg/mL for Sa375-G30W (Figure 4.4), placing each isolate within the susceptible range for vancomycin (≤2 μg/mL). This was greater than a two-fold decrease compared to the Sa375 progenitor isolate, with had vancomycin MIC of 4 μg/mL.

Cross resistance to the lipopeptide antibiotic daptomycin has previously been observed for VISA isolates that possess mutations within *walK* (Bayer et al., 2013, Chen et al., 2015, Howden et al., 2011). In a previous study, van Hal et al identified that the Sa375 progenitor isolate (Q369R) was daptomycin non-susceptible, which was likely due to the identified SNP within *walK* (van Hal et al., 2013). Further MIC testing was then completed for the mutant Sa375 isolates with daptomycin, which revealed a significant decrease in MIC from 4 μg/mL (Sa375) to 0.5 μg/mL for Sa375-L37F, and 1 μg/mL for Sa375-G560S and Sa375-G30W. Similarly, the reduction in MICs places these mutants within the susceptible range for daptomycin (≤1 μg/mL).

4.5.4 Gly560Ser Alters the Cell Wall Phenotype

In sections 4.5.2 and 4.5.3, we identified the phenotypic effects of *walK* mutations on cell wall thickness and vancomycin/daptomycin susceptibility, in Sa375 mutant isolates. Allelic exchange was then performed to introduce the mutation Gly560Ser from a series 2 mutant, into the progenitor isolate Sa375, in order to confirm its exclusive role in producing the aforementioned phenotype (i.e., decreased cell wall thickness and increased sensitivity to vancomycin and daptomycin).

Allelic exchange was successfully performed using the plasmid vector pIMAY-Z, which was used to clone a PCR fragment derived from Sa375-G560S (carrying the identified *walK* SNP) prior to transformation into Sa375. Subsequently, the cloned fragment was successfully incorporated into the genome of Sa375, producing the genetically modified strain Sa375-iG560S which was confirmed with Sanger sequencing. MIC tests were then performed on the derived mutant (Sa375-iG560S), which was found to have a significantly lower vancomycin MIC and higher BDM-I MIC of 1 μg/mL and 3-4 μg/mL, respectively; this is compared to the vancomycin and BDM-I MICs of Sa375, which are 4 μg/mL and 2 μg/mL respectively. Additionally, TEM was performed on Sa375-iG560S, and this revealed a significant decrease in cell wall thickness from 30.1 nm to 24.48 nm (Figure 4.4).

As such, based on the observed changes in MICs and cell wall thickness for Sa375-iG560S, and its phenotypic similarities to Sa375-G560S, it is highly likely that the identified compensatory mutations within *walK* (for the Sa375 mutants generated via the induction experiments) are solely driving increased resistance to BDM-I.

4.6 Discussion

With access to mutants with increased resistance to antimicrobials, as well as their progenitor isolates, whole genome sequencing can be utilised to identify mutations that are likely relevant to a drugs MoA. In the context of BDM-I, previous studies have failed to produce mutant isolates with increased resistance (Denisenko et al., 2010, White et al., 2014). However, in Chapter 3 we described the generation of mutant VRE and MRSA isolates with increased BDM-I resistance (>2x MIC) following prolonged exposure to the compound. Derived VRE and MRSA mutant isolates were then subjected to whole genome sequencing in order to identify mutations that may be driving increased resistance to BDM-I. Mutations were considered significant in relation to the BDM-I MoA if they were identified in all (or the majority) of the sequenced mutant isolates from each series. In this regard, analysis of the sequencing data revealed two cellular processes that were affected by prolonged BDM-I exposure, namely ATP synthesis within VRE and peptidoglycan synthesis within MRSA.

Sequencing analysis of Efm003 and Efm008 mutants revealed that mutations within the ATP synthase operon were common. Interestingly, the types of mutations identified as well as their locations within the operon varied considerably between colonies, series and isolates. In the case of Efm003, a SNP was identified within *atpB* for all three series, while SNPs were identified within *atpD* for series 1 and 2 of Efm008, as well as a large IS-mediated deletion of several genes for series 3. Furthermore, mutations were identified within 5 *atp* genes for the day 10 Efm008 mutant series. Considering the unpredictability regarding where mutations are present (within the ATP synthase operon), as well as the fact that mutant isolates remain susceptible to increased BDM-I concentrations, it is

unlikely that ATP synthase is the direct target of BDM-I. Instead, it is likely that altering the activity of ATP synthase may be a compensatory mechanism by which VRE can adapt to BDM-I exposure. To explore the effect that BDM-I has on the activity of ATP synthase, ATP assays were performed to assess intracellular ATP levels within both VRE (Efm0008) and MRSA (Sa057) isolates when treated with BDM-I. Interestingly, results from these assays revealed that such treatment (with BDM-I MIC_{50}) significantly reduced intracellular ATP concentrations in both isolates (section 4.4.2). While ATP synthesis appears to be inhibited by BDM-I within MRSA, no mutations were identified within the ATP synthase operon for any of the MRSA mutant isolates. As such, the inability to knockout ATP synthase in response to BDM-I exposure may support previous observations that is essential for MRSA growth, at least under the conditions tested (Balemans et al., 2012).

Additional evidence for the inhibition of ATP synthesis was gathered via checkerboard assays combining BDM-I and polymyxin B (section 4.4.3). As discussed in section 4.4.3, these assays examined changes in Sa057 sensitivity to polymyxin B (CAMP) when used in combination with BDM-I. Results from these studies identified a reduction in the intrinsic resistance to CAMPs typically associated with *S. aureus*. The significance of this outcome relates to observations that inhibiting ATP synthase in *S. aureus* alters the membrane potential, which increases the susceptibility of *S. aureus* to CAMPs (Vestergaard et al., 2017).

Therefore, these results in combination strongly indicate that BDM-I treatment affects ATP synthase activity, and thus the availability of intracellular ATP. However, sequencing analysis of MRSA mutant isolates revealed that they could not circumvent

decreased levels of intracellular ATP in the same way (i.e., by knocking out ATP synthase), and adapt differently. In this regard, peptidoglycan synthesis was shown to be negatively affected by BDM-I exposure, as mutations were identified within genes that regulate cell wall maintenance. Specifically, SNPs were identified within the *walK* gene for all Sa375 mutant isolates, while for the Sa057 mutant isolates mutations were identified in several genes that function both directly (*murA* and *atlA*) and indirectly (*mvaA*) in cell wall synthesis.

As discussed in section 4.5, *walK* is part of the walKR TCS, which often plays a role in the vancomycin and daptomycin resistance displayed by hVISA/VISA isolates. This resistance is commonly driven by SNPs within *walK* that result in a thickened cell wall phenotype, as observed for Sa375 (section 4.5.2). By conducting TEM analysis of Sa375 BDM-I mutants, we revealed that the identified *walK* mutations produce a phenotype that is similar to that of VSSA isolates (i.e., thinner cell walls). Additional MIC studies also revealed that these mutant isolates were susceptible to both vancomycin and daptomycin, as a result of the cell wall thinning. As such, it appears that in the case of the VISA isolate (Sa375), it has reverted to a VSSA phenotype (by acquiring compensatory mutations in *walK*) as an adaptive response to BDM-I exposure. Thus, this implies that the VSSA phenotype is less susceptible to BDM-I, which again coincides with the observed vancomycin/BDM-I inverse relationship (see section 3.4).

In summary, the data generated in this chapter provides further insight into the BDM-I MoA. By examining the genotype and phenotype of mutant isolates with increased resistance to BDM-I, we have identified that the compound likely inhibits ATP synthesis via the oxidative phosphorylation pathway (i.e., by affecting ATP synthase). The

observed reduction in intracellular ATP levels would limit the availability of free ATP for various cellular processes and thus favour cell phenotypes that utilize less ATP. This is most evident in the case of Sa375 mutants reverting to a VSSA phenotype (upon BDM-I exposure), which is likely due to the significant amount of energy required to synthesize and maintain a thickened cell wall (Jarick et al., 2018).

Chapter 5

Proteomic Analysis of BDM-I Treated Isolates

5.1 Introduction

Whole genome sequencing was previously utilized to identify mutations that contributed to increased BDM-I resistance (see Chapter 4). As discussed, the data generated strongly indicated that BDM-I negatively affects the functionality of ATP synthase. However, such an approach does not reveal how cells more broadly adapt (to BDM-I exposure) at a protein expression level, which would provide a greater understanding of the cellular pathways affected and the overall MoA.

To investigate this proteomic studies were carried out using Efm008 and Sa057 treated with BDM-I (MIC_{50}), as well as the Efm008 deletion mutant $Efm008_{\Delta atpACDG}$ (Chapter 4, section 4.2). In this regard, two different methodological approaches were utilized, and these were 2-Dimensional Gel Electrophoresis (2-DGE) and shotgun proteomics. 2-DGE was initially used for first pass analysis of protein changes in collaboration with the proteomics research group from the Western Sydney University School of Medicine. In this initial study we analysed both membrane and soluble proteins that displayed greater than a 90% change when cells were treated with BDM-I. In this regard, following separation by 2-DGE, proteins with such an expression change were identified (using mass spectrometry) based on changes in protein spot intensity as identified using Delta2D software. This approach was initially performed using BDM-I treated Efm008, as well as the $Efm008_{\Delta atpACDG}$ deletion mutant (see section 4.2).

Due to the limitations associated with 2-DGE proteomics, a shotgun approach was then adopted in collaboration with the Stuart Cordwell laboratory at the University of Sydney School of Life and Environmental Sciences. Subsequently, by utilizing shotgun proteomics, an in-depth dataset was generated that provided insight into the cellular response of BDM-I treated MRSA and VRE. Specifically, common pathways and proteins for both bacterial species were identified that are differentially regulated due to BDM-I exposure, and these results were then be compared to whole genome sequencing data (Chapter 4) in order to gain further insight into the BDM-I MoA.

5.2 2-D Gel Proteomics of BDM-I Treated Efm008 and Efm008$_{\Delta atpACDG}$

Proteome analysis of BDM-I treated Efm008 and the mutant isolate Efm008$_{\Delta atpACDG}$ was initially performed using 2-DGE. This methodology relies on gel-based protein separation according to a proteins isoelectric point (first dimension) and molecular weight (second dimension). Each isolate was grown to mid-exponential phase in the presence (Efm008) or absence (Efm008$_{\Delta atpACDG}$) of BDM-I, before the cells were harvested, and the protein was extracted for proteomic analysis. Separated proteins were analysed using the Delta2D software to detect protein spots with visible changes in intensity. Subsequently, spots of interest (i.e., those displaying greater than 90% change) were then identified using mass spectrometry.

In this regard, several proteins were identified with altered expression, as shown in Figure 5.1 (soluble fraction) and Figure 5.2 (membrane fraction). Spots that are circled green and red indicate those which are present or absent, respectively, in comparison to the WT

Efm0008 isolate. In total, 17 soluble and 11 membrane bound proteins spots were identified with mass spectrometry and are summarised in Tables 5.1 and 5.2, respectively.

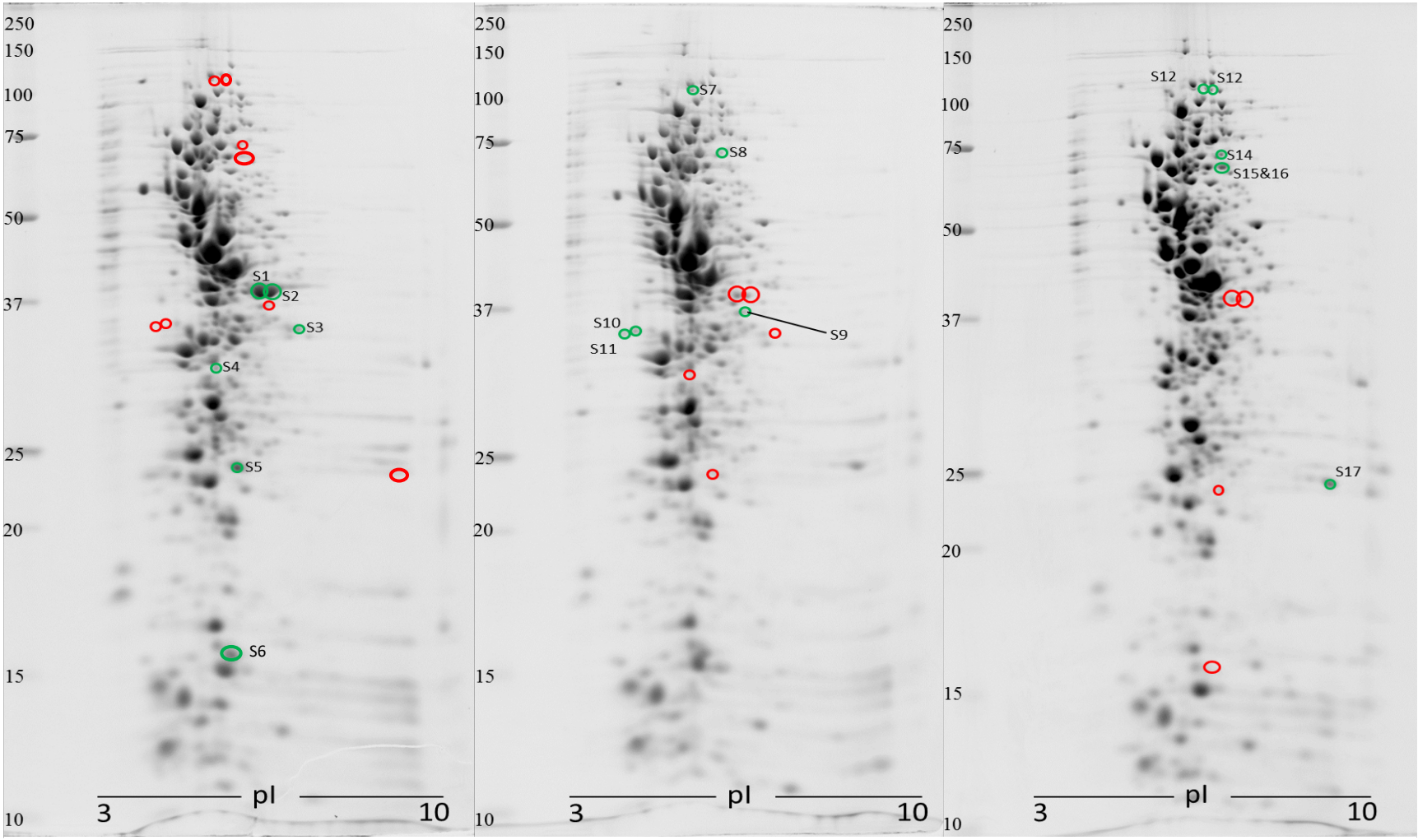

Figure 5.1 2-DGE of soluble protein fractions from Efm008 (left), Efm008$_{\Delta atpACDG}$ (middle) and BDM-I treated Efm008 (MIC$_{50}$) (right).

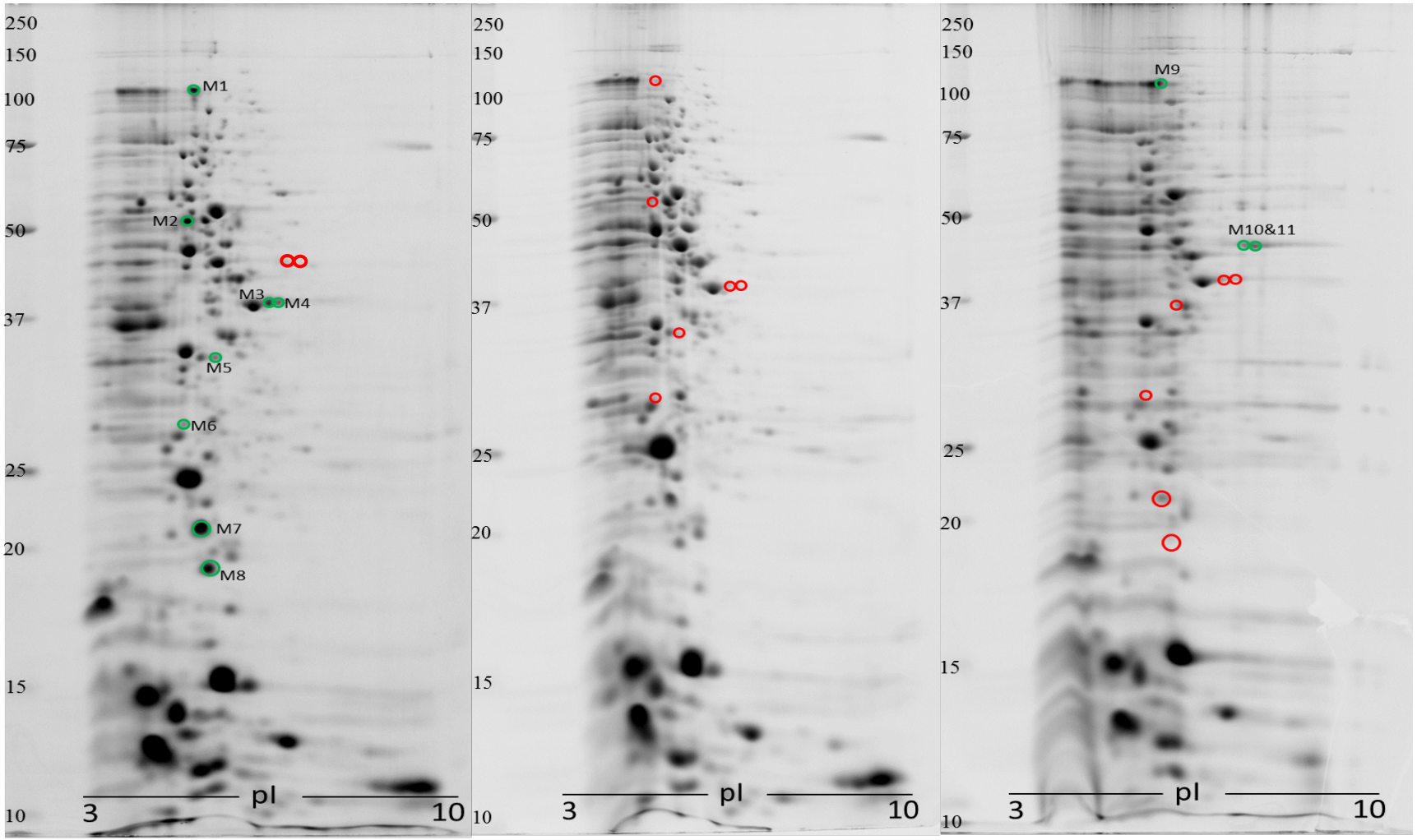

Figure 5.2 2-DGE of membrane protein fractions from Efm008 (left), Efm008$_{\Delta atpACDG}$ (middle) and BDM-I treated Efm008 (MIC$_{50}$) (right).

Table 5.1 Identification of differentially expressed soluble proteins within Efm008$_{\Delta atpACDG}$ and BDM-I Treated (MIC$_{50}$) Efm008

Protein Band No.	Protein ID	Protein Name	Score	MW (kDa)	pI	Expression[a]	
						MIC$_{50}$	$\Delta_{atpACDG}$
S1	VANA_ENTFC	Vancomycin/teicoplainin A-type resistance protein	3566	37.4	5.8	↓	↓
S2	VANA_ENTFC	Vancomycin/teicoplainin A-type resistance protein	3680	37.3	5.2	↓	↓
S3	VANH_ENTFC	D-specific alpha-keto acid dehydrogenase	2263	35.7	6.2	↓	↓
S4	RL2_ENTFA	50S ribosomal subunit	335	30.2	-	=	↓
S5	VANX_ENTFC	D-alanyl-D-alanine dipeptidase	3371	23.3	5.58	↓	↓
S6	PTHP_LACSK	Phosphocarrier protein	146	9.4	4.9	↓	=
S7	L2IW34	Valine tRNA ligase	1847	101.7	4.9	↑	=
S8	D0AG92	Asparagine synthetase	1310	72.8	5.4	↑	↑
S9	AROB_ENTFA	3-dehydroquinate synthase	148	38.9	5.3	=	↑
	KOZN21	3-dehydroquinate synthase	1095	38.4	5.8		
	KOZ2V5	Tryptophanyl-tRNA synthetase II	434	37.2	5.7		
	K0Z3U9	Fructosamine deglycase	321	38.1	5.6		
	K0YZ15	Polyprenyl synthetase	189	37.0	5.9		
	D0AGA2	Ferredoxin-NADP reductase	147	36.5	5.7		
S10	L2MZX4	LPXTG-domain containing protein cell wall anchor domain	1577	53.1	4.7	=	↑
	R2WNK2	Fimbrial isopeptide formation D2 domain-containing protein	1415	53.0	4.8		
S11	K0Z0H4	Pyruvate dehydrogenase complex, E1 component, beta subunit	143	35.4	4.6	=	↑
S12	SYV_ENTFA	Valine tRNA ligase	642	101.5	4.8	↑	=
	MUTS_ENTFA	DNA mismatch repair protein	489	96.8	5.0		

Table 5.1 *continued*

Protein Band No.	Protein ID	Protein Name	Score	MW (kDa)	pI	Expression[a]	
						MIC_{50}	$\Delta_{atpACDG}$
S13	L2IW34	Valine tRNA ligase	607	101.6	4.9	↑	=
	I3U2E8	DNA polymerase	197	100.4	5.3		
	C9AHE3	DNA mismatch repair protein	161	99.5	5.2		
	K0ZBX1	Sigma-54 factor interaction domain-containing protein	102	102.6	5.2		
S14	D0AG92	Asparagine synthetase	1705	72.8	5.4	↑	=
S15&16	K0Z3Y4	Coenzyme A disulfide reductase	4203	60.3	5.5	↑	=
	K0Z3H2	Glucan 1,6-alpha gucosidase	239	63.0	5.3	↑	=
	K0ZR27	Phosphoenolpyruvate-protein phosphotransferase	226	63.2	4.8	↑	=
	R2CRN4	Uncharacterized protein	206	65.0	5.4	↑	=
	D0AE22	Proline tRNA ligase	145	64.4	5.0	↑	=
	K1A8R9	Phosphoglucomutase/mannomutase family protein	142	63.8	5.0	↑	=
S17	K0ZS04	3-ketoacyl-(Acyl carrier protein) reductase	2102	26.1	7.7	↑	=
	C9APL7	3-oxoacyl-(Acyl carrier protein) reductase	966	26.1	7.7	↑	=
	L2HFL0	CBS protein	627	24.2	8.3	↑	=

[a] ↑ signifies upregulated, ↓ signifies downregulated, = signifies no change

Table 5.2 Identification of Differentially Expressed Membrane Bound Proteins within Efm008$_{\Delta atpACDG}$ and BDM-I Treated (MIC_{50}) Efm008

Protein Band No.	Protein ID	Protein Name	Score	MW (kDa)	pI	Expression	
						MIC_{50}	$\Delta_{atpACDG}$
M1	L2IZM7	Dihydrolipoamide S-succinyltransferase	2545	45.9	5.3	↑	↓
	C8NEA0	Dihydrolipoyllysine-residue acetyltransferase	351	55.6	4.9		
M2	ATPB_ENTHA	ATP synthase subunit beta	3675	50.9	4.7	=	↓
M3	VANA_ENTFC	Vancomycin/teicoplanin A-type resistance protein	3121	37.4	5.8	↓	↓
M4	VANA_ENTFC	Vancomycin/teicoplanin A-type resistance protein	2371	37.4	5.8	↓	↓
M5	RS2_ENTFA	30S ribosomal protein	1383	29.4	5.0	=	↓
M6	C9CAX1	50s ribosomal protein	1301	21.9	4.6	↓	↓
M7	CLPP_ENTFA	ATP dependent Clp protease proteolytic subunit	167	21.6	4.7	↓	=
		ATP synthase subunit delta	107	20.6	5.5		
M8	K0Z016	Uncharacterized protein	593	12.8	4.9	↓	=
M9	L2IZM7	Dihydrolipoamide S-succinyltransferase	2767	45.9	5.3	↑	=
	K0Z094	fusA Elongation factor G	297	76.7	4.8	↑	=
	L2S531	Penicillin-binding protein transpeptidase	170	73.7	4.9	↑	=
M10	MSMK_STRMU	Multiple sugar-binding transport ATP-binding protein	203	41.9	5.9	↑	=
	D0AGE3	ABC transporter	2022	41.1	6.2	↑	=
M11	C2E3E2	Glycerol-3-phosphate-transporting ATPase	144	41.3	5.8	↑	=

Of the 17 soluble protein spots selected for analysis, four (SP1, SP2, SP3 and SP5) were identified as being encoded by the *vanHAX* operon, which functions in facilitating high-level vancomycin resistance. These four spots were heavily down-regulated in both the BDM-I treated and mutant isolates. Two membrane spots (M3 and M4) were also identified as one of these proteins (in both isolates) and were similarly down-regulated. The downregulation of the *vanHAX* operon is likely due to the lack of selective pressures (imposed by exposure to glycopeptides) and reduced availability of ATP.

In accordance with the whole genome sequencing data generated for the VRE mutants described in section 4.2, subunits of ATP synthase were downregulated in the mutant and drug treated isolates. Interestingly, several proteins are upregulated that function in the metabolism of substrates essential for ATP synthesis via the glycolytic pathway. The E1 component of the pyruvate dehydrogenase complex (S11) was upregulated within the deletion mutant and catalyses the conversion of pyruvate to Acetyl-CoA. Furthermore, coenzyme A disulphide reductase (S15 and 16), asparagine synthetase (S8 and 14) and Dihydrolipoamide S-succinyltransferase (M1) were upregulated within the BDM-I treated isolate. Respectively, these proteins are involved in the production of coenzyme A, oxaloacetate (via asparagine) and succinyl-CoA which are all utilized in the TCA cycle.

Several transport proteins were also upregulated within BDM-I treated Efm008, including MsmK, an ABC transporter (M10) and a Glycerol-3-phosphate-transporting-ATPase (M11). Additionally, both the 30S (M5) and 50S (M6) ribosomal proteins were downregulated within Efm008$_{\Delta apACDG}$, possibly indicating a disruption in transcription as a result of decreased ATP levels.

5.3 Shotgun Proteomics Identifies Several Key Pathways Affected by BDM-I Treatment

Due to the limitations associated with 2-DGE proteomics, such as poor resolution and the limited amount of data that can be obtained, additional studies were conducted on the proteomes of MRSA (Sa057) and VRE (Efm008) isolates treated with BDM-I (MIC_{50}). Each isolate was grown to mid-exponential phase in the presence of BDM-I before being harvested and utilized for whole proteome analysis using liquid chromatography-mass spectrometry (LC/MS) of enriched peptides.

Analysis of the proteome data was completed in collaboration with Stuart Cordwell and William Klare at the Charles Perkins Centre, University of Sydney. In short, total proteome data was identified and quantified using MaxQuant (ver 1.6.0.16) software and the Uniprot *Staphylococcus aureus* strain JKD6008 (4/2/17, 2652 proteins) and the Uniprot *Enterococcus faecium* strain Aus0004 (4/2/17, 2826 proteins) with the default settings of 20 and 4.5 ppm for first and main search precursor tolerance, respectively. Peptides were identified using the LFQ algorithm for normalisation allowing for two missed tryptic cleavages, while Oxidation of methionine, protein N-terminal acetylation and carbamidomethylation of cysteine were set as variable modifications. The quantify option was enabled with a minimum of two unique razor peptides used for protein quantification. The peptide spectral match and false discovery rate (FDR) were set to 1% when all searches were made.

Proteins were selected for analysis if ≥2 peptides were successfully mapped, while proteins that occurred in only a single replicate were discarded. Missing values for the remaining proteins were imputed from a normal distribution using Perseus (ver 1.6.07).

Multiple t-tests were performed on log_2 transformed LFQ intensities, with a FDR cut-off of p_{adj} <0.05, with a log_2 difference of ≥ 2-fold being considered differentially expressed between groups for statistically significant results.

A total of 1589 proteins were identified with >2 peptides mapping to the *S. aureus* strain JKD6008. Of these, 1070 were identified in ≥2 replicates within both samples, while 287 proteins were significantly different (p_{adj} <0.05) between the WT and treated isolates. In total, 30 proteins met the log_2 fold change cut-off as shown in Figure 5.3 (a). In the case of Efm0008, 1459 proteins were identified with >2 peptides mapping to the *E. faecium* strain Aus0004. 1068 of these proteins were present in ≥2 replicates, while 190 were significantly different (p_{adj} <0.05) between WT and treated isolates, with 12 proteins meeting the final log_2 fold cut-off of ≥2 (Figure 5.3 (b)).

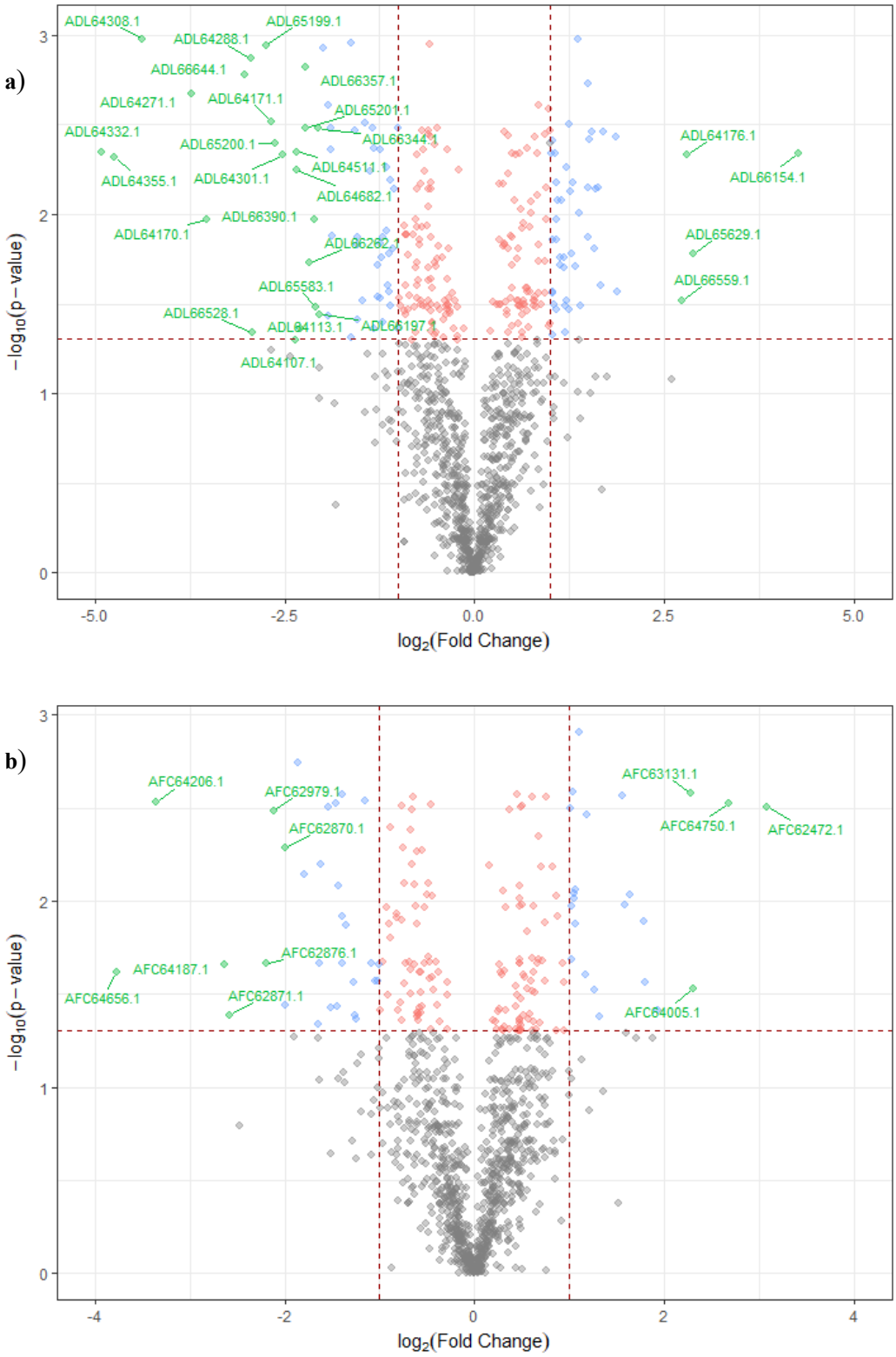

Figure 5.3 Volcano Plots identifying the number of proteins differentially expressed within Sa057 (a) and Efm008 (b) following exposure to BDM-I. Data points labelled blue indicate proteins with a ≥±1-fold change, while green data points indicate proteins with a ≥±2-fold change. Fold change is relative to the untreated isolates.

Proteins that met the log_2 fold change cut-off of ≥2 were identified and are shown in Supplementary Tables 6 to 9, including the fold change relative to untreated cells. Interestingly (and importantly), several proteins were differentially regulated in both Sa057 and Efm008 and these are summarised in Table 5.3.

Table 5.3 Proteins Differentially Regulated in both Sa057 and Efm008 following BDM-I Treatment

Protein	Gene	Log_2 Fold Change	
		Efm008	Sa057
Uracil-DNA glycosylase	*ung*	+2.06	+2.46
Nitroredutase family proteins	-	+6.58	+4.14
6-phospho-beta-galactosidase	*lacG*	-17.69	-13.62
Primosomal protein N'	*priA*	-11.32	-2.01
Zinc-containing alcohol dehydrogenase	-	-3.8	-6.47
Aspartate carbamoyltransferase	*pyrB*	-3.4	-5.34
Carbamoyl-phosphate synthase	*pyrA*	-2.68	-4.96
ATP Synthase F1, gamma subunit	*atpG*	-2.42	-2.13
Dihydroxyacetone kinase, phosphotransfer subunit	-	-2.12	-2.07
Phosphomevalonate kinase	*mvaK2*	-2.12	-2.62
Acetyltransferase, GNAT family	-	-2.09	-2.25
Orotate phosphoribosyltransferase	*pyrE*	-2.04	-3.6
ABC transporter ATP binding protein	-	-2.02	-3.86

The most significant change observed in both isolates was in the expression of 6-phospho-galactosidase, which was downregulated in Efm008 by 17.69-fold, and in Sa057 by 13.61-fold. Of note, this protein is involved in the multi-step conversion of lactose to D-tagatose-6P. Several glycosyl transferases were also downregulated in both isolates, including glycosyl transferase family 1 by 32.09-fold in Sa057, and glycosyl transferase family 8 by 18.35-fold in Efm008 (Supplementary Tables 6 and 8).

Interestingly, phosphomevalonate kinase (*mvaK2*), which is indirectly involved in peptidoglycan synthesis (via the mevalonate pathway) was downregulated in Sa057 and Efm008 by 2.62-fold and 2.12-fold respectively. Furthermore, analysis revealed the

downregulation of WalK (see section 4.5) by 9.21-fold in Sa057, as well as several other upregulated proteins involved in peptidoglycan hydrolysis including; a transglycosylase (*sceD*) in Sa057 by 34.05-fold, and a LysM containing protein in Efm008 by 7.45-fold.

Several pathways were also found to be differentially regulated following BDM-I treatment. Analysis revealed that all proteins involved in *de novo* Uridine Monophosphate (UMP) biosynthesis were downregulated in Sa057 following drug treatment. In total, 7 proteins are involved in the step-wise production of UMP from carbamoyl phosphate (Figure 5.4a). All 7 proteins were downregulated by ≥2.5-fold within Sa057, as well as several in Efm008; including aspartate carbamoyltransferase (*pyrB*), carbamoyl-phosphate synthase (*pyrAB*) and orotate phosoribosyltransferase (*pyrF*), by 3.4-fold, 2.68-fold and 2.04-fold respectively (Figure 5.4b).

a)

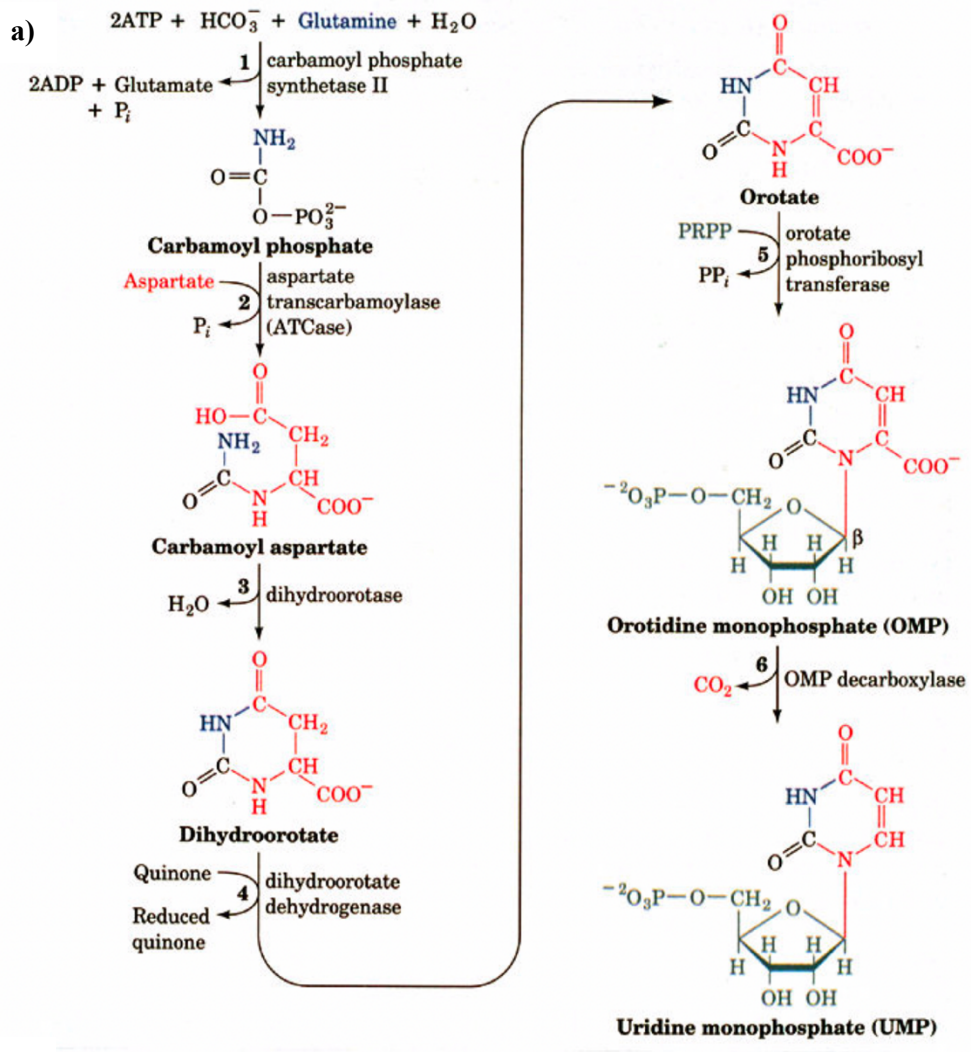

b)

Product	Gene	Log$_2$ Fold Change[a]	
		Sa057	Efm008
Dihydroorotate dehydrogenase	*pyrD*	-6.85	-
Dihydroorotase	*pyrC*	-5.69	-
Aspartate carbamoyltransferase	*pyrB*	-5.33	-3.4
Carbamoyl phosphate synthase (small chain)	*pyrAA*	-4.96	-
Carbamoyl phosphate synthase (large chain)	*pyrAB*	-4.44	-2.68
Orotate phosphoribosyltransferase	*pyrE*	-3.59	-2.04
Orotidine 5'-phosphate decarboxylase	*pyrF*	-2.81	-

[a]Indicates no change in expression following BDM-I treatment compared to WT.

Figure 5.4 UMP Biosynthesis Pathway (a) and associated proteins downregulated in BDM-I treated Sa057 and Efm008 (b). Interestingly, all proteins within this pathway were downregulated in Sa057, while three were also downregulated in Efm008.

Interestingly, proteins involved in pyruvate metabolism also exhibited altered expression, including L-lactate oxidase (converts L-lactate to acetate) and Phosphoenolpyruvate carboxykinase (converts phosphoenolpyruvate to oxaloacetate), which were downregulated by 13.76-fold and 3.04-fold, respectively within Efm008. Furthermore, L-lactate dehydrogenase (converts pyruvate to L-lactate in a reversible reaction) was upregulated by 2.8-fold within Efm008, as well as a Class II Aldolase and Adducin N-terminal domain protein (upregulated 30.54-fold), which likely functions in the synthesis of L-lactaldehyde. Interestingly, L-lactaldehyde is an important precursor for the synthesis of L-lactate, possibly indicating that Efm008 is favouring the production of pyruvate/L-lactate following drug treatment. Furthermore, the bifunctional acetylaldehyde CoA dehydrogenase (converts Acetyl-CoA to acetaldehyde) enzyme and formate C-acetyltransferase (converts Acetyl-CoA to CoA and pyruvate using formate) were downregulated in Sa057 by 60.93-fold and 10.53-fold, respectively. Interestingly, acetyl-coenzyme A synthase (converts acetyladenylate to acetyl-CoA) was upregulated by 2.19-fold, suggesting that Sa057 may be responding to drug treatment by increasing the production of acetyl-CoA. Interestingly, both pyruvate and acetyl-CoA are essential substrates of the TCA cycle.

Furthermore, several proteins were identified which showed drastically altered expression profiles, in some cases showing >10-fold changes in expression compared to the WT isolates. With regard to Sa057, threonine dehydratase (responsible for the synthesis of 2-ketobutyrate from L-threonine) was significantly downregulated by 78.33-fold, as well as a respiratory nitrate reductase which was downregulated by 52.97-fold. Additionally, the osmotically inducible protein OsmC was upregulated by 13.16-fold. Interestingly, OsmC is a homologue to hydroperoxide peroxidase and is known to play a role in

alleviating oxidative stress. Respective to Efm008, a SIS domain containing protein was downregulated 26.65-fold, as well as a mannose/fructose/sorbose-specific IIB component of the phosphotransferase system, which was downregulated 10.45-fold. Interestingly, it is likely that both of these proteins function in sugar metabolism. Additionally, a D-alanyl-D-alanine dipeptidase (VanX) was downregulated by 7.54-fold, which corresponds to previous proteomic work as described in section 5.2.

STRINGdb analysis was also used to identify protein clusters which were downregulated or upregulated following BDM-I exposure. Regarding Sa057, major clusters which were downregulated include those associated with virulence factors (EssA, ExsAB), metabolism (Ldh1, Ldh2, LdhD) and nucleotide metabolism (Tgt, UvrB, RlmN), as shown in Figure 5.5. Clusters which were upregulated include proteins associated with the stress response, iron acquisition, urease biosynthesis and capsule biosynthesis (Figure 5.6). STRINGdb analysis of Efm008 identified two primary protein clusters downregulated following exposure to BDM-I, including proteins associated with phosphoenolpyruvate-dependent sugar phosphotransferase activity and ATPase activity (Figure 5.7a). Protein clusters which were upregulated include those associated with nitroreductase activity and cell redox homeostasis (Figure 5.7b).

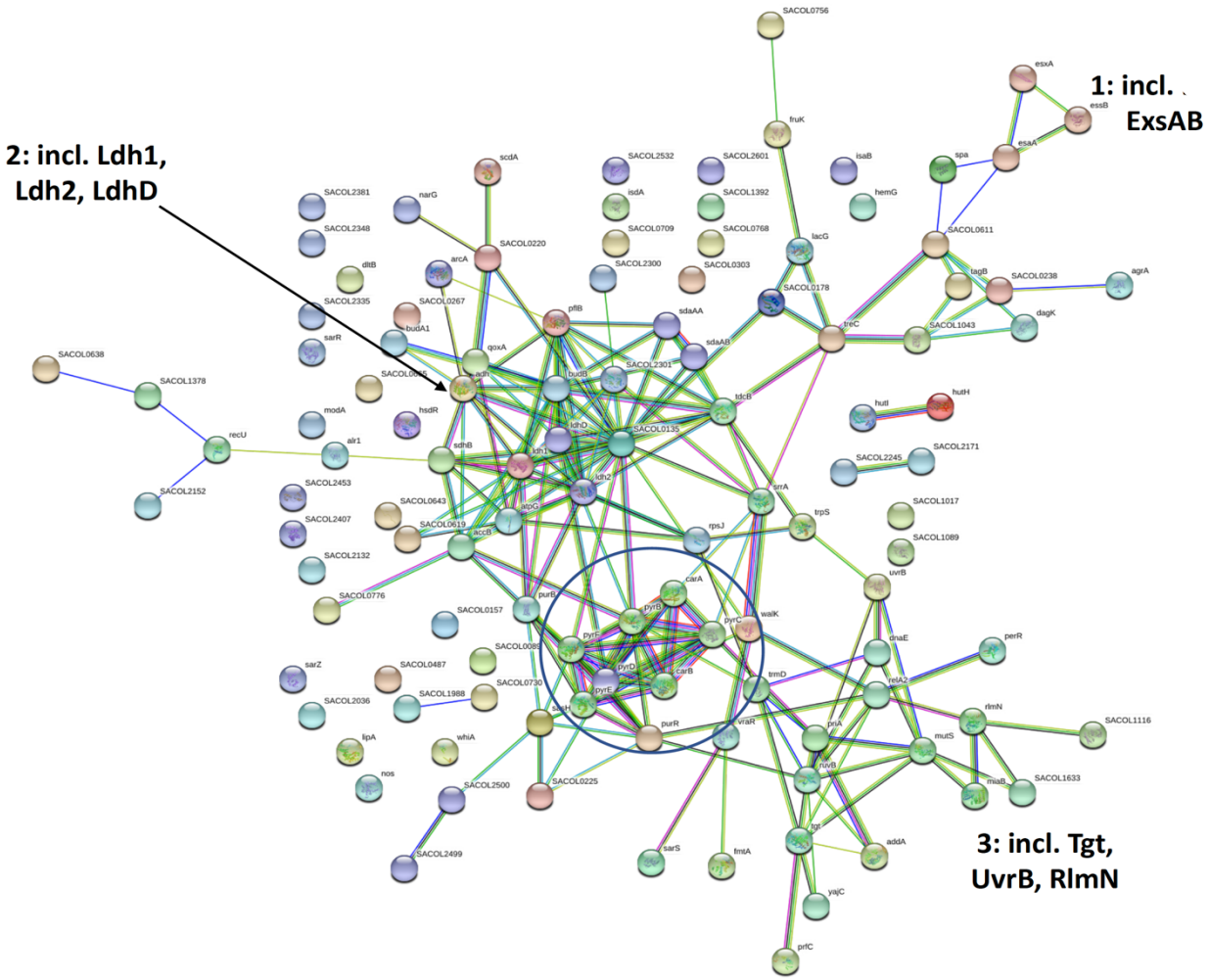

Figure 5.5: STRINGdb analysis identifying protein clusters downregulated in BDM-I treated Sa057. Highlighted clusters include proteins associated with virulence (1), metabolism (2) and nucleotide metabolism (3).

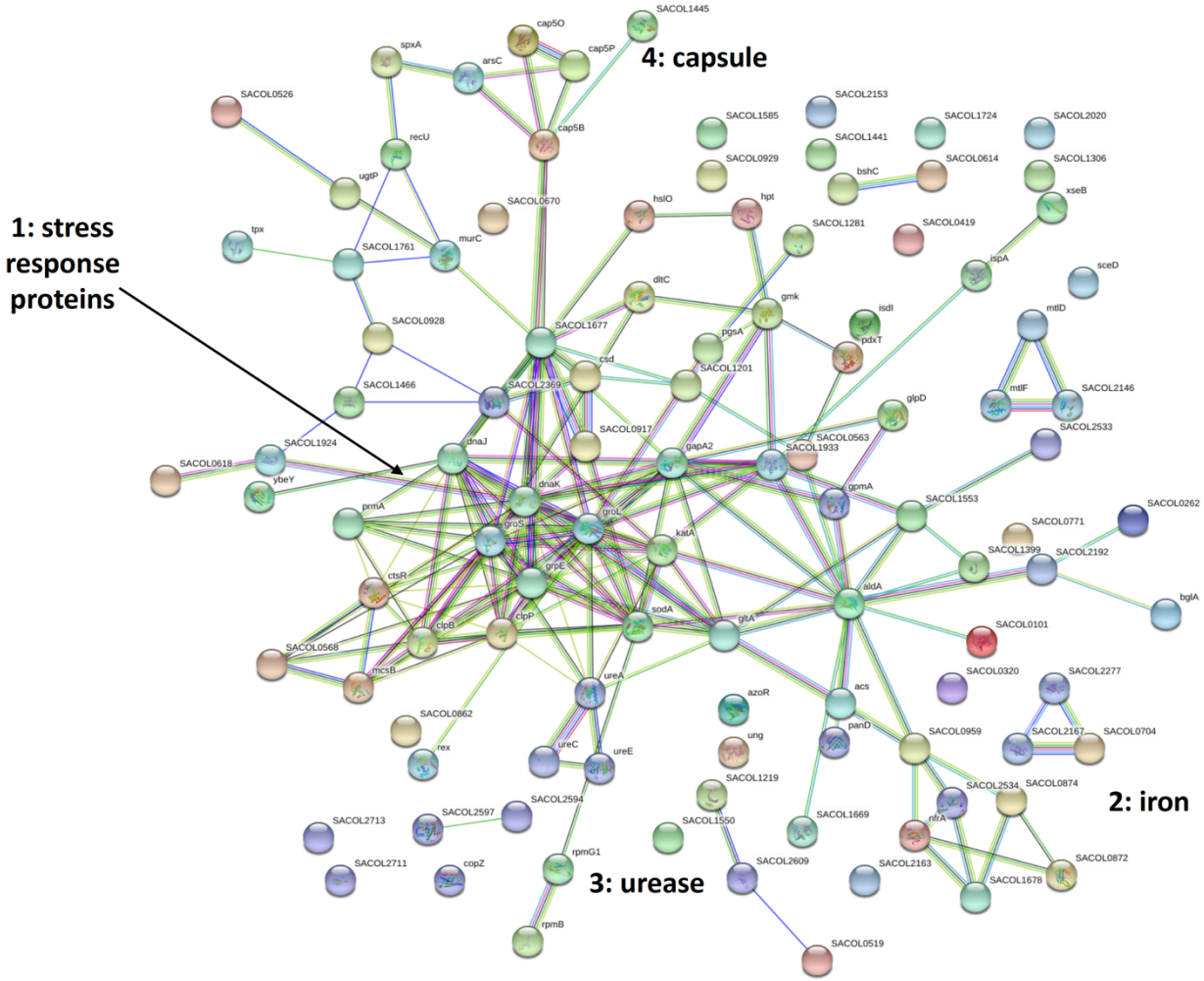

Figure 5.6: STRINGdb analysis identifying protein clusters upregulated in BDM-I treated Sa057. Highlighted clusters include proteins associated with the stress response (1), iron acquisition (2) and urease metabolism (3).

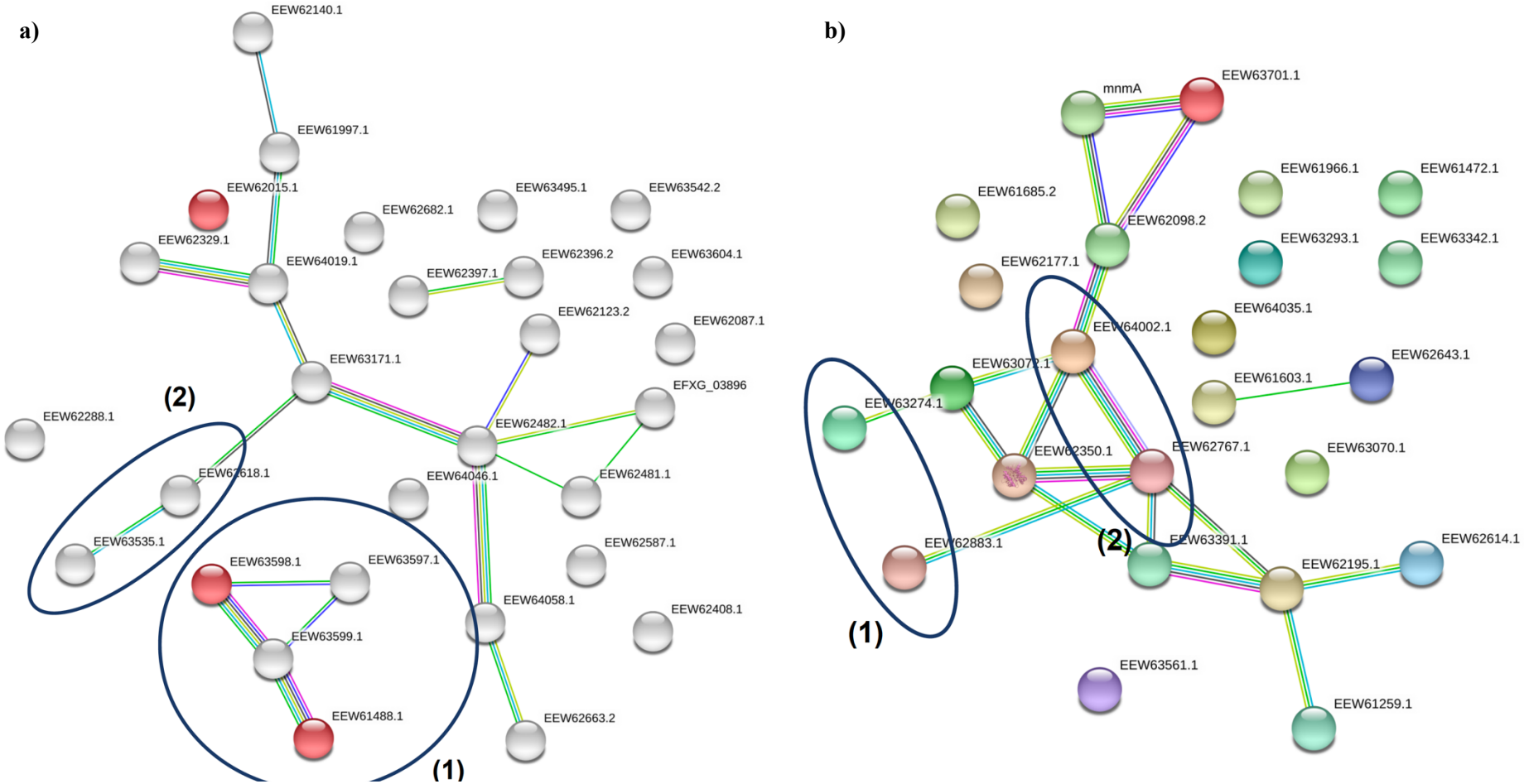

Figure 5.7: STRINGdb analysis identifying protein clusters downregulated (a) and upregulated (b) in BDM-I treated Efm008. Highlighted clusters which were downregulated (a) include proteins associated with phosphophenylpyruvate- dependent sugar phosphotransferase activity (1) and ATPase activity (2). Clusters which were upregulated (b) include proteins with nitroreductase activity (1) and proteins functioning in cell redox homeostasis (2).

5.4 Discussion

Whole proteome analysis of drug treated cells is a well-documented approach to understanding the MoA of a compound (Bandow et al., 2003, Thangamani et al., 2016, Wang and Chiu, 2008). Following the identification of compensatory mutations within mutant isolates with increased resistance to BDM-I, we aimed to utilize proteomics to study the cellular response to BDM-I treatment. Two methods were used and discussed in Chapter 5, including 2-DGE (section 5.2) as a first pass approach and shotgun proteomics (section 5.3), which provided significantly more quantifiable data.

Results discussed in Chapter 4 strongly indicated that BDM-I negatively affects ATP synthase, therefore we hypothesized that cellular responses to BDM-I treatment would, at least in part, relate to reduced ATP synthesis via the oxidative phosphorylation pathway. As shown above, a large number of proteins were found to be differentially expressed as a result of BDM-I exposure. Interestingly, a number of these proteins (and associated pathways) correlate to data obtained in Chapter 4. For example, multiple subunits of ATP synthase were downregulated in drug treated Efm008 (subunits δ and γ, section 5.2 and 5.3, respectively) and Sa057 (subunit γ, section 5.3). As a possible response to this, several proteins that function in pyruvate and acetyl-CoA metabolism exhibited altered expression, as shown in Figure 5.8.

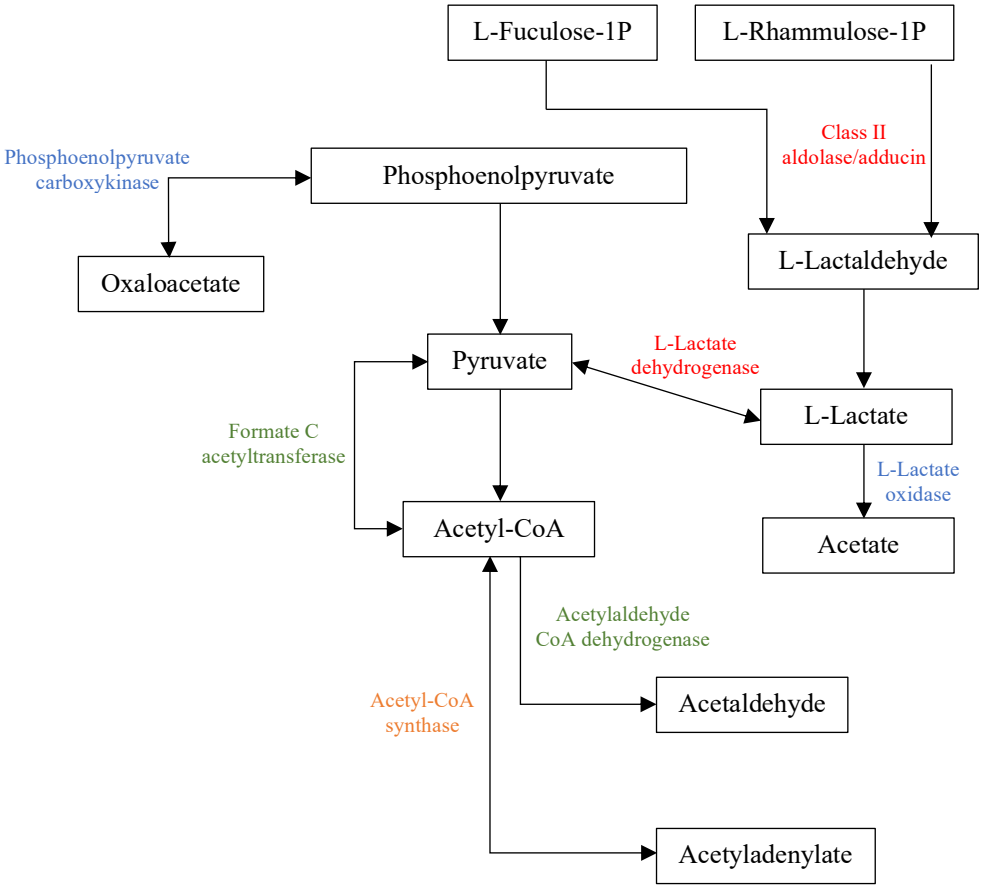

Figure 5.8 Proteins associated with the synthesis of pyruvate and acetyl-CoA that are differentially regulated following BDM-I treatment. Proteins involved in the synthesis of L-Lactaldehyde and L-lactate/pyruvate were upregulated within Efm008 (red), while those that convert L-lactate to acetate and phosphoenolpyruvate to oxaloacetate were downregulated (blue). Within Sa057, acetyl-CoA synthase was upregulated (orange), while acetylaldehyde CoA dehydrogenase and formate C acetyltransferase were downregulated (green).

In the context of Efm008, shifts in protein expression appear to favour the production of L-lactate. This is most evident based on the upregulation of proteins involved in the synthesis of L-lactate, and most importantly, the protein L-lactate dehydrogenase, which is responsible for the reversible conversion of pyruvate to lactate. Furthermore, proteins that convert L-lactate to other substrates (such as L-lactate oxidase) are downregulated following BDM-I treatment. This increased production of L-Lactate and pyruvate is likely a compensatory mechanism in response to the disruption of ATP synthase activity, and the reduced production of ATP via oxidative phosphorylation. Enterococci are capable of utilizing multiple pathways to generate ATP (at the substrate level) depending on environmental conditions. In the absence of functioning ATP synthase, the up-regulation of lactate and pyruvate synthesizing enzymes indicates that BDM-I treated Efm008 may be utilizing lactic acid fermentation as an alternative pathway to generate ATP (Ramsey M, 2014). Lactate is commonly utilized by lactic acid bacteria as a source of energy and can be generated by the reduction of pyruvate, which also produces NAD^+. Ensuring a continuous supply of NAD^+ promotes ATP production via the glycolytic pathway (Jiang et al., 2014, Ramsey M, 2014).

Unlike Efm008, several lactate dehydrogenase proteins were downregulated in Sa057. Anaerobic growth of *S. aureus* occurs in the absence of external electron acceptors such as oxygen and nitrate. When switching to anaerobic growth, glycolytic enzymes such as lactate dehydrogenases, alcohol dehydrogenases, α-acetolactate decarboxylase and acetolactate synthase are upregulated, signifying that mixed acid and butanediol fermentation is taking place (Fuchs et al., 2007). However, BDM-I treatment resulted in the downregulation of all proteins associated with anaerobic growth in *S. aureus*. Furthermore, proteins functioning in the synthesis of acetyl-CoA were upregulated

suggesting that ATP synthesis via the TCA cycle and oxidative phosphorylation is still favoured. Instead of changes in cellular respiration, the primary pathway affected by BDM-I treatment in Sa057 is UMP synthesis, which is the initial step in pyrimidine (nucleotide) metabolism (Hammer et al., 2005). Previous results (sections 4.6 and 5.2) indicate that changes to cell wall synthesis is the primary mechanism by which *S. aureus* can adapt to BDM-I exposure. Interestingly, proteins involved in pyrimidine metabolism have been associated with cell wall homeostasis in other bacteria. Research by Solopova et al identified that cell wall rigidity is regulated by aspartate carbamoyltransferase (*pyrB*) in *Lactococcus lactis* (Solopova et al., 2016). Furthermore, UMP can be phosphorylated to uridine diphosphate (UDP), which is required for the production of UDP-N-acetylglucosamine in the early stages of peptidoglycan synthesis (Jarick et al., 2018). WalK was also downregulated (>9-fold) following BDM-I treatment, which correlates with results discussed in Chapter 4. The WalKR TCS regulates the expression of a large number of proteins, several of which play key roles in peptidoglycan synthesis and hydrolysis. Proteomic analysis revealed the up-regulation of a WalKR regulated transglycosylase (*sceD*), with known cell wall degradative functions (Dubrac et al., 2007). This data suggests that Sa057 is restricting cell wall synthesis and promoting cell wall turnover in response to BDM-I treatment.

In Chapter 3 and 4, it was observed that *S. aureus* was unable to adapt to BDM-I in the same way as *E. faecium* via mutations within the ATP synthase operon. One possible explanation is that ATP synthase may be essential (or more essential) within *S. aureus* under the conditions tested. Balemans et al and Ko et al identified that ATP synthase knockout mutants suffered from a severely decreased growth rate, suggesting that ATP synthase plays an important role in the growth and survival of *S. aureus* (Balemans et al.,

2012, Ko et al., 2006). Therefore, in order to compensate for the decreased levels of intracellular ATP, *S. aureus* may instead downregulate cellular processes that require large amounts of ATP, such as cell wall synthesis. The ability of *E. faecium* to develop increased resistance to BDM-I is likely due to its metabolic and physiological characteristics as a lactic acid bacteria. Inhibition of ATP synthase promotes anaerobic respiration through fermentation and the glycolytic pathway, causing the increased production of lactate (Jiang et al., 2014). Unlike enterococci, *S. aureus* is not capable of generating ATP via the same pathway and this likely explains the difficulty experienced in generating BDM-I mutants with increased resistance, as well as the alternate compensatory mechanisms observed for *S. aureus* isolates (i.e., decreasing cell wall thickness, for example).

In Chapter 5, the effects of BDM-I treatment on exponentially growing Efm008 and Sa057 cells were examined in order to gain further insight into its MoA. The data obtained provides further evidence that BDM-I negatively affects ATP synthase. Additionally, regulation of lactate production within Efm008 explains the ability of *E. faecium* to develop increased resistance to BDM-I, by knocking down ATP synthase activity and utilising lactic acid fermentation. As *S. aureus* cannot undergo lactic acid fermentation, alternate compensatory mechanisms are utilized following BDM-I treatment, relying primarily on reducing the activity of pathways that require large amounts of ATP.

Chapter 6

Identifying the Binding Partner of BDM-I

6.1 Introduction

In previous chapters we have revealed that BDM-I affects ATP Synthase, as well as other interconnected cellular processes within both MRSA and VRE cells. However, the specific binding partner(s) of BDM-I has not yet been identified as part of the genomic and proteomic experiments performed to date. As discussed in Chapter 1, it has been proposed that BDM-I binds to and inhibits bacterial tyrosine phosphatases, although there is little data available that directly supports this hypothesis directly (White et al., 2014). In this chapter, we utilised relatively novel methods of target identification, including Drug Affinity Responsive Target Stability (DARTS) analysis and Thermal Proteome Profiling (TPP), which have both previously been used to identify binding partners of small molecules.

DARTS (Figure 6.1a) is a novel method that has been used successfully to identify the binding partner of several drugs that affect eukaryotic cell lines, including; rapamycin, resveratrol and ecumicin (Cui et al., 2003, Shoji et al., 2011). DARTS analysis relies on the observation that proteins are less susceptible to proteolysis when bound to a small molecule. Specifically, protein lysates are compared using SDS-PAGE following treatment with a small molecule and a broad-spectrum protease, and this facilitates the identification of proteins that exhibit increased stability (in the presence of a small molecule drug). DARTS offers several advantages over traditional methods, such as affinity chromatography, as it does not rely on chemical modification of the test

compound and it facilitates the identification of targets with low binding affinities due to the lack of washing steps (Chang et al., 2016).

TPP (Figure 6.1b) is similar in principal to DARTS, however it offers significant advantages in terms of the quality and sensitivity of the data generated. TPP combines the principals of cellular thermal shift and multiplexed quantitative mass spectrometry to identify the binding partner(s) of a compound; identification is based on a target's relative abundance/change in melting temperature following drug treatment and exposure to increased temperatures. Specifically, TPP involves the treatment of whole cells or cell lysates with a small molecule compound prior to exposing the samples to a range of temperatures. Protein-drug interactions have been shown to increase the thermostability of bound proteins, and stabilized proteins can be identified using quantitative mass spectrometry (Mateus et al., 2018, Mateus et al., 2017). As such, analysis of the resulting data allows identification of proteins with higher melting temperatures as a result of drug binding.

Due to the relative simplicity of DARTS and TPP analysis, as well as their proven accuracy in identifying protein targets (of small molecules), each method was used in an attempt to identify the binding partner(s) of BDM-I. DARTS analysis was initially performed using whole cell lysates derived from the MRSA isolate Sa057, while TPP was completed in collaboration with Professor Stuart Cordwell using Sa057 whole cells treated with BDM-I.

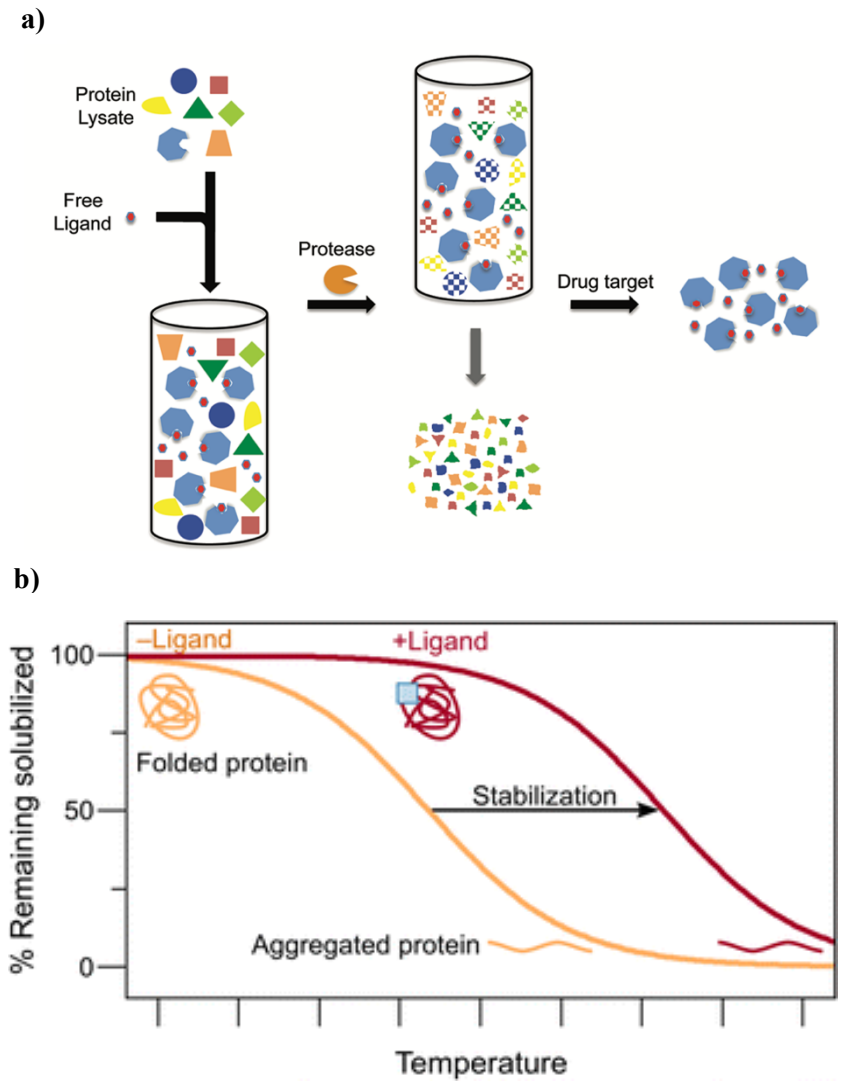

Figure 6.1: Theory of DARTS (a) and TPP (b) analysis for identifying the targets of small molecule drugs. Both methods are based on the same concept that the binding of a drug (ligand) will stabilise the target protein against protease activity (DARTS) and increase its melting temperature (TPP). The detection methods differ for each procedure, with DARTS relying on gel separation of treated lysates coupled with MS, while TPP utilizes protein enrichment coupled with LC/MS for greater degrees of sensitivity. Figures a and b are derived from Lomenick et al and Mateus et al, respectively (Lomenick et al., 2011, Mateus et al., 2017).

6.2 DARTS Analysis of BDM-I Treated MRSA Protein Lysate

Protein lysates were isolated from Sa057 grown to mid-exponential phase in 500 mL of LBB, using lysostaphin digestion and probe sonication, and then quantified using the BSA assay and diluted to a concentration of 4 mg/mL. The lysates were then treated with DMSO (vehicle control) or BDM-I at working concentrations of 3 μg/mL (MIC) and 15 μg/mL (MICx5) for 30 min at 25°C. Each sample was then treated with a mixture of proteases using Pronase:Protein ratios of 1:50, 1:100, 1:250 and 1:500 for another 30 min at 25°C; digestion reactions were stopped using protease inhibitors. The samples were then separated on 4-15% Mini-PROTEAN TGX precast gels (Bio-Rad) for 90 min at 100 V before being stained with Coomassie Brilliant Blue and imaged using white light and a UV Gel Dock system.

Subsequently, duplicate Mini-PROTEAN gels were analysed visually in order to identify any differences in protein bands between the vehicle control (DMSO) and BDM-I treated lysates. Unfortunately, as shown in Figure 6.2, we were unable to identify any proteins that were stabilized against Pronase digestion following treatment with BDM-I. Note that multiple BDM-I concentrations were tested, including 3 μg/mL (MICx1) and 15 μg/mL (MICx5), in an attempt to saturate the sample and increase the chance of BDM-I binding to its target(s) under the conditions used.

Based on the results (i.e., no observable difference in banding patterns between the samples), it is unlikely that DARTS is a viable method for the elucidation of the BDM-I binding partner(s). This could be due to several reasons, including the BDM-I binding affinity is weak (under the conditions used) or its target is present in low abundance.

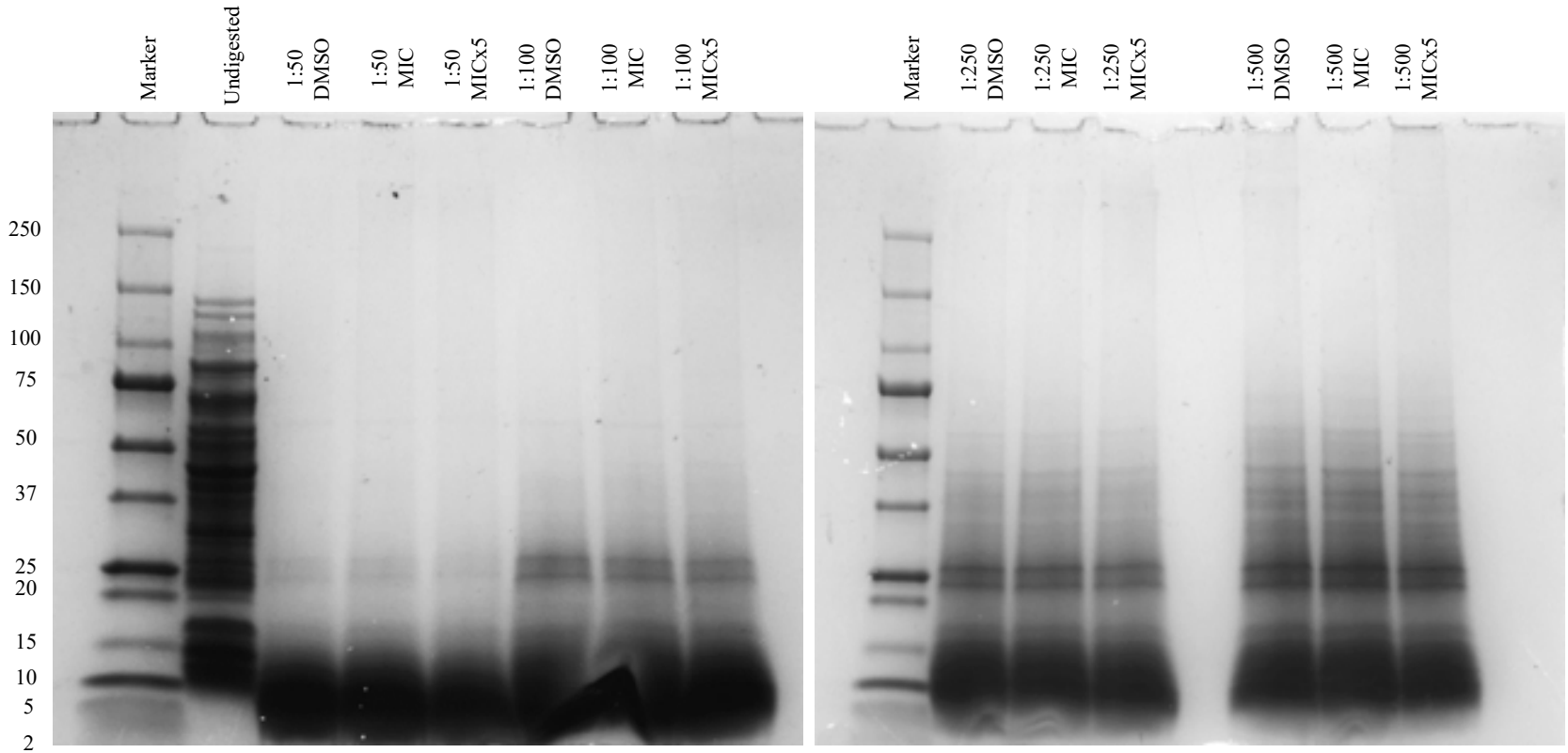

Figure 6.2 4-15% Mini-Protean Gels loaded with lysate samples derived from Sa057. Samples were treated with DMSO as well as BDM-I at 3 µg/mL (MIC) and 15 µg/mL (MICx5) before treatment with Pronase. Wells are grouped based on the Pronase:Protein ratio and treatment type.

6.3 TPP of the MRSA Proteome Following Exposure to BDM-I

BDM-I treated Sa057 whole cells were selected for TPP experiments as described by Mateus et al (Mateus et al., 2018). As a first pass approach, Sa057 cultures were grown to mid-exponential phase before being treated with BDM-I or DMSO and incubated for a further 10 min at 37°C. The cells were then harvested and resuspended in sterile PBS to an OD_{600} of 10, prior to heat treatment at 63°C for 3 min. Cell lysates were then prepared followed by peptide enrichment and LC/MS for protein identification.

Preliminary data revealed a total of 57 proteins present in higher abundance for drug treated Sa057, following treatment at 63°C (Supplementary Table 10); the majority (n=51) were 1-fold to 5-fold more abundant relative to the vehicle treated control. Interestingly, a significant number of these proteins function in ATP binding (n=7), oxidoreductase activity (n=3), DNA binding (n=2) and rRNA binding (n=5).

The greatest difference in relative abundance observed was for a luciferase family oxidoreductase and the DNA topoisomerase protein ParC, which were 23.87-fold and 22.02-fold more abundant, respectively. Interestingly, adenylate cyclase was also identified to be present in higher abundance (by 17.24-fold) following BDM-I treatment. At this stage, it is difficult to ascertain why ParC and a luciferase family oxidoreductase are present in significantly higher abundance without additional studies. In the case of adenylate cyclase, it is known to function in the conversion of ATP to 3',5'cyclic-AMP (cAMP), which can be recycled further to adenine monophosphate (AMP).

6.4 Discussion

A key step in drug development is exploring protein-drug interactions in order to identify the binding partner of a novel compound, and the gold standard methodology often utilized is affinity chromatography. However, this method is limited (especially in regards to small molecules) due to the need to chemically modify a compound which may affect its bioactivity, as well as the potential for high levels of non-specific protein binding to matrix columns (Lomenick et al., 2009). Recent methodological approaches have attempted to study drug target interactions *in situ* on a proteome wide scale, removing the need to modify a compound prior to target identification. In this regard, the two most promising methods that have been used successfully to identify the binding partner(s) of small molecule compounds are DARTS and TPP. Both techniques rely on the principal that a ligand bound protein is more tolerant to stressors, such as proteolysis and increased temperatures (Cui et al., 2003, Mateus et al., 2018, Mateus et al., 2017, Shoji et al., 2011).

DARTS analysis offers a major advantage due to its relative simplicity, as this technique utilizes standard laboratory techniques including SDS-PAGE protein separation and mass spectrometry. In section 6.2, DARTS analysis was utilized in an attempt to identify the BDM-I binding partner(s) within drug treated Sa057 protein lysates. Several BDM-I concentrations (MICx1 and MICx5) and Pronase:protein ratios (1:50, 1:100, 1:250 and 1:500) were utilized, however no observable differences (in banding patterns) were observed between BDM-I and control lysates (Figure 6.2) which potentially illustrate the limitations of DARTS analysis. In this regard, successful DARTS analysis relies on several characteristics that must be associated with the protein target interaction. Firstly, the target protein must be sufficiently abundant within the cell to be visible following

separation and staining. Secondly, if the target protein comigrates with other proteins of similar MW, it may be masked depending on the abundance of these comigrating proteins. Finally, the technique relies on a strong binding interaction between the drug and its protein target (Lomenick et al., 2011). Based on these limitations, it is likely that the drug-protein interaction between BDM-I and its target(s) may not be suitable for identification using DARTS, although more sensitive stains, such as Sypro Ruby, could be tested.

Following DARTS analysis, an alternative approach was utilized that offers higher sensitivity and accuracy when determining the target of a novel compound. TPP combines the principal of the cellular thermal shift assay with quantitative mass spectrometry, to identify changes in protein abundance following drug and heat treatment. Through TPP, the melting behaviour of the proteome can be examined post drug treatment, as protein-drug interactions typically increase the thermal tolerance of proteins (Mateus et al., 2018). Recently, TPP was optimized for usage with bacterial proteomes to identify the (known) target of several antibiotics. Mateus et al examined the dynamics of the *E. coli* proteome following treatment with ampicillin and ciprofloxacin in an attempt to identify their cellular targets. Using TPP, they observed that the known targets of ampicillin (penicillin-binding proteins (PBPs)) and ciprofloxacin (DNA Gyrase) were stabilized within cells treated with each compound. Furthermore, they noted that TPP can also be used to study resistance determinants as well as a compound's mechanism of action (downstream consequences to cellular physiology) (Mateus et al., 2018).

Using this optimized methodology, we collaborated with Stuart Cordwell's group at the University of Sydney to perform TPP on BDM-I treated Sa057. As a first pass approach to confirm the validity of TPP, the cells were incubated at 63°C to confirm protein

thermostabilization following BDM-I binding. Analysis identified a total of 57 proteins that were stabilized by BDM-I treatment relative to the vehicle control. Considering the data presented in Chapters 4 to 5, the high abundance of adenylate cyclase within BDM-I treated Sa057 may be relevant to the observation that BDM-I negatively affects ATP synthase. As stated previously, adenylate cyclase converts ATP to cAMP. Interestingly, De Rasmo et al identified that depleted intracellular concentrations of cAMP result in reduced ATP synthesis and hydrolysis activity by the mammalian ATP synthase (De Rasmo et al., 2016). This finding may indicate a possible mechanism by which ATP synthase is inhibited by BDM-I treatment, via the inhibition of adenylate cyclase and therefore cAMP synthesis.

However, it is critical to note that without additional TPP studies it is not possible to make any conclusions based on the available data. Based on work by Mateus et al, TPP analysis of drug treated cells yields significantly higher numbers of stabilized proteins compared to drug treated cell lysates. In the case of ciprofloxacin, DNA gyrase was only identified to be stabilized based on the data generated from TPP of drug treated lysates (Mateus et al., 2018). Therefore, additional studies are required to complete TPP on BDM-I treated Sa057 protein lysates exposed to a range of temperatures.

Chapter 7

Discussion

7.1 Introduction

The need for novel antibiotics is becoming increasingly important, as bacteria are masters of adaptation and can rapidly become resistant to antimicrobial compounds. In this regard, BDM-I represents a novel antimicrobial compound that has good *in vitro* activity against a broad range of microbial organisms, including multi-drug resistant bacteria. Although this activity has been demonstrated previously (at least in part), its MoA is not fully understood. Currently, the primary target of BDM-I is believed to be protein tyrosine phosphatases (PTPs), and this is largely based on a previous study that revealed it inhibits the bacterial phosphatases PTP1B and Yop, at rates of 46% and 42% respectively. Additionally, virulence factors that rely on PTP activity such as motility in *Proteus* spp and attachment/invasion in *Yersinia* spp were also shown to be inhibited by BDM-I (White et al., 2014). Furthermore, a study by Park et al on structurally similar compounds to BDM-I identified the likely binding partner to be PTPs (Park and Pei, 2004).

Although the data from previous studies suggest that BDM-I is likely inhibiting bacterial PTPs, the function of these proteins in bacteria is not well understood. This makes it difficult to ascertain the mechanism by which BDM-I inhibits microbial growth, assuming it is through the inhibition of PTPs. As such, this study aimed to gain further insight into the MoA of BDM-I by using an omics approach; whole genome sequencing and proteomic analysis of *in vitro* derived BDM-I mutants, as well as BDM-I treated

isolates. Additionally, this study also aimed to determine the efficacy of BDM-I as a treatment option for the common bacterial pathogens *S. aureus* and *E. faecium*.

7.2 Examining the Utility of BDM-I Against the ESKAPE Pathogens

7.2.1 BDM-I Displays Increased Activity Against MRSA

As stated previously, BDM-I has been shown to be effective against a broad range of microbial organisms. Significant activity has typically been observed against gram-positive species including, *S. pyogenes*, *C. perfringens* and *S. aureus* (unpublished data). As part of this study, we aimed to assess the utility of BDM-I against a library of clinical *S. aureus* and *E. faecium* isolates with varying degrees of vancomycin susceptibility, in order to identify potential cross-resistance in isolates with reduced vancomycin susceptibility. As described in section 3.3, MIC analysis was conducted using 103 clinical MRSA isolates comprised of 43 VSSA, 54 hVISA, and 6 VISA isolates; this isolate set also included 26 isogenic pairs and 3 isogenic series. As observed in Table 3.2, there were no significant differences in BDM-I MICs between initial and recurrent/persistent isolates, indicating that cross-resistance (to BDM-I) did not develop during prolonged periods of exposure to other antibiotics, which can potentially occur (Chen et al., 2015). Interestingly, as shown in Table 3.3 we did observe a gradual decrease in BDM-I MICs within series C. The initial VSSA isolate Sa057 exhibited an observed MIC of 4 μg/mL, which decreased to 3 μg/mL for the persistent hVISA isolates, and finally 2 μg/mL for the final VISA isolate. This shift in BDM-I MIC indicated a possible seesaw effect between BDM-I and vancomycin MICs.

A seesaw effect refers to an inverse correlation of susceptibility between two types of antibiotics. It is a phenomenon that has previously been described for *S. aureus*, in relation

to the *in vivo* evolution of resistance to glycopeptides and daptomycin, which was shown to inversely correlate to β-lactam susceptibility following prolonged treatment periods (Vignaroli et al., 2011, Yang et al., 2010). As described in section 3.4, a Spearman's test was used to confirm the potential see saw effect between BDM-I and vancomycin, by utilising the average MIC values for each vancomycin phenotype (Table 3.7). Analysis revealed a definitive negative correlation between both compounds (Rho = -0.24; P = 0.0145), with VSSA isolates having a higher BDM-I MIC and lower vancomycin MIC, while the opposite was true for VISA isolates.

MIC testing was also completed using 30 clinical *E. faecium* isolates (10 VSE, 10 *vanB* and 10 *vanA*) to identify any similar trends to those observed with MRSA isolates. MIC results between the three phenotypes were comparable, with the majority of the isolates having MICs ranging from 6-8 μg/mL (Table 3.5). Interestingly, several isolates were identified to be more susceptible to BDM-I, with MICs of 3-3.5 μg/mL. In the case of the *vanB* isolate Efm0002, previous work had identified it possesses a SNP mutation within the gene *walK* which results in a thickened cell wall (unpublished data). Considering the VISA isolates are approximately 2-fold more susceptible to BDM-I than VSSA, it is interesting that a VRE isolate with a similar phenotype is also approximately 2-fold more susceptible to BDM-I compared to WT *E. faecium*. The mechanism driving this negative correlation between the MICs of WT isolates, and those with thickened cell walls, will be discussed further in section 7.3.2.

As described in section 3.4, checkerboard assays were completed using three clinical MRSA isolates and three clinical VRE isolates: Sa057 (VSSA), Sa060 (hVISA), Sa375 (VISA), Efm008 (*vanA*) and Efm123 (*vanB*) and Efm201 (*vanB*). BDM-I was identified

to exert an additive effect in combination with vancomycin for Sa060 and Sa375; vancomycin MICs decreasing significantly when combined with BDM-I at MIC_{50}. However, this relationship was unique to Sa060 and Sa375, as there were no synergistic or additive relationships observed for Sa057, Efm008, Efm123 and Efm201.

Combination therapy has been described since the 1950s as a viable method of treatment that can significantly reduce the probability of resistance developing (Elek, 1956). Currently, there are three categories of combination therapy that are outlined in a review by Fischbach (Fischbach, 2011). These categories include drugs that inhibit targets in different pathways, drugs that inhibit different nodes in the same pathway, and drugs that inhibit the same target in different ways (Fischbach, 2011). An important factor that needs to be considered in selecting antibiotics for combination therapy is their synergistic relationship. Certain drugs can often be antagonistic to another compound's MoA, which represents the greatest limiting factor in terms of using antibiotics in combination. Considering the previously discussed seesaw effect and checkerboard data, BDM-I and vancomycin could be used in combination therapy to treat MRSA infections, particularly those associated with hVISA/VISA isolates. Additionally, it is important to note that there was no antagonism observed between BDM-I and vancomycin, which as described previously, is a limiting factor when using compounds in combination.

Upon identifying the additive effect in the case of the hVISA and VISA isolates, additional checkerboard assays were completed combining BDM-I with other cell wall active antibiotics, specifically the penicillin-binding protein inhibitors Flucloxacillin and Ceftaroline Fosamil. However, combination studies with these compounds identified no additive or synergistic effects for MRSA or VRE isolates, suggesting that the previously

observed additive effect is unique between BDM-I and vancomycin and is likely related to cell wall thickness.

7.2.2 *E. faecium* Readily Develops Increased Resistance to BDM-I

The data gathered in section 3.3 identifies BDM-I as a viable treatment option for MRSA infections, particularly those associated with hVISA and VISA isolates. It is important then to determine the potential for bacteria to develop increased resistance to BDM-I *in vitro*, in order to examine its usability during long term treatment, as well as producing mutant isolates for use in WGS studies. Section 3.5 described induction experiments using two MRSA (VSSA and VISA) and two VRE (*vanA* and *vanB*) clinical isolates, which were sub-cultured in sub-inhibitory concentrations of BDM-I for ≥70 days. Results from these studies indicate that MRSA isolates have a limited capacity to develop increased resistance to BDM-I, particularly Sa057 (VSSA), which was unable to adapt following an extended period of BDM-I exposure (100 days). However, Sa375 (VISA) did appear to generate limited resistance to BDM-I by the final day of treatment, with endpoint MICs being determined as 5 μg/mL, higher than that of the progenitor Sa375 with an MIC of 2 μg/mL (section 3.2.1). In comparison, both VRE isolates were readily capable of adapting to BDM-I, with final MIC values for both Efm003 and Efm008 being more than double that of the progenitor isolates. Significant increases in BDM-I MICs were observed within 10 days of BDM-I exposure, which continued to increase throughout the entire duration of the experiment (70 days), which may limit the potential utility of BDM-I as a treatment option for *E. faecium* associated infections.

7.3 Developing a Model of the BDM-I Mechanism of Action

7.3.1 BDM-I Affects ATP Synthase Activity

While the data produced in section Chapter 3 revealed lower activity of BDM-I against *E. faecium* (in comparison to *S. aureus*), we were able to generate mutant isolates with significantly higher MICs compared to the corresponding progenitor isolates. *In vitro* derived VRE and MRSA mutant isolates were then subjected to whole genome sequencing, in order to identify mutations driving the increased MICs which can potentially provide insight into the BDM-I MoA. Given the ability of both VRE isolates to rapidly develop increased BDM-I resistance, they were selected for initial WGS from two timepoints (approximately 10 and 60 days of exposure). Three colonies were isolated from each of the three series, giving a total of nine data sets from each time point.

Following variant analysis, 15 mutations were identified across the Efm003 day 10 colonies, and 10 were identified across the final day Efm003 colonies (Supplementary Tables 1 and 2). Analysis of the sequencing data identified no common mutation present within all day 10 colonies, with the most common mutation identified being a SNP in the gene EFAU004_00165, which encodes an M-protein Trans-acting positive regulator. The location of these mutations within EFAU004_00165 varied between each colony, ruling out a site-specific response to BDM-I exposure. Currently, it is unclear why mutations within an M-protein regulator may be advantageous in the presence of BDM-I, given the primary role of M-proteins is in bacterial virulence. Interestingly, research on the well-studied *S. pyogenes* M-protein has shown that it is regulated by phosphorylation on both serine and tyrosine sites, catalysed by the activity of bacterial protein kinases (Chiang et

al., 1989). This may be linked to the activity of bacterial tyrosine phosphatases, which are the predicted target of BDM-I.

Analysis of the sequencing data for the remaining time points identified common mutations within the ATP synthase operon, for both Efm003 and Efm008. Interestingly, mutations were not specific to a single gene, but were spread across the entire operon as outlined in Tables 4.1 and 4.2. SNP mutations were commonly identified in the final day mutant isolates within *atpD* (Efm008) and *atpB* (Efm003), which encode the β-subunit of the F_1 complex and the c-subunit of the F_0 complex of ATP synthase, respectively. Mutations within the day 10 Efm008 mutants were more varied, and included SNPs and IS*1256*-like insertion sequences (and associated deletions) within *atpE*, *atpD*, *atpG* and *atpF* (see Table 4.1). Considering the presence of mutations within various ATP synthase genes for all mutant *E. faecium* isolates, it is likely that ATP synthase is strongly linked to the BDM-I MoA. However, it is unlikely to be its only target due to the fact that day 60 Efm008 mutant isolates, which have an IS*1256*-like insertion sequence mediated deletion of *atpC*, *atpD*, *atpG,* and partial deletion of *atpA*, remained sensitive to increased concentrations (≥18 μg/mL) of BDM-I. Therefore, it is likely that mutations identified within these genes are only partly compensating for the BDM-I MoA; note that this compensatory mechanism may only be possible in the case of *E. faecium*, as ATP synthase appears to be more essential for *S. aureus* growth.

ATP assays were then utilized to confirm that BDM-I is inhibiting ATP synthase within both Efm008 and Sa057 (Chapter 4). Subsequently, results revealed a significant decrease in intracellular ATP concentrations for both isolates. These results were the first indication that ATP synthase was also affected in *S. aureus*. Interestingly, such an affect

was also confirmed via BDM-I and polymyxin B combination studies using Sa057. Research by Vestergaard et al identified that inhibition of ATP synthase reduces the innate resistance of *S. aureus* to CAMPS, such as polymyxin B. Specifically, it was proposed that ATP synthase inhibition results in the hyperpolarization of the cell membrane and (as a result) increased activity of CAMPS (Vestergaard et al., 2017). Considering these observations, checkerboard assays revealed that when used in combination (BDM-I MIC_{50}), the MIC of polymyxin B decreased from 256 μg/mL to 64 μg/mL (FICI = 0.75), which is indicative of ATP synthase inhibition.

Additional evidence was obtained regarding the importance of ATP synthase in association with the BDM-I MoA, based on the proteomic analysis of BDM-I treated *S. aureus* and *E. faecium* cells (Chapter 5). Initial analysis was completed using 2-D gel electrophoresis of proteins extracted from BDM-I treated Efm008, in order to identify changes in expression following drug treatment. Two subunits of ATP synthase (subunit-β and subunit-δ) were downregulated following exposure to BDM-I. Furthermore, a pyruvate dehydrogenase complex within the $Efm008_{\Delta atpACDG}$ mutant was upregulated, possibly indicating a shift to substrate level ATP synthesis due to the inactivity of ATP synthase. Due to the limitations associated with gel based proteomic methods (see section 5.4), additional studies were conducted using shotgun proteomics on BDM-I treated Efm008 and Sa057 cells. By using shotgun proteomics, significantly more data was obtained which provided a deeper understanding of the cellular response to BDM-I treatment. Importantly, analysis revealed that the ATP synthase γ-subunit was downregulated in both Sa057 and Efm008 by 2.13-fold and 2.42-fold, respectively.

Proteomic analysis also revealed the potential mechanism by which *E. faecium* is able to readily adapt to BDM-I. Data revealed that Efm008 is likely utilizing lactic acid fermentation to synthesize ATP as a result of BDM-I treatment. Several proteins were differentially regulated that promote the production of L-lactate and pyruvate, including a lactate dehydrogenase, which was upregulated >2-fold. Enterococci are capable of undergoing fermentation in anaerobic environments through the metabolism of glucose. During this process, pyruvate and NADH are produced, the latter of which can be further oxidised to NAD^+ following the conversion of pyruvate to L-lactate (Doi, 2018). This continual conversion of pyruvate to L-lactate ensures there is a constant supply of NAD^+, which is required for the conversion of glyceraldehyde-3-phosphate to 1,3-bisphosphoglycerate during glycolysis (Figure 7.1) (Ramsey M, 2014, Jiang et al., 2014). By utilizing this pathway, Efm008 is able to compensate for the reduced activity of ATP synthase by producing ATP at a substrate level.

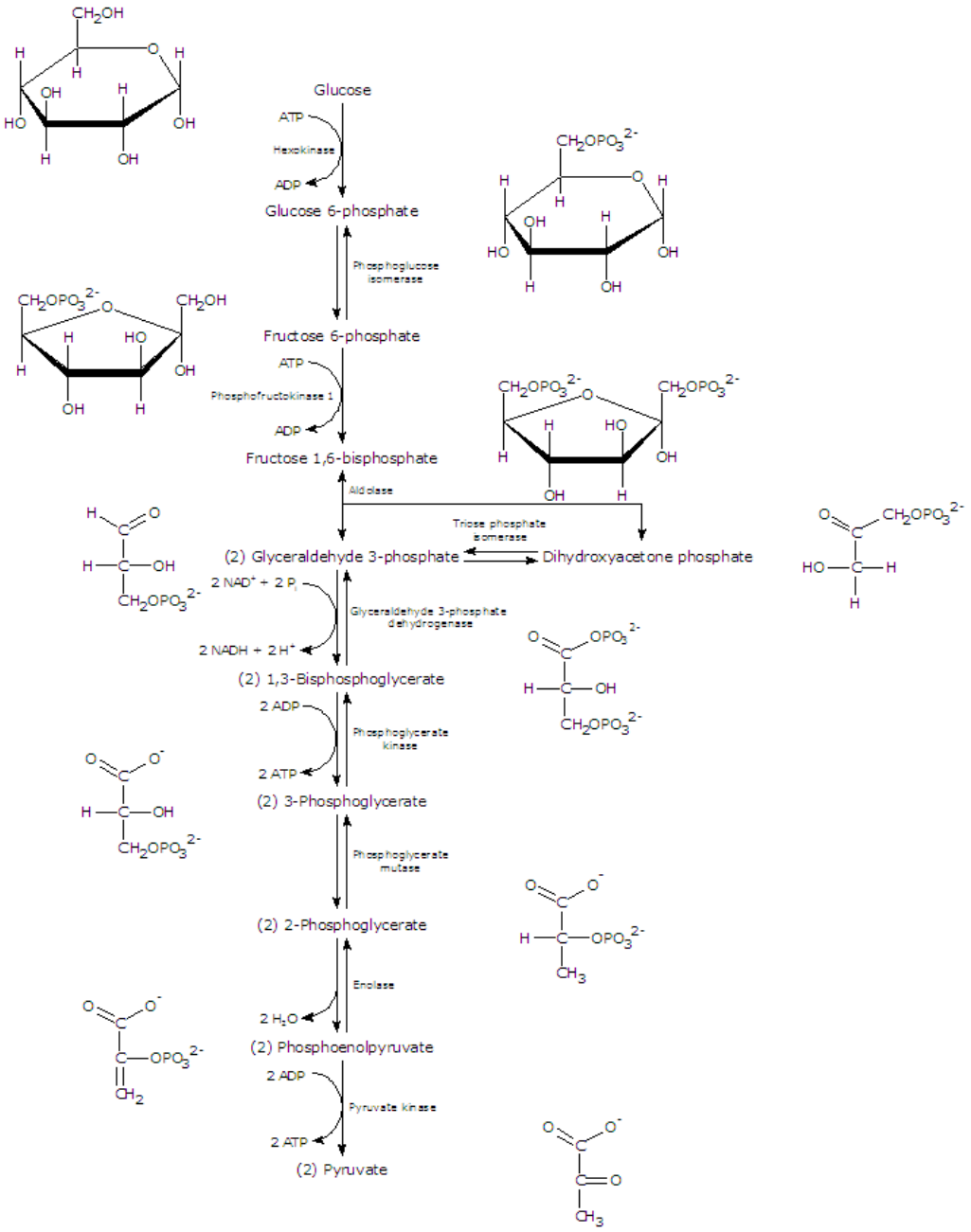

Figure 7.1 Glycolysis pathway involved in the stepwise production of Pyruvate from Glucose. Through the production of L-lactate from pyruvate, glycolysis can be utilized by lactic acid bacteria as an alternative method to produce ATP. Lactate dehydrogenase catalyses the reversible conversion of pyruvate to lactate, which releases a continual supply of NAD^+ which is required for glycolysis to occur.

Unlike *E. faecium*, *S. aureus* is not capable of using lactic acid fermentation as an alternative to oxidative phosphorylation. Proteomic data revealed that BDM-I treated Sa057 was still favouring ATP synthesis via oxidative phosphorylation, based on the downregulation of all proteins associated with anaerobic respiration (Fuchs et al., 2007), as well as the up-regulation of proteins that produce acetyl-CoA which can be used in the TCA cycle. Sa057 may be relying on ATP synthase based on its essentiality within *S. aureus* (see section 5.4), which would explain the increased BDM-I sensitivity observed for MRSA isolates (relative to VRE), as well as the difficulty in generating MRSA mutants with increased resistance to BDM-I (Chapter 3).

Although no mutations were identified within the ATP synthase operon for either MRSA isolates, common mutations were identified within the Sa057 gene SAA6008_00679, which encodes a putative phosphate uptake regulator (which is distantly related to PhoU). PhoU is a negative regulator of P_i uptake in (predominantly) gram-negative bacteria, although it has been identified in several gram-positive species (Zheng et al., 2016). The mechanisms involved in the transport of inorganic phosphate (P_i) molecules has been studied extensively in *E. coli*, as well as other species (although to a lesser extent) including *B. subtilis* (Qi et al., 1997, Rao and Torriani, 1990, Willsky et al., 1973). Acquisition of P_i can be carried out by three classes of importers found within bacteria; PstSCAB (phosphate-specific-transport), PitA/PitB (phosphate inorganic transport) and the NptA (Na-dependent phosphate transport) systems (Kelliher et al., 2018). PstSCAB is a high affinity P_i transporter belonging to the ABC family which is regulated by PhoU via the PhoBR two-component regulatory system. In short, when P_i concentrations are below or above 0.4 μM, PhoU will initiate the expression or repression of *pstA*. Therefore, Sa057 mutants may be responding to reduced ATP synthase activity by regulating the

transport of P_i into the cell. Currently, it is not believed that BDM-I is binding to ATP synthase and inhibiting it directly. Mutant VRE isolates bearing mutations within the ATP synthase operon still remain susceptible to BDM-I at higher concentrations, including the previously discussed deletion mutant (Efm008$_{\Delta atpACDG}$). Therefore, we hypothesize that ATP synthase inhibition is a downstream consequence of the primary BDM-I target.

In the context of the proposed BDM-I MoA as a PTP inhibitor, previous studies have identified that ATP synthase is regulated through phosphorylation in eukaryotic cells and some prokaryotic cells (*e.g.* Streptococcus species) (Ge and Shan, 2011, Kane and Van Eyk, 2009, Sun et al., 2010). Additional studies of the eukaryotic ATP synthase have revealed that it is unable to release ADP efficiently when phosphorylated (Arrell et al., 2006), possibly indicating that a hyper-phosphorylated form of the enzyme could be deleterious to the cell's metabolism. If bacterial ATP synthase is regulated by a similar mechanism, the inhibition of bacterial PTP may be deleterious to the activity of ATP synthase.

Alternatively, preliminary TPP data (Chapter 6) identified adenylate cyclase was thermostabilized by BDM-I treatment within Sa057. Adenylate cyclase catalyses the conversion of ATP to cAMP, which can be converted further to AMP via phosphodiesterases (De Rasmo et al., 2016). cAMP has been identified as a regulator of ATP synthase activity within mammalian cells, following observations that the depletion of cAMP is associated with decreased ATP and hydrolysis by ATP synthase. Furthermore, cAMP is also associated with maintaining the expression of ATP synthase subunits within mammalian cells (De Rasmo et al., 2016). Currently, it is not possible to state with confidence that BDM-I inhibits ATP synthase by depleting the intracellular

concentration of cAMP. Significantly more work is required to confirm that both; BDM-I is binding to and inhibiting adenylate cyclase, and that bacterial ATP synthase activity is regulated by cAMP levels.

7.3.2 *S. aureus* Responds to BDM-I by Regulating Peptidoglycan Synthesis

As discussed in section 7.3.1, the data generated in this study suggests that the BDM-I MoA is (at least in part) inhibition of ATP synthesis. Sequencing and proteomic analysis of mutant/BDM-I treated MRSA and VRE isolates, as well as results from ATP assays, strongly support this apparent mechanism. BDM-I treatment of Efm008 resulted in the utilization of lactic acid fermentation to compensate for the decreased activity of ATP synthase. However, due to the essentiality of ATP synthase in *S. aureus*, as well as the inability for *S. aureus* to undergo lactic acid fermentation, we observed a unique adaptive mechanism within MRSA isolates through the regulation of peptidoglycan synthesis.

Peptidoglycan synthesis is an essential, multi-stage process that is critical in ensuring bacterial cell viability and pathogenicity. The gram-positive cell wall is composed of cross-linked peptidoglycan, which consists of chains (of repeating disaccharide units) of *N*-acetylglucosamine (GlcNAC) and *N*-acetylmuramic acid (MurNAc). In *S. aureus*, these polysaccharide chains are cross-linked by interpeptide bridges composed of five glycyl residues that protrude from the L-lysine of the stem-peptides (Jarick et al., 2018). Briefly, peptidoglycan is synthesized in three stages: first, the nucleotide sugar-linked UDP-MurNAc-pentapeptide is formed, second, lipid II is formed by the addition of UDP-GlcNAc to lipid I, lastly, lipid II is transported across the membrane and added to the

growing peptidoglycan sacculus by penicillin binding proteins (see Figure 7.2) (Jarick et al., 2018).

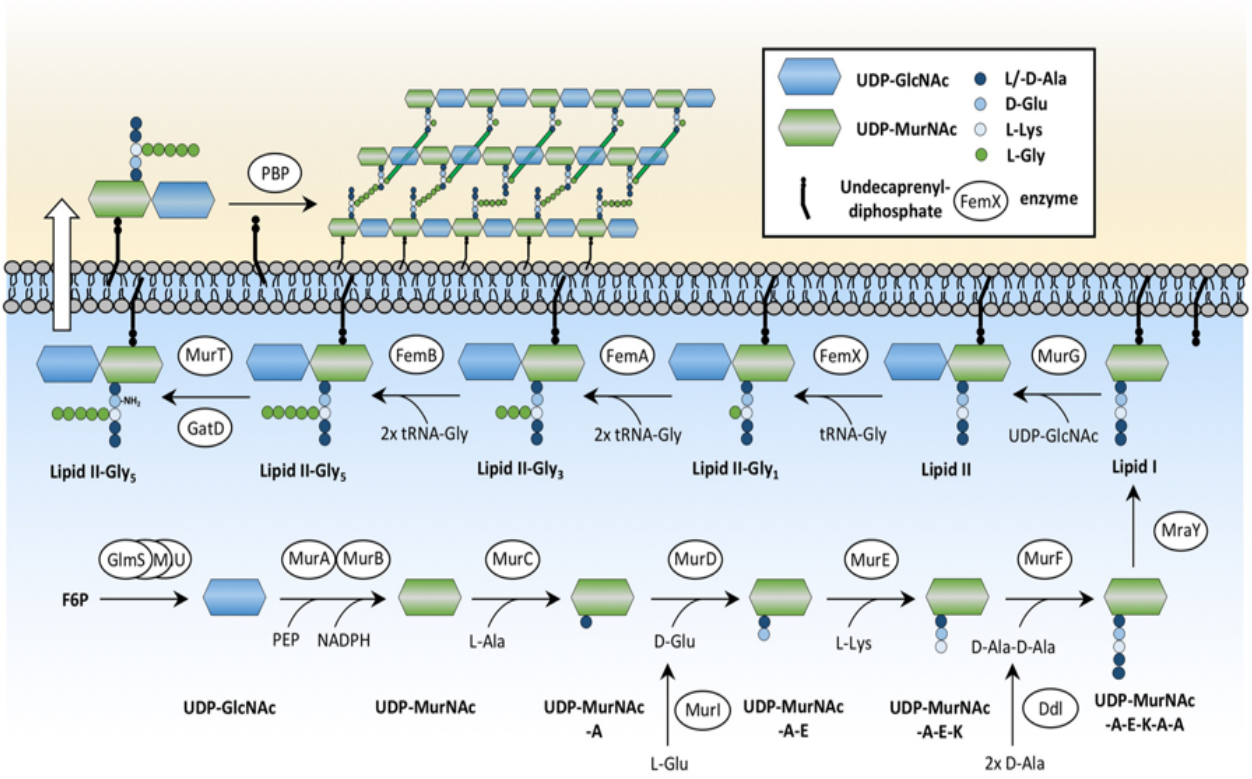

Figure 7.2 Structure and synthesis of Peptidoglycan in *S. aureus*. Fructose-6-phosphate is initially converted to GlcN6P by the aminotransferase GlmS, before being processed to N-acetylglucosamine-6-phsphate (UDP-GlcNAc) by GlmM and GlmU. UDP-GlcNAc is then converted to N-acetylmuramic acid (UDP-MurNAc) by MurA and MurB, followed by the sequential addition of the amino acids L-Ala, D-Glu and L-Lys as well as the dipeptide D-Ala-D-Ala which is catalysed by MurC-F. The resulting product, UDP-MurNAc-L-Ala-D-Glu-L-Lys-D-Ala-D-Ala is then linked to the lipid carrier undecaprenyl-diphosphate by the translocase MraY, which produces the membrane bound Lipid I. UDP-GlcNAc is then linked to the Lipid I molecule by the glycosyltransferase MurG, forming Lipid II. Lipid II is then modified by the addition of five glycine residues by the FemX/A/B proteins, which use glycyl tRNAs to transfer glycine to the PGN-lysl side chain of Lipid II. Following several modifications including the deamination of D-Glu of the stem peptide by MurT/GatD, the pentaglycine-Lipid II molecule is translocated to the outer side of the membrane. Here, penicillin binding proteins incorporate extracellular Lipid II to the growing PGN through transglycosylation and transpeptidation. Image and caption derived from Jarick et al, 2018 (Jarick et al., 2018).

As discussed in Chapter 3, VISA isolates are more sensitive to BDM-I in comparison to hVISA and VSSA isolates, as they have a lower average MIC of 2.5 μg/mL. Additionally, Efm0002, which also has a thickened cell wall like VISA isoaltes, was also more sensitive to BDM-I compared to WT *E. faecium*. Interestingly, Sa375 (VISA) exhibited the greatest capacity to generate increased (and stable) resistance to BDM-I following prolonged periods of exposure in comparison to Sa057 (VSSA). WGS of Sa375 mutants identified SNPs within the gene *walK* for all sequenced mutant colonies. As mentioned previously, *walK* belongs to the essential WalKR two-component regulatory system, which is associated with controlling cell wall homeostasis and cell viability (Delauné et al., 2012). In context of the VISA phenotype, mutations within *walK* have been attributed to reduced vancomycin susceptibility via the production of thickened cell walls with reduced permeability, which can also be associated with daptomycin cross-resistance (Bayer et al., 2013, Howden et al., 2010, Howden et al., 2011, Kelley et al., 2011, Shoji et al., 2011). Regarding Sa375, its VISA phenotype is driven by a SNP within *walK* (Q369R) that results in thickened cell walls. Interestingly, this mutation is still present within BDM-I mutants (van Hal et al., 2013)

Given the well-established role of *walK* in maintaining cell wall homeostasis, as well as the presence of novel mutations in *walK* within all BDM-I mutants, it was hypothesized that these mutations were driving increased BDM-I resistance by altering the phenotype of the cell wall. Electron microscopy (section 4.5.2) of Sa375 mutants revealed significant reductions in cell wall thickness which were also associated with increased sensitivity to both vancomycin and daptomycin (Figure 4.4). The SNP within mutant series 2 (G560S) was then introduced into Sa375-WT, which exhibited similar sensitivity profiles to the mutant isolate (increased BDM-I resistance, increased vancomycin sensitivity, increased

daptomycin sensitivity, decreased cell wall thickness), confirming that the *walK* mutations identified within mutant Sa375 isolates are driving the observed phenotype, as well as the increased resistance to BDM-I.

Furthermore, the importance of cell wall regulation as an adaptive mechanism against BDM-I was further illustrated following proteomic analysis of BDM-I treated Sa057 cells (section 5.3). Analysis revealed the downregulation of *walK* by 9.21-fold following drug treatment, which corresponds with previous sequencing data. Transcriptome profiling of the WalKR regulon has revealed its role in regulating the expression of a large number of proteins involved in cell wall metabolism, regulatory pathways, the stress response, transport and metabolism. Regarding cell wall metabolism, inhibition of WalKR activity is associated with reduced peptidoglycan synthesis and cell wall turnover, as well as increased autolytic activity (Delauné et al., 2012, Dubrac et al., 2007). Interestingly, WalKR is essential in regulating the expression of proteins responsible for cell wall degradation, namely *lytM*, *atlA*, *isaA*, *sceD* and *ssaA*. Proteomic analysis of BDM-I treated Sa057 revealed the upregulation of *sceD* by >30-fold as a result of WalKR inactivation. As shown in Figure 7.3, the increased expression of *sceD* is likely due to the repression of *isaA*, which is positively regulated by *walR* under optimal conditions (Stapleton et al., 2007).

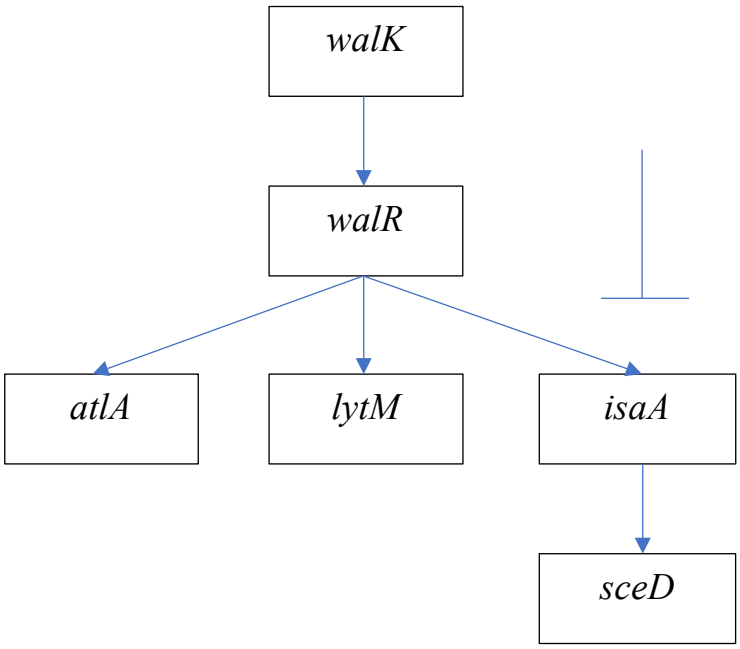

Figure 7.3 WalKR regulates the expression of several genes with known autolytic activities. Several genes including *atlA*, *lytM* and *isaA* have been identified to be positively regulated by *walK*. Evidence also suggests that *sceD* is positively expressed when *isaA* is repressed, which occurs when *walK* activity is reduced.

Additionally, it is worth noting that mutations were identified within the gene *murC* in 50% of Sa057 BDM-I mutants (Table 4.3). *murC* encodes UDP-N-acetylmuramic acid L-alanine ligase, which plays an essential role in peptidoglycan synthesis in *S. aureus* by catalysing the ligation of L-Ala to UDP-MurNAc in the early stages of peptidoglycan synthesis (Figure 7.2) (Kurokawa et al., 2008). Furthermore, proteomic analysis of BDM-I treated Efm008 identified the upregulation of a LysM domain containing protein by 7.45-fold. While the majority of evidence suggesting that BDM-I affects cell wall synthesis has been observed in *S. aureus*, the identification of a cell wall hydrolase being

upregulated (similar to *sceD*) in *E. faecium* is notable and may be worth further investigation (Buist et al., 2008). Furthermore, the downregulation of all proteins involved in UMP biosynthesis following BDM-I treatment may be another mechanism to limit cell wall synthesis, considering that UMP is a precuroor to UDP, which is a major component of precursors utilized in peptidoglycan synthesis.

Through whole genome sequencing, proteomics and electron microscopy, we have identified that *S. aureus* responds to BDM-I treatment through the regulation of peptidoglycan synthesis. This observation provides further evidence for the apparent MoA of BDM-I as an (in)direct inhibitor of ATP synthesis. Peptidoglycan synthesis is an essential process that requires significant amounts of energy, more so in the case of VISA isolates such as Sa375 (and Efm0002), as they have significantly thicker cell walls. This phenomenon would explain the observed alterations to the phenotype of mutant Sa375 isolates with increased resistance to BDM-I. By reverting to a VSSA cell wall phenotype, ATP that would have been required for peptidoglycan synthesis can be utilised in other essential cellular pathways, which may also explain why VISA isolates have lower BDM-I MICs compared to VSSA isolates.

7.4 Proposed Model of the BDM-I MoA

Considering the results presented in this study, which are discussed in detail above, we propose that the key BDM-I MoA is inhibition of ATP synthesis via ATP synthase and oxidative phosphorylation (outlined in Figure 7.4).

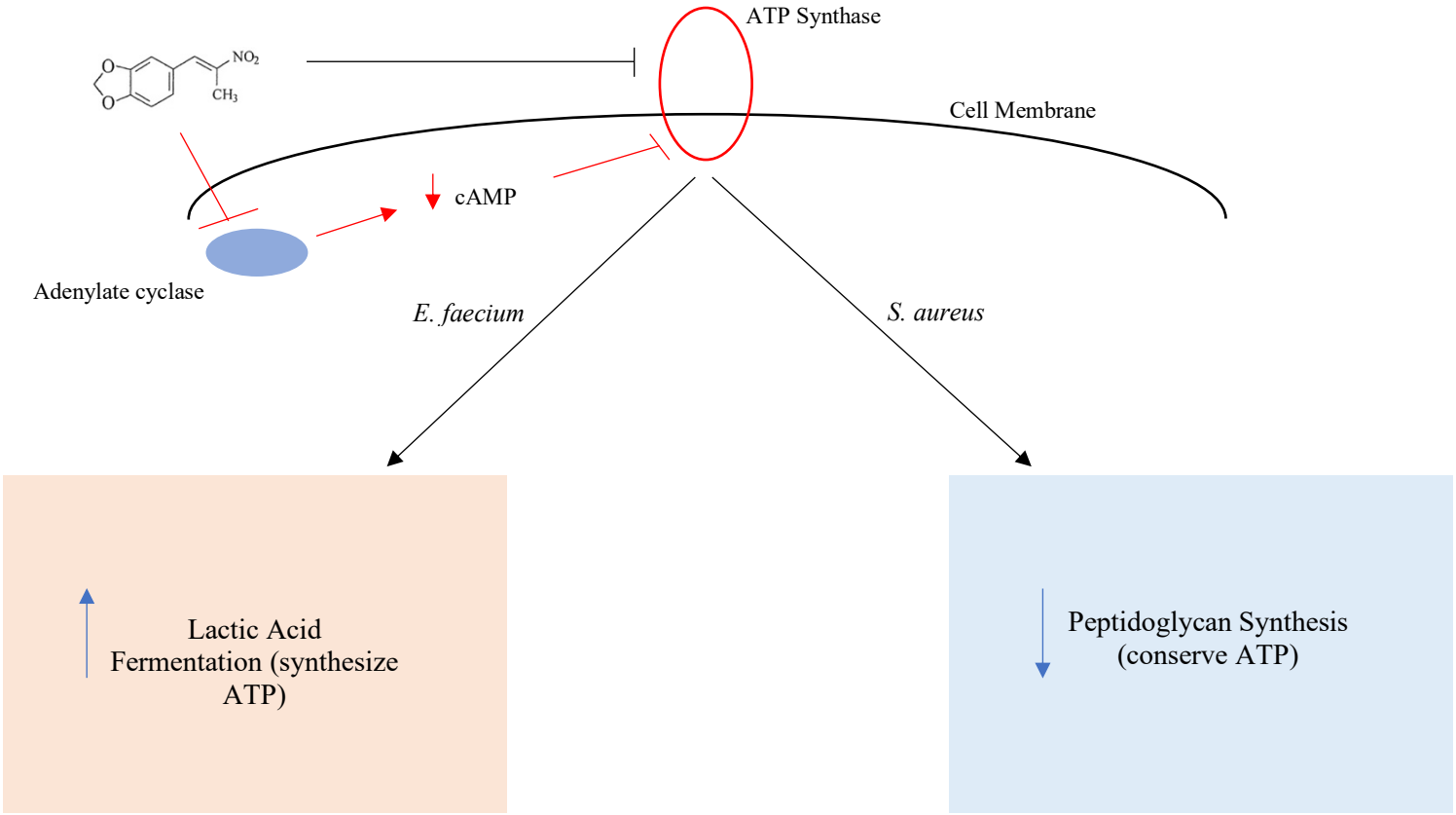

Figure 7.4 Proposed BDM-I MoA is inhibition of ATP synthase. ATP assays indicate that BDM-I treatment reduces the intracellular concentration of ATP within *S. aureus* and *E. faecium*. Proteomic and sequencing data indicates that *E. faecium* responds (and adapts) to BDM-I treatment by knocking down the activity of ATP synthase in favour of lactic acid fermentation. As *S. aureus* cannot utilize this pathway, it compensates for reduced ATP availability by repressing cellular pathways (such as peptidoglycan synthesis) that require large amounts of ATP. Red lines connecting adenylate cyclase to BDM-I and ATP synthase inhibition represent theoretical interactions which have not yet been proven experimentally.

Briefly, BDM-I inhibits ATP synthase indirectly (or possibly directly) by a currently unknown mechanism. One possible explanation could be that BDM-I negatively affects adenylate cyclase, which would result in cAMP depletion within a cell and potential repression of ATP synthase activity. In any case, how bacteria respond to this appears to be species specific, as *E. faecium* appears to utilize lactic acid fermentation as an alternative pathway to produce ATP, while *S. aureus*, which cannot utilize lactic acid fermentation, downregulates cellular processes (such as cell wall synthesis) that require large amounts of ATP. This inhibitory mechanism explains why *S. aureus* is more susceptible to BDM-I than *E. faecium* (particularly VISA isolates that need to synthesize significantly thicker cell walls) and the observed difficulty for *S. aureus* to develop increased resistance to BDM-I (compared to *E. faecium*).

7.5 Future Directions

Currently, we are unable to confidently identify the binding partner of BDM-I. While TPP analysis did identify a potential binding partner that corresponds with other results outlined in this study, the data is preliminary and requires significantly more work before conclusions can be made regarding the BDM-I target. As such, future experiments are required to optimise the TPP protocol for *S. aureus*, and to repeat the experiment on drug treated protein lysates to improve data resolution and narrow the pool of potential binding partners (Mateus et al., 2018). Additionally, TPP analysis should also be completed using *E. faecium* to confirm the BDM-I target across species, which would increase reliability of the results and proposed MoA.

It is also important to conduct further studies examining the relationship between BDM-I and cell wall synthesis in *S. aureus*. While we have confirmed that BDM-I exposure

drives mutations that favour a thinner cell wall phenotype and increased sensitivity to glycopeptide antibiotics, it is also important to study associated changes in peptidoglycan morphology and structure. Following proteomic analysis of *S. aureus*, we identified significant downregulation (≥3-fold) of all proteins involved in UMP metabolism. In this regard, previous research has identified a correlation between pyrimidine metabolism and peptidoglycan morphology in *L. lactis* (Solopova et al., 2016). Therefore, additional steps should be taken to analyse the peptidoglycan morphology within BDM-I treated MRSA.

Considering the poor success rate associated with clinical drug development, additional research could also be undertaken to identify alternative uses for BDM-I. Considering it negatively affects ATP synthase, BDM-I could potentially be used as a component of industrial antiseptics and cleaning agents to inhibit the spread of plasmids carrying multiple antibiotic resistance determinants. Plasmid partitioning (Par) systems in bacteria ensure the stable transmission of low-copy plasmids to daughter cells during cell division. These systems consist of two proteins called ParA and ParB, as well as a centromere like *parS* partition site. During cell division, ParB binds to the *parS* site forming the partition complex, and this is followed by DNA segregation which is driven by the hydrolysis of either ATP or GTP by ParA (Funnell, 2016, Brooks and Hwang, 2017). There are three well characterized partitioning systems and these are classified based on their ATPase activity; Walker-type ATPase (type I), Actin-like ATPase (type II) and Tubulin-like GTPase (type III) (Brooks and Hwang, 2017). Walker-type ATPase (type I) systems represent the most commonly observed Par systems in bacteria, and can be further divided into type Ia and type Ib subgroups (Yin et al., 2006).

Considering that ATP is required for these systems to function effectively, BDM-I could be explored as a potential inhibitor of plasmid (and therefore resistance) segregation. Preliminary work was undertaken to examine the stability of a Type 1b plasmid (pJEG1) in the presence of sub-inhibitory concentrations of BDM-I, with results finding that BDM-I treatment resulted in the rapid loss of pJEG1 in the absence of selective pressures (erythromycin) (Figure 7.5). While promising, further studies are required to confirm the potential use of BDM-I to inhibit plasmid segregation and spread amongst bacteria, particularly in a hospital environment.

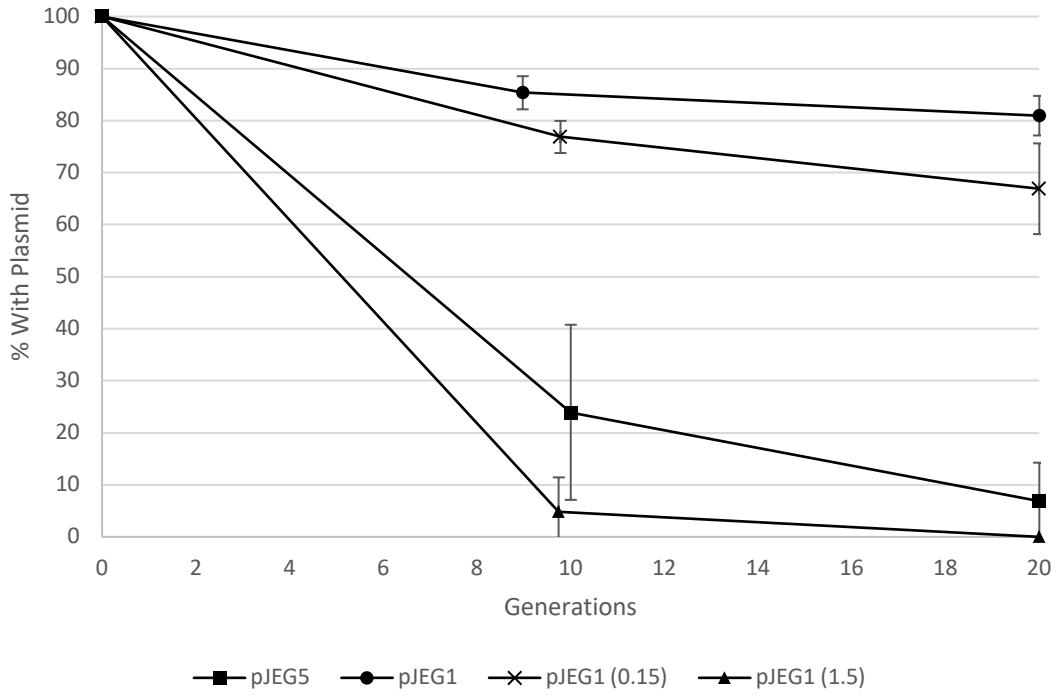

Figure 7.5 Reduced plasmid stability following treatment with BDM-I. Stability assays were performed using the S. aureus strain RN4220 containing pJEG001 treated with BDM-I (0.15 and 1.5 µg/mL) and pJEG005 as a control. Assays determined that following treatment with BDM-I and in the absence of antibiotic selection (erythromycin), the percentage of cells retaining pJEG001 decreasd to <10% within 10 generations. This trend was comparable to the pJEG005 control, which carries in inactive *parA* gene.

Finally, recent research (unpublished) has also revealed that BDM-I displays activity *in vitro* against the clinically important species *N. gonorrhoea*. *N. gonorrhoea* causes the sexually transmitted infection (STI) gonorrhoea, which is highly prevalent worldwide and increasingly difficult to treat due to a high incidence of multi-drug resistance (Unemo and Shafer, 2014). Additional MIC studies should be undertaken to examine the efficacy of BDM-I against reference *N. gonorrhoea* strains using the agar dilution method (see section 3.3).

7.6 Concluding Remarks

In order to combat the now global threat that antibiotic resistance represents, a significant shift in prioritization back to the research and development of novel antimicrobials is required by large pharmaceutical companies. Such a shift also requires strong support from relevant government bodies. However, until this happens, the primary responsibility of developing new and novel antibiotics will remain with smaller biotechnology companies and within academia, often in partnership with each other.

When developing any potential therapeutic it is critically important to broadly examine its efficacy and understand its MoA. 3,4-methylenedioxy-β-nitropropene (BDM-I) is a small molecule compound that is currently being developed at Opal Biosciences, and has emerged as a potential antimicrobial that could be used for the treatment of complicated infections caused by important hospital bacterial pathogens. One aspect of BDM-I which is not currently understood is its MoA.

A previous study by White et al confirmed that BDM-I does not target typical cellular processes associated with antibiotics, such as cell wall synthesis, nucleotide synthesis, or protein synthesis, but likely acts intracellularly by inhibiting protein tyrosine phosphatases. As part of this study, it was observed that BDM-I is readily capable of permeating the cell membrane and inhibit several bacterial virulence factors that are associated with PTP activity (White et al., 2014). In any case, while these results are interesting, the roles of PTPs in bacterial physiology are not well understood outside of their roles as secreted virulence factors. Therefore, through further studies we aimed to examine the BDM-I MoA within bacteria, as well as study its activity against the ESKAPE pathogens, which are most often associated with antibiotic resistance and nosocomial infections.

Initial studies included large scale BDM-I MIC screening using several different bacterial species, including *P. aureginosa*, *K. pneumoniae*, *E. coli*, *E. faecium* and *S. aureus*. MIC data gathered revealed that BDM-I displays no antimicrobial activity against gram-negative bacteria (of the ESKAPE pathogen group), limiting its utility to gram-positive species members. In this regard, BDM-I displayed the greatest activity against *S. aureus*, particuarly MRSA isolates with reduced susceptibility to vancomycin (hVISA and VISA). Additional checkerboard studies also revealed a synergistic relationship between BDM-I and vancomycin when used in combination against such isolates, illuminating a potential treatment option for problematic/persistent staphylococcal infections. Induction experiments also revealed the limited capacity for *S. aureus* isolates to develop increased resistance to BDM-I during prolonged periods of exposure.

Combined, these results indicate that BDM-I is a potential treatment option for MRSA, either as monotherapy or in combination with vancomycin for difficult to treat VISA isolates. While BDM-I did display activity against VRE isolates, the higher average MICs and the rapid rate at which VRE is able to develop resistance against BDM-I severely limits its usability for this pathogen in a clinical setting.

Unlike previous studies, a broader omics approach was taken to studying the BDM-I MoA, using techniques such as whole genome sequencing and proteomics. The ability to generate BDM-I mutants allowed us to explore novel mutations that are associated with increased BDM-I resistance. The discovery of mutations within ATP synthase genes (for all mutant VRE isolates) revealed an important connection between ATP synthesis and the BDM-I MoA. This was reinforced through proteomic analysis of BDM-I treated MRSA and VRE cells using 2-D gel electrophoresis and shotgun proteomics, which revealed downregulation of several subunits of ATP synthase, as well as the regulation of proteins involved in lactic acid fermentation (in the case of VRE). To study the relationship between BDM-I and ATP synthesis further, ATP assays were performed in order to identify changes in intracellular ATP concentrations following treatment with BDM-I. Subsequently, results from these assays confirmed a significant reduction in intracellular ATP levels, strongly supporting the idea that BDM-I inhibits ATP synthesis. However, without further research it is difficult to confirm whether this occurs by direct inhibition, or more likely, is occurring as a downstream consequence of BDM-I inhibiting another cellular target, the latter of which is more likely.

In any case, we propose that the primary MoA of BDM-I is the disruption of ATP synthesis by ATP synthase, which subsequently limits the availability of ATP for various

cellular processes. Additionally, we have confirmed the potential utility of BDM-I (via *in vitro* testing) as a treatment option for MRSA infections, either as monotherapy, in combination with vancomycin, or as salvage therapy in the context of vancomycin treatment failure.

Chapter 8

References

Clinical Laboratory Standards Institute, Methods for Dilution Antimicrobial Susceptibility Tests for Bacteria That Grow Aerobically: Ninth Edition: Approved Standard M07-A9, CLSI, Wayne, PA, USA, 2012.

2009. Classification of staphylococcal cassette chromosome mec (SCCmec): guidelines for reporting novel SCCmec elements. *Antimicrob Agents Chemother,* 53**,** 4961-7.

ALLEN, H. K., DONATO, J., WANG, H. H., CLOUD-HANSEN, K. A., DAVIES, J. & HANDELSMAN, J. 2010. Call of the wild: Antibiotic resistance genes in natural environments. *Nature Reviews Microbiology,* 8**,** 251-259.

ANDERSSON, D. I. & HUGHES, D. 2010. Antibiotic resistance and its cost: is it possible to reverse resistance? *Nat Rev Micro,* 8**,** 260-271.

ANDRIES, K., VERHASSELT, P., GUILLEMONT, J., GOHLMANN, H. W., NEEFS, J. M., WINKLER, H., VAN GESTEL, J., TIMMERMAN, P., ZHU, M., LEE, E., WILLIAMS, P., DE CHAFFOY, D., HUITRIC, E., HOFFNER, S., CAMBAU, E., TRUFFOT-PERNOT, C., LOUNIS, N. & JARLIER, V. 2005. A diarylquinoline drug active on the ATP synthase of Mycobacterium tuberculosis. *Science,* 307**,** 223-7.

ANTUNES, L. C. S., VISCA, P. & TOWNER, K. J. 2014. Acinetobacter baumannii: evolution of a global pathogen. *Pathogens and Disease,* 71**,** 292-301.

ARIAS, C. A. & MURRAY, B. E. 2012. The rise of the Enterococcus: beyond vancomycin resistance. *Nat Rev Microbiol,* 10**,** 266-78.

ARRELL, D. K., ELLIOTT, S. T., KANE, L. A., GUO, Y., KO, Y. H., PEDERSEN, P. L., ROBINSON, J., MURATA, M., MURPHY, A. M., MARBAN, E. & VAN EYK, J. E. 2006. Proteomic analysis of pharmacological preconditioning: novel protein targets converge to mitochondrial metabolism pathways. *Circ Res,* 99**,** 706-14.

ARZANLOU, M., CHAI, WERN C. & VENTER, H. 2017. Intrinsic, adaptive and acquired antimicrobial resistance in Gram-negative bacteria. *Essays In Biochemistry,* 61**,** 49-59.

BALEMANS, W., VRANCKX, L., LOUNIS, N., POP, O., GUILLEMONT, J., VERGAUWEN, K., MOL, S., GILISSEN, R., MOTTE, M., LANCOIS, D., DE BOLLE, M., BONROY, K., LILL, H., ANDRIES, K., BALD, D. & KOUL, A. 2012. Novel antibiotics targeting respiratory ATP synthesis in Gram-positive pathogenic bacteria. *Antimicrob Agents Chemother,* 56**,** 4131-9.

BALIBAR, C. J., SHEN, X. & TAO, J. 2009. The mevalonate pathway of Staphylococcus aureus. *Journal of bacteriology,* 191**,** 851-861.

BANDOW, J. E., BRÖTZ, H., LEICHERT, L. I. O., LABISCHINSKI, H. & HECKER, M. 2003. Proteomic Approach to Understanding Antibiotic Action. *Antimicrobial Agents and Chemotherapy,* 47**,** 948.

BARLOW, M. 2009. What Antimicrobial Resistance Has Taught Us About Horizontal Gene Transfer. *In:* GOGARTEN, M. B., GOGARTEN, J. P. & OLENDZENSKI, L. C. (eds.) *Horizontal Gene Transfer: Genomes in Flux.* Totowa, NJ: Humana Press.

BAYER, A. S., SCHNEIDER, T. & SAHL, H.-G. 2013. Mechanisms of daptomycin resistance in Staphylococcus aureus: role of the cell membrane and cell wall. *Annals of the New York Academy of Sciences,* 1277**,** 139-158.

BERENDONK, T. U., MANAIA, C. M., MERLIN, C., FATTA-KASSINOS, D., CYTRYN, E., WALSH, F., BURGMANN, H., SORUM, H., NORSTROM, M., PONS, M. N., KREUZINGER, N., HUOVINEN, P., STEFANI, S., SCHWARTZ, T., KISAND, V., BAQUERO, F. & MARTINEZ, J. L. 2015. Tackling antibiotic resistance: the environmental framework. *Nat Rev Microbiol,* 13**,** 310-7.

BLAKE, K. L., O'NEILL, A. J., MENGIN-LECREULX, D., HENDERSON, P. J. F., BOSTOCK, J. M., DUNSMORE, C. J., SIMMONS, K. J., FISHWICK, C. W. G., LEEDS, J. A. & CHOPRA, I. 2009. The nature of Staphylococcus aureus MurA and MurZ and approaches for detection of peptidoglycan biosynthesis inhibitors. *Molecular Microbiology,* 72**,** 335-343.

BOUCHER, H. W., TALBOT, G. H., BRADLEY, J. S., EDWARDS, J. E., GILBERT, D., RICE, L. B., SCHELD, M., SPELLBERG, B. & BARTLETT, J. 2009. Bad bugs, no drugs: no ESKAPE! An update from the Infectious Diseases Society of America. *Clin Infect Dis,* 48**,** 1-12.

BREIDENSTEIN, E. B. M., DE LA FUENTE-NÚÑEZ, C. & HANCOCK, R. E. W. 2011. Pseudomonas aeruginosa: all roads lead to resistance. *Trends in Microbiology,* 19**,** 419-426.

BROOKS, A. C. & HWANG, L. C. 2017. Reconstitutions of plasmid partition systems and their mechanisms. *Plasmid,* 91**,** 37-41.

BROWN, E. D. & WRIGHT, G. D. 2016. Antibacterial drug discovery in the resistance era. *Nature,* 529**,** 336-43.

BUIST, G., STEEN, A., KOK, J. & KUIPERS, O. P. 2008. LysM, a widely distributed protein motif for binding to (peptido)glycans. *Molecular Microbiology,* 68**,** 838-847.

BUSH, K. 2013. The ABCD's of β-lactamase nomenclature. *Journal of Infection and Chemotherapy,* 19**,** 549-559.

BUSH, K., COURVALIN, P., DANTAS, G., DAVIES, J., EISENSTEIN, B., HUOVINEN, P., JACOBY, G. A., KISHONY, R., KREISWIRTH, B. N., KUTTER, E., LERNER, S. A., LEVY, S., LEWIS, K., LOMOVSKAYA, O., MILLER, J. H., MOBASHERY, S., PIDDOCK, L. J. V., PROJAN, S., THOMAS, C. M., TOMASZ, A., TULKENS, P. M., WALSH, T. R., WATSON, J. D., WITKOWSKI, J., WITTE, W., WRIGHT, G., YEH, P. & ZGURSKAYA, H. I. 2011. Tackling antibiotic resistance. *Nat Rev Micro,* 9**,** 894-896.

BUSH, K. & JACOBY, G. A. 2010. Updated Functional Classification of β-Lactamases. *Antimicrobial Agents and Chemotherapy,* 54**,** 969.

BUTLER, M. S., BLASKOVICH, M. A. T. & COOPER, M. A. 2016. Antibiotics in the clinical pipeline at the end of 2015. *The Journal Of Antibiotics,* 70**,** 3.

CABEZÓN, E., RIPOLL-ROZADA, J., PEÑA, A., DE LA CRUZ, F. & ARECHAGA, I. 2015. Towards an integrated model of bacterial conjugation. *FEMS Microbiology Reviews,* 39**,** 81-95.

CAIN, J. A., SOLIS, N. & CORDWELL, S. J. 2014. Beyond gene expression: The impact of protein post-translational modifications in bacteria. *Journal of Proteomics,* 97**,** 265-286.

CATTOIR, V. & GIARD, J.-C. 2014. Antibiotic resistance in Enterococcus faecium clinical isolates. *Expert Review of Anti-Infective Therapy,* 12**,** 239-48.

CETINKAYA, Y., FALK, P. & MAYHALL, C. G. 2000. Vancomycin-Resistant Enterococci. *Clinical Microbiology Reviews,* 13**,** 686-707.

CHANG, J., KIM, Y. & KWON, H. J. 2016. Advances in identification and validation of protein targets of natural products without chemical modification. *Natural Product Reports,* 33**,** 719-730.

CHAO, J. D., WONG, D. & AV-GAY, Y. 2014. Microbial protein-tyrosine kinases. *J Biol Chem,* 289**,** 9463-72.

CHEN, C.-J., HUANG, Y.-C. & CHIU, C.-H. 2015. Multiple pathways of cross-resistance to glycopeptides and daptomycin in persistent MRSA bacteraemia. *Journal of Antimicrobial Chemotherapy,* 70**,** 2965-2972.

CHIANG, T. M., REIZER, J. & BEACHEY, E. H. 1989. Serine and tyrosine protein kinase activities in Streptococcus pyogenes. Phosphorylation of native and synthetic peptides of streptococcal M proteins. *J Biol Chem,* 264**,** 2957-62.

COLOMER-LLUCH, M., CALERO-CACERES, W., JEBRI, S., HMAIED, F., MUNIESA, M. & JOFRE, J. 2014. Antibiotic resistance genes in bacterial and bacteriophage fractions of Tunisian and Spanish wastewaters as markers to compare the antibiotic resistance patterns in each population. *Environ Int,* 73**,** 167-75.

COLOMER-LLUCH, M., IMAMOVIC, L., JOFRE, J. & MUNIESA, M. 2011. Bacteriophages carrying antibiotic resistance genes in fecal waste from cattle, pigs, and poultry. *Antimicrob Agents Chemother,* 55**,** 4908-11.

COOMBS, G. W., PEARSON, J. C., DALEY, D. A., LE, T., ROBINSON, O. J., GOTTLIEB, T., HOWDEN, B. P., JOHNSON, P. D., BENNETT, C. M., STINEAR, T. P. & TURNIDGE, J. D. 2014. Molecular epidemiology of enterococcal bacteremia in Australia. *J Clin Microbiol,* 52**,** 897-905.

COX, G. & WRIGHT, G. D. 2013. Intrinsic antibiotic resistance: Mechanisms, origins, challenges and solutions. *International Journal of Medical Microbiology,* 303**,** 287-292.

CUI, L., MA, X., SATO, K., OKUMA, K., TENOVER, F. C., MAMIZUKA, E. M., GEMMELL, C. G., KIM, M. N., PLOY, M. C., EL-SOLH, N., FERRAZ, V. & HIRAMATSU, K. 2003. Cell wall thickening is a common feature of vancomycin resistance in Staphylococcus aureus. *J Clin Microbiol,* 41**,** 5-14.

CZAPLEWSKI, L., BAX, R., CLOKIE, M., DAWSON, M., FAIRHEAD, H., FISCHETTI, V. A., FOSTER, S., GILMORE, B. F., HANCOCK, R. E. W., HARPER, D., HENDERSON, I. R., HILPERT, K., JONES, B. V., KADIOGLU, A., KNOWLES, D., ÓLAFSDÓTTIR, S., PAYNE, D., PROJAN, S., SHAUNAK, S., SILVERMAN, J., THOMAS, C. M., TRUST, T. J., WARN, P. & REX, J. H. 2016. Alternatives to antibiotics—a pipeline portfolio review. *The Lancet Infectious Diseases,* 16**,** 239-251.

DANTAS, G. & SOMMER, M. O. A. 2014. How to Fight Back Against Antibiotic Resistance. *American Scientist,* 102**,** 42-51.

DE RASMO, D., MICELLI, L., SANTERAMO, A., SIGNORILE, A., LATTANZIO, P. & PAPA, S. 2016. cAMP regulates the functional activity, coupling efficiency and structural organization of mammalian FOF1 ATP synthase. *Biochimica et Biophysica Acta (BBA) - Bioenergetics,* 1857**,** 350-358.

DECKERS-HEBESTREIT, G. & ALTENDORF, K. 1996. The F0F1-type ATP synthases of bacteria: structure and function of the F0 complex. *Annu Rev Microbiol,* 50**,** 791-824.

DELAUNÉ, A., DUBRAC, S., BLANCHET, C., POUPEL, O., MÄDER, U., HIRON, A., LEDUC, A., FITTING, C., NICOLAS, P., CAVAILLON, J.-M., ADIB-CONQUY, M. & MSADEK, T. 2012. The WalKR System Controls Major Staphylococcal Virulence Genes and Is Involved in Triggering the Host Inflammatory Response. *Infection and Immunity,* 80**,** 3438-3453.

DENISENKO, P. P., SAPRONOV, N. S. & TARASENKO, A. A. 2010. Antimicrobial and radioprotective compounds. Google Patents.

DOI, Y. 2018. Lactic acid fermentation is the main aerobic metabolic pathway in Enterococcus faecalis metabolizing a high concentration of glycerol. *Applied Microbiology and Biotechnology,* 102**,** 10183-10192.

DUBRAC, S., BISICCHIA, P., DEVINE, K. M. & MSADEK, T. 2008. A matter of life and death: cell wall homeostasis and the WalKR (YycGF) essential signal transduction pathway. *Mol Microbiol,* 70**,** 1307-22.

DUBRAC, S., BONECA, I. G., POUPEL, O. & MSADEK, T. 2007. New Insights into the WalK/WalR (YycG/YycF) Essential Signal Transduction Pathway Reveal a Major Role in Controlling Cell Wall Metabolism and Biofilm Formation in Staphylococcus aureus</em&gt. *Journal of Bacteriology,* 189**,** 8257.

ELEK, S. D. 1956. Principles and Problems of Combined Antibiotic Therapy. *Postgraduate Medical Journal,* 32**,** 324-327.

ESPOSITO, S. & DE SIMONE, G. 2017. Update on the main MDR pathogens: prevalence and treatment options. *Infez Med,* 25**,** 301-310.

EVANS, B. A. & AMYES, S. G. B. 2014. OXA β-Lactamases. *Clinical Microbiology Reviews,* 27**,** 241.

FISCHBACH, M. A. 2011. Combination therapies for combating antimicrobial resistance. *Current opinion in microbiology,* 14**,** 519-523.

FISCHBACH, M. A. & WALSH, C. T. 2009. Antibiotics for emerging pathogens. *Science,* 325**,** 1089-93.

FOLKESSON, A., JELSBAK, L., YANG, L., JOHANSEN, H. K., CIOFU, O., HOIBY, N. & MOLIN, S. 2012. Adaptation of Pseudomonas aeruginosa to the cystic fibrosis airway: an evolutionary perspective. *Nat Rev Microbiol,* 10**,** 841-51.

FOURNIER, P.-E., VALLENET, D., BARBE, V., AUDIC, S., OGATA, H., POIREL, L., RICHET, H., ROBERT, C., MANGENOT, S., ABERGEL, C., NORDMANN, P., WEISSENBACH, J., RAOULT, D. & CLAVERIE, J.-M. 2006. Comparative Genomics of Multidrug Resistance in Acinetobacter baumannii. *PLoS Genetics,* 2**,** e7.

FREIBERG, C., FISCHER, H. P. & BRUNNER, N. A. 2005. Discovering the mechanism of action of novel antibacterial agents through transcriptional profiling of conditional mutants. *Antimicrob Agents Chemother,* 49**,** 749-59.

FRENCH, G. L. 2010. The continuing crisis in antibiotic resistance. *International Journal of Antimicrobial Agents,* 36, Supplement 3**,** S3-S7.

FUCHS, S., PANÉ-FARRÉ, J., KOHLER, C., HECKER, M. & ENGELMANN, S. 2007. Anaerobic Gene Expression in Staphylococcus aureus</em&gt. *Journal of Bacteriology,* 189**,** 4275.

FUNNELL, B. E. 2016. ParB Partition Proteins: Complex Formation and Spreading at Bacterial and Plasmid Centromeres. *Frontiers in Molecular Biosciences,* 3**,** 44.

GE, R. & SHAN, W. 2011. Bacterial Phosphoproteomic Analysis Reveals the Correlation Between Protein Phosphorylation and Bacterial Pathogenicity. *Genomics, Proteomics & Bioinformatics,* 9**,** 119-127.

GOSBELL, I. B. 2014. VISA and hVISA in hospitals. *Microbiology Australia,* 35**,** 29-34.

GOULD, I. M., DAVID, M. Z., ESPOSITO, S., GARAU, J., LINA, G., MAZZEI, T. & PETERS, G. 2012. New insights into meticillin-resistant Staphylococcus aureus (MRSA) pathogenesis, treatment and resistance. *Int J Antimicrob Agents,* 39**,** 96-104.

GRANGEASSE, C., COZZONE, A. J., DEUTSCHER, J. & MIJAKOVIC, I. 2007. Tyrosine phosphorylation: an emerging regulatory device of bacterial physiology. *Trends Biochem Sci,* 32**,** 86-94.

GRILO, I. R., LUDOVICE, A. M., TOMASZ, A., DE LENCASTRE, H. & SOBRAL, R. G. 2014. The glucosaminidase domain of Atl - the major Staphylococcus aureus autolysin - has DNA-binding activity. *MicrobiologyOpen,* 3**,** 247-256.

HALL, B. G. & BARLOW, M. 2004. Evolution of the serine beta-lactamases: past, present and future. *Drug Resist Updat,* 7**,** 111-23.

HAMMER, K., KILSTRUP, M., RUHDAL JENSEN, P. & MARTINUSSEN, J. 2005. Nucleotide metabolism and its control in lactic acid bacteria. *FEMS Microbiology Reviews,* 29**,** 555-590.

HARRIS, P., PATERSON, D. & ROGERS, B. 2015. Facing the challenge of multidrug-resistant gram-negative bacilli in Australia. *Med J Aust,* 202**,** 243-7.

HENSON, K. E., LEVINE, M. T., WONG, E. A. & LEVINE, D. P. 2015. Glycopeptide antibiotics: evolving resistance, pharmacology and adverse event profile. *Expert Rev Anti Infect Ther,* 13**,** 1265-78.

HIDRON, A. I., EDWARDS, J. R., PATEL, J., HORAN, T. C., SIEVERT, D. M., POLLOCK, D. A. & FRIDKIN, S. K. 2008. NHSN annual update: antimicrobial-resistant pathogens associated with healthcare-associated infections: annual summary of data reported to the National Healthcare Safety Network at the Centers for Disease Control and Prevention, 2006-2007. *Infect Control Hosp Epidemiol,* 29**,** 996-1011.

HIRAMATSU, K., HANAKI, H., INO, T., YABUTA, K., OGURI, T. & TENOVER, F. C. 1997. Methicillin-resistant Staphylococcus aureus clinical strain with reduced vancomycin susceptibility. *J Antimicrob Chemother,* 40**,** 135-6.

HOWDEN, B. P., DAVIES, J. K., JOHNSON, P. D., STINEAR, T. P. & GRAYSON, M. L. 2010. Reduced vancomycin susceptibility in Staphylococcus aureus, including vancomycin-intermediate and heterogeneous vancomycin-intermediate strains: resistance mechanisms, laboratory detection, and clinical implications. *Clin Microbiol Rev,* 23**,** 99-139.

HOWDEN, B. P., MCEVOY, C. R. E., ALLEN, D. L., CHUA, K., GAO, W., HARRISON, P. F., BELL, J., COOMBS, G., BENNETT-WOOD, V., PORTER, J. L., ROBINS-

BROWNE, R., DAVIES, J. K., SEEMANN, T. & STINEAR, T. P. 2011. Evolution of Multidrug Resistance during Staphylococcus aureus Infection Involves Mutation of the Essential Two Component Regulator WalKR. *PLoS Pathogens,* 7**,** e1002359.

HUTTER, B., SCHAAB, C., ALBRECHT, S., BORGMANN, M., BRUNNER, N. A., FREIBERG, C., ZIEGELBAUER, K., ROCK, C. O., IVANOV, I. & LOFERER, H. 2004. Prediction of mechanisms of action of antibacterial compounds by gene expression profiling. *Antimicrob Agents Chemother,* 48**,** 2838-44.

IOERGER, T. R., O'MALLEY, T., LIAO, R., GUINN, K. M., HICKEY, M. J., MOHAIDEEN, N., MURPHY, K. C., BOSHOFF, H. I., MIZRAHI, V., RUBIN, E. J., SASSETTI, C. M., BARRY, C. E., 3RD, SHERMAN, D. R., PARISH, T. & SACCHETTINI, J. C. 2013. Identification of new drug targets and resistance mechanisms in Mycobacterium tuberculosis. *PLoS One,* 8**,** e75245.

JACOBY, G. A. 2009. AmpC β-Lactamases. *Clinical Microbiology Reviews,* 22**,** 161.

JARICK, M., BERTSCHE, U., STAHL, M., SCHULTZ, D., METHLING, K., LALK, M., STIGLOHER, C., STEGER, M., SCHLOSSER, A. & OHLSEN, K. 2018. The serine/threonine kinase Stk and the phosphatase Stp regulate cell wall synthesis in Staphylococcus aureus. *Scientific Reports,* 8**,** 13693.

JIANG, T., GAO, C., MA, C. & XU, P. 2014. Microbial lactate utilization: enzymes, pathogenesis, and regulation. *Trends in Microbiology,* 22**,** 589-599.

KANE, L. A. & VAN EYK, J. E. 2009. Post-translational modifications of ATP synthase in the heart: biology and function. *J Bioenerg Biomembr,* 41**,** 145-50.

KANG, H.-K. & PARK, Y. 2015. Glycopeptide Antibiotics: Structure and Mechanisms of Action. *J Bacteriol Virol,* 45**,** 67-78.

KELLEY, P. G., GAO, W., WARD, P. B. & HOWDEN, B. P. 2011. Daptomycin non-susceptibility in vancomycin-intermediate Staphylococcus aureus (VISA) and heterogeneous-VISA (hVISA): implications for therapy after vancomycin treatment failure. *Journal of Antimicrobial Chemotherapy,* 66**,** 1057-1060.

KELLIHER, J. L., RADIN, J. N., GRIM, K. P., PÁRRAGA SOLÓRZANO, P. K., DEGNAN, P. H. & KEHL-FIE, T. E. 2018. Acquisition of the Phosphate Transporter NptA Enhances Staphylococcus aureus Pathogenesis by Improving Phosphate Uptake in Divergent Environments. *Infection and Immunity,* 86**,** e00631-17.

KMIETOWICZ, Z. 2017. Few novel antibiotics in the pipeline, WHO warns. *BMJ,* 358.

KO, K. S., LEE, J. Y., SONG, J. H., BAEK, J. Y., CHUN, J. S. & YOON, H. S. 2006. Screening of Essential Genes in Staphylococcus aureus N315 Using Comparative Genomics and Allelic Replacement Mutagenesis. v. 16.

KOHANSKI, M. A., DWYER, D. J. & COLLINS, J. J. 2010. How antibiotics kill bacteria: from targets to networks. *Nat Rev Microbiol,* 8**,** 423-35.

KREISWIRTH, B. N., LÖFDAHL, S., BETLEY, M. J., O'REILLY, M., SCHLIEVERT, P. M., BERGDOLL, M. S. & NOVICK, R. P. 1983. The toxic shock syndrome exotoxin structural gene is not detectably transmitted by a prophage. *Nature,* 305**,** 709-712.

KUROKAWA, K., NISHIDA, S., ISHIBASHI, M., MIZUMURA, H., UENO, K., YUTSUDO, T., MAKI, H., MURAKAMI, K. & SEKIMIZU, K. 2008. Staphylococcus aureus MurC Participates in l-Alanine Recognition via Histidine 343, a Conserved Motif in the Shallow Hydrophobic Pocket. *The Journal of Biochemistry,* 143**,** 417-424.

LEVY, S. B. & MARSHALL, B. 2004. Antibacterial resistance worldwide: causes, challenges and responses. *Nat Med,* 10**,** S122-9.

LEWIS, K. 2013. Platforms for antibiotic discovery. *Nat Rev Drug Discov,* 12**,** 371-87.

LEWIS, K. 2016. New approaches to antimicrobial discovery. *Biochem Pharmacol*.

LIN, M. H., SUGIYAMA, N. & ISHIHAMA, Y. 2015. Systematic profiling of the bacterial phosphoproteome reveals bacterium-specific features of phosphorylation. *Sci Signal,* 8**,** rs10.

LIU, Y. Y., WANG, Y., WALSH, T. R., YI, L. X., ZHANG, R., SPENCER, J., DOI, Y., TIAN, G., DONG, B., HUANG, X., YU, L. F., GU, D., REN, H., CHEN, X., LV, L., HE, D., ZHOU, H., LIANG, Z., LIU, J. H. & SHEN, J. 2016. Emergence of plasmid-mediated

colistin resistance mechanism MCR-1 in animals and human beings in China: a microbiological and molecular biological study. *Lancet Infect Dis,* 16**,** 161-8.
LOMENICK, B., HAO, R., JONAI, N., CHIN, R. M., AGHAJAN, M., WARBURTON, S., WANG, J., WU, R. P., GOMEZ, F., LOO, J. A., WOHLSCHLEGEL, J. A., VONDRISKA, T. M., PELLETIER, J., HERSCHMAN, H. R., CLARDY, J., CLARKE, C. F. & HUANG, J. 2009. Target identification using drug affinity responsive target stability (DARTS). *Proceedings of the National Academy of Sciences,* 106**,** 21984.
LOMENICK, B., OLSEN, R. W. & HUANG, J. 2011. Identification of Direct Protein Targets of Small Molecules. *ACS Chemical Biology,* 6**,** 34-46.
MACEK, B., MIJAKOVIC, I., OLSEN, J. V., GNAD, F., KUMAR, C., JENSEN, P. R. & MANN, M. 2007. The serine/threonine/tyrosine phosphoproteome of the model bacterium Bacillus subtilis. *Mol Cell Proteomics,* 6**,** 697-707.
MATEUS, A., BOBONIS, J., KURZAWA, N., STEIN, F., HELM, D., HEVLER, J., TYPAS, A. & SAVITSKI, M. M. 2018. Thermal proteome profiling in bacteria: probing protein state in vivo. *Mol Syst Biol,* 14**,** e8242.
MATEUS, A., MÄÄTTÄ, T. A. & SAVITSKI, M. M. 2017. Thermal proteome profiling: unbiased assessment of protein state through heat-induced stability changes. *Proteome Science,* 15**,** 13.
MCDERMOTT, P. F., WALKER, R. D. & WHITE, D. G. 2003. Antimicrobials: modes of action and mechanisms of resistance. *Int J Toxicology,* 22.
MCGUINNESS, W. A., MALACHOWA, N. & DELEO, F. R. 2017. Vancomycin Resistance in Staphylococcus aureus. *The Yale journal of biology and medicine,* 90**,** 269-281.
MOELLERING, R. C., JR. 1992. Emergence of Enterococcus as a Significant Pathogen. *Clinical Infectious Diseases,* 14**,** 1173-1176.
MONK, I. R., SHAH, I. M., XU, M., TAN, M. W. & FOSTER, T. J. 2012. Transforming the untransformable: application of direct transformation to manipulate genetically Staphylococcus aureus and Staphylococcus epidermidis. *MBio,* 3.
MONK, I. R., TREE, J. J., HOWDEN, B. P., STINEAR, T. P. & FOSTER, T. J. 2015. Complete Bypass of Restriction Systems for Major Staphylococcus aureus Lineages. *MBio,* 6**,** e00308-15.
MUNITA, J. M. & ARIAS, C. A. 2016. Mechanisms of Antibiotic Resistance. *Microbiology spectrum,* 4**,** 10.1128/microbiolspec.VMBF-0016-2015.
NAVON-VENEZIA, S., KONDRATYEVA, K. & CARATTOLI, A. 2017. Klebsiella pneumoniae: a major worldwide source and shuttle for antibiotic resistance. *FEMS Microbiol Rev,* 41**,** 252-275.
NORMARK, B. H. & NORMARK, S. 2002. Evolution and spread of antibiotic resistance. *Journal of Internal Medicine,* 252**,** 91-106.
O'DRISCOLL, T. & CRANK, C. W. 2015. Vancomycin-resistant enterococcal infections: epidemiology, clinical manifestations, and optimal management. *Infection and Drug Resistance,* 8**,** 217-230.
ORHAN, G., BAYRAM, A., ZER, Y. & BALCI, I. 2005. Synergy tests by E test and checkerboard methods of antimicrobial combinations against Brucella melitensis. *J Clin Microbiol,* 43**,** 140-3.
PAI, M. Y., LOMENICK, B., HWANG, H., SCHIESTL, R., MCBRIDE, W., LOO, J. A. & HUANG, J. 2015. Drug Affinity Responsive Target Stability (DARTS) for Small Molecule Target Identification. *Methods in molecular biology (Clifton, N.J.),* 1263**,** 287-298.
PARK, J. & PEI, D. 2004. trans-Beta-nitrostyrene derivatives as slow-binding inhibitors of protein tyrosine phosphatases. *Biochemistry,* 43**,** 15014-21.
PARTRIDGE, S. R., KWONG, S. M., FIRTH, N. & JENSEN, S. O. 2018. Mobile Genetic Elements Associated with Antimicrobial Resistance. *Clinical Microbiology Reviews,* 31.
PENDLETON, J. N., GORMAN, S. P. & GILMORE, B. F. 2013. Clinical relevance of the ESKAPE pathogens. *Expert Review of Anti-Infective Therapy,* 11**,** 297-308.
PESCHEL, A., JACK, R. W., OTTO, M., COLLINS, L. V., STAUBITZ, P., NICHOLSON, G., KALBACHER, H., NIEUWENHUIZEN, W. F., JUNG, G., TARKOWSKI, A., VAN

KESSEL, K. P. M. & VAN STRIJP, J. A. G. 2001. Resistance to Human Defensins and Evasion of Neutrophil Killing via the Novel Virulence Factor Mprf Is Based on Modification of Membrane Lipids with Lysine. *The Journal of Experimental Medicine,* 193**,** 1067-1076.

PESCHEL, A., OTTO, M., JACK, R. W., KALBACHER, H., JUNG, G. & GOTZ, F. 1999. Inactivation of the dlt operon in Staphylococcus aureus confers sensitivity to defensins, protegrins, and other antimicrobial peptides. *J Biol Chem,* 274**,** 8405-10.

POGUE, J. M., MANN, T., BARBER, K. E. & KAYE, K. S. 2013. Carbapenem-resistant Acinetobacter baumannii: epidemiology, surveillance and management. *Expert Review of Anti-infective Therapy,* 11**,** 383-393.

POIREL, L., BONNIN, R. A. & NORDMANN, P. 2011. Genetic basis of antibiotic resistance in pathogenic Acinetobacter species. *IUBMB Life,* 63**,** 1061-1067.

PRISIC, S., DANKWA, S., SCHWARTZ, D., CHOU, M. F., LOCASALE, J. W., KANG, C. M., BEMIS, G., CHURCH, G. M., STEEN, H. & HUSSON, R. N. 2010. Extensive phosphorylation with overlapping specificity by Mycobacterium tuberculosis serine/threonine protein kinases. *Proc Natl Acad Sci U S A,* 107**,** 7521-6.

QI, Y., KOBAYASHI, Y. & HULETT, F. M. 1997. The pst operon of Bacillus subtilis has a phosphate-regulated promoter and is involved in phosphate transport but not in regulation of the pho regulon. *Journal of Bacteriology,* 179**,** 2534-2539.

QUEENAN, A. M. & BUSH, K. 2007. Carbapenemases: the versatile beta-lactamases. *Clin Microbiol Rev,* 20**,** 440-58, table of contents.

RAMSEY M, H. A., HUYCKE M. 2014. The Physiology and Metabolism of Enterococci. *Enterococci: From Commensals to Leading Causes of Drug Resistant Infection.*

RAO, N. N. & TORRIANI, A. 1990. Molecular aspects of phosphate transport in Escherichia coli. *Mol Microbiol,* 4**,** 1083-90.

RASAMIRAVAKA, T., LABTANI, Q., DUEZ, P. & EL JAZIRI, M. 2015. The Formation of Biofilms by Pseudomonas aeruginosa: A Review of the Natural and Synthetic Compounds Interfering with Control Mechanisms. *BioMed Research International,* 2015**,** 17.

RYAN, R. P. & DOW, J. M. 2008. Diffusible signals and interspecies communication in bacteria. *Microbiology,* 154**,** 1845-58.

SANTAJIT, S. & INDRAWATTANA, N. 2016. Mechanisms of Antimicrobial Resistance in ESKAPE Pathogens. *BioMed Research International,* 2016**,** 2475067.

SCHENK, S. & LADDAGA, R. A. 1992. Improved method for electroporation of Staphylococcus aureus. *FEMS Microbiology Letters,* 94**,** 133-138.

SENIOR, A. E., NADANACIVA, S. & WEBER, J. 2002. The molecular mechanism of ATP synthesis by F1F0-ATP synthase. *Biochimica et Biophysica Acta (BBA) - Bioenergetics,* 1553**,** 188-211.

SHOJI, M., CUI, L., IIZUKA, R., KOMOTO, A., NEOH, H. M., WATANABE, Y., HISHINUMA, T. & HIRAMATSU, K. 2011. walK and clpP mutations confer reduced vancomycin susceptibility in Staphylococcus aureus. *Antimicrob Agents Chemother,* 55**,** 3870-81.

SHOUSHA, A., AWAIWANONT, N., SOFKA, D., SMULDERS, F. J., PAULSEN, P., SZOSTAK, M. P., HUMPHREY, T. & HILBERT, F. 2015. Bacteriophages Isolated from Chicken Meat and the Horizontal Transfer of Antimicrobial Resistance Genes. *Appl Environ Microbiol,* 81**,** 4600-6.

SILBERGELD, E. K., GRAHAM, J. & PRICE, L. B. 2008. Industrial Food Animal Production, Antimicrobial Resistance, and Human Health. *Annual Review of Public Health,* 29**,** 151-169.

SKOV, R., CHRISTIANSEN, K., DANCER, S. J., DAUM, R. S., DRYDEN, M., HUANG, Y.-C. & LOWY, F. D. 2012. Update on the prevention and control of community-acquired meticillin-resistant Staphylococcus aureus (CA-MRSA). *International Journal of Antimicrobial Agents,* 39**,** 193-200.

SOLDO, B., LAZAREVIC, V., PAGNI, M. & KARAMATA, D. 1999. Teichuronic acid operon of Bacillus subtilis 168. *Molecular Microbiology,* 31**,** 795-805.

SOLOPOVA, A., FORMOSA-DAGUE, C., COURTIN, P., FURLAN, S., VEIGA, P., PÉCHOUX, C., ARMALYTE, J., SADAUSKAS, M., KOK, J., HOLS, P., DUFRÊNE, Y. F., KUIPERS, O. P., CHAPOT-CHARTIER, M.-P. & KULAKAUSKAS, S. 2016. Regulation of Cell Wall Plasticity by Nucleotide Metabolism in Lactococcus lactis. *The Journal of biological chemistry,* 291**,** 11323-11336.

SOPIRALA, M. M., MANGINO, J. E., GEBREYES, W. A., BILLER, B., BANNERMAN, T., BALADA-LLASAT, J. M. & PANCHOLI, P. 2010. Synergy testing by Etest, microdilution checkerboard, and time-kill methods for pan-drug-resistant Acinetobacter baumannii. *Antimicrob Agents Chemother,* 54**,** 4678-83.

SOUFI, B., GNAD, F., JENSEN, P. R., PETRANOVIC, D., MANN, M., MIJAKOVIC, I. & MACEK, B. 2008. The Ser/Thr/Tyr phosphoproteome of Lactococcus lactis IL1403 reveals multiply phosphorylated proteins. *Proteomics,* 8**,** 3486-93.

STAPLETON, M. R., HORSBURGH, M. J., HAYHURST, E. J., WRIGHT, L., JONSSON, I.-M., TARKOWSKI, A., KOKAI-KUN, J. F., MOND, J. J. & FOSTER, S. J. 2007. Characterization of IsaA and SceD, two putative lytic transglycosylases of Staphylococcus aureus. *Journal of bacteriology,* 189**,** 7316-7325.

STEFANI, S., CHUNG, D. R., LINDSAY, J. A., FRIEDRICH, A. W., KEARNS, A. M., WESTH, H. & MACKENZIE, F. M. 2012. Meticillin-resistant Staphylococcus aureus (MRSA): global epidemiology and harmonisation of typing methods. *International Journal of Antimicrobial Agents,* 39**,** 273-282.

SUN, X., GE, F., XIAO, C.-L., YIN, X.-F., GE, R., ZHANG, L.-H. & HE, Q.-Y. 2010. Phosphoproteomic Analysis Reveals the Multiple Roles of Phosphorylation in Pathogenic Bacterium Streptococcus pneumoniae. *Journal of Proteome Research,* 9**,** 275-282.

THANGAMANI, S., MOHAMMAD, H., ABUSHAHBA, M. F. N., SOBREIRA, T. J. P., HEDRICK, V. E., PAUL, L. N. & SELEEM, M. N. 2016. Antibacterial activity and mechanism of action of auranofin against multi-drug resistant bacterial pathogens. *Scientific reports,* 6**,** 22571-22571.

THOMAS, C. M. & NIELSEN, K. M. 2005. Mechanisms of, and barriers to, horizontal gene transfer between bacteria. *Nat Rev Microbiol,* 3**,** 711-21.

TYPAS, A., BANZHAF, M., GROSS, C. A. & VOLLMER, W. 2011. From the regulation of peptidoglycan synthesis to bacterial growth and morphology. *Nat Rev Microbiol,* 10**,** 123-36.

UNEMO, M. & SHAFER, W. M. 2014. Antimicrobial Resistance in Neisseria gonorrhoeae in the 21st Century: Past, Evolution, and Future. *Clinical Microbiology Reviews,* 27**,** 587.

VAN HAL, S. J., STEEN, J. A., ESPEDIDO, B. A., GRIMMOND, S. M., COOPER, M. A., HOLDEN, M. T. G., BENTLEY, S. D., GOSBELL, I. B. & JENSEN, S. O. 2013. In vivo evolution of antimicrobial resistance in a series of Staphylococcus aureus patient isolates: the entire picture or a cautionary tale? *Journal of Antimicrobial Chemotherapy*.

VESTERGAARD, M., NØHR-MELDGAARD, K., BOJER, M. S., KROGSGÅRD NIELSEN, C., MEYER, R. L., SLAVETINSKY, C., PESCHEL, A. & INGMER, H. 2017. Inhibition of the ATP Synthase Eliminates the Intrinsic Resistance of Staphylococcus aureus towards Polymyxins. *mBio,* 8**,** e01114-17.

VIGNAROLI, C., RINALDI, C. & VARALDO, P. E. 2011. Striking "seesaw effect" between daptomycin nonsusceptibility and beta-lactam susceptibility in Staphylococcus haemolyticus. *Antimicrob Agents Chemother,* 55**,** 2495-6; author reply 296-7.

VON WINTERSDORFF, C. J. H., PENDERS, J., VAN NIEKERK, J. M., MILLS, N. D., MAJUMDER, S., VAN ALPHEN, L. B., SAVELKOUL, P. H. M. & WOLFFS, P. F. G. 2016. Dissemination of Antimicrobial Resistance in Microbial Ecosystems through Horizontal Gene Transfer. *Frontiers in Microbiology,* 7.

WACKER, S. A., HOUGHTALING, B. R., ELEMENTO, O. & KAPOOR, T. M. 2012. Using transcriptome sequencing to identify mechanisms of drug action and resistance. *Nat Chem Biol,* 8**,** 235-237.

WALSH, C. 2000. Molecular mechanisms that confer antibacterial drug resistance. *Nature,* 406**,** 775-81.

WANG, Y. & CHIU, J.-F. 2008. Proteomic approaches in understanding action mechanisms of metal-based anticancer drugs. *Metal-based drugs,* 2008**,** 716329-716329.

WEBER, J. 2010. Structural biology: Toward the ATP synthase mechanism. *Nat Chem Biol,* 6**,** 794-795.

WHITE, K. 2008. *The antimicroboial mechanism of action of 3,4-methylenedioxy-beta-nitropropene.* Doctor of Philosophy, RMIT.

WHITE, K. S., NICOLETTI, G. & BORLAND, R. 2014. Nitropropenyl Benzodioxole, An Anti-Infective Agent with Action as a Protein Tyrosine Phosphatase Inhibitor. *The Open Medicinal Chemistry Journal,* 8**,** 1-16.

WHITMORE, S. E. & LAMONT, R. J. 2012. Tyrosine phosphorylation and bacterial virulence. *Int J Oral Sci,* 4**,** 1-6.

WILLETTS, N. S. & FINNEGAN, D. J. 1970. Characteristics of E. coli K12 strains carrying both an F prime and an R factor. *Genetical Research,* 16**,** 113-122.

WILLSKY, G. R., BENNETT, R. L. & MALAMY, M. H. 1973. Inorganic Phosphate Transport in Escherichia coli: Involvement of Two Genes Which Play a Role in Alkaline Phosphatase Regulation. *Journal of Bacteriology,* 113**,** 529-539.

WISPLINGHOFF, H., BISCHOFF, T., TALLENT, S. M., SEIFERT, H., WENZEL, R. P. & EDMOND, M. B. 2004. Nosocomial bloodstream infections in US hospitals: analysis of 24,179 cases from a prospective nationwide surveillance study. *Clin Infect Dis,* 39**,** 309-17.

WYRES, K. L. & HOLT, K. E. 2018. Klebsiella pneumoniae as a key trafficker of drug resistance genes from environmental to clinically important bacteria. *Current Opinion in Microbiology,* 45**,** 131-139.

YANG, S.-J., XIONG, Y. Q., BOYLE-VAVRA, S., DAUM, R., JONES, T. & BAYER, A. S. 2010. Daptomycin-Oxacillin Combinations in Treatment of Experimental Endocarditis Caused by Daptomycin-Nonsusceptible Strains of Methicillin-Resistant Staphylococcus aureus with Evolving Oxacillin Susceptibility (the "Seesaw Effect"). *Antimicrobial Agents and Chemotherapy,* 54**,** 3161-3169.

YIN, P., LI, T. Y., XIE, M. H., JIANG, L. & ZHANG, Y. 2006. A Type Ib ParB protein involved in plasmid partitioning in a gram-positive bacterium. *J Bacteriol,* 188**,** 8103-8.

ZHENG, J. J., SINHA, D., WAYNE, K. J. & WINKLER, M. E. 2016. Physiological Roles of the Dual Phosphate Transporter Systems in Low and High Phosphate Conditions and in Capsule Maintenance of Streptococcus pneumoniae D39. *Frontiers in Cellular and Infection Microbiology,* 6.

Chapter 9

Appendix

Supplementary Table 1: Mutations Identified within day 8 Efm003 Mutant Isolates

Series	Colony	Mutation	AA Change	Gene	Product
1	1	G→T	Gly235Val	EFAU004_00433	SPFH Domain/Band 7 family protein
	2	C→T	Gln171*	EFAU004_00165	M-protein Trans-acting positive regulator
		C→A	Leu7Ile	EFAU004_02233	Transcriptional regulator, Fis family
		C→T	Gly366Arg	*guaB*	Inosine-5-monophosphate dehydrogenase
	3	C→T	Gln57*	EFAU004_00165	M-protein Trans-acting positive regulator
		C→A	Arg254Leu	EFAU004_01140	Helix-turn-helix protein
2	1	G→T	Glu134*	EFAU004_00165	M-protein Trans-acting positive regulator
		G→A	Ala869Val	EFAU004_02606	Transcription repair coupling factor
	2	C→A	Thr443Lys	EFAU004_00165	M-protein Trans-acting positive regulator
		C→A	Gln184Lys	EFAU004_1360	Beta-lactamase
	3**	-	-	-	-
3	1	G→A	Asp51Asn	EFAU004_00117	Translation initiation factor, IF-1
		G→T	Ala230Asp	EFAU004_00162	Glycerol uptake facilitator protein
		G→A	Thr159Ile	EFAU004_00965	Dihydroorotate dehydrogenase, electron transfer subunit
	2	G→T	Glu275*	EFAU004_00165	M-protein Trans-acting positive regulator
	3	DEL	Gly173fs	EFAU004_00165	M-protein Trans-acting positive regulator

**No mutations identified within colony 3

Supplementary Table 2: Mutations identified within final day Efm003 Mutant Isolates

Series	Colony(s)	Mutation	AA Change	Gene	Product
1	1-3	C→A	Thr172Asn	*ylov*	DAK2 domain fusion protein YIoV
	1-3	C→T	Met27Ile	*apt*	adenine phosphoribosyltransferase
	1-3	C→A	Glu*	*fur*	transcriptional regulator, FUR family
	1-3	G→A	Trp104*	EFAU004_01238	hypothetical protein
	1-3	C→G	Ser214Thr	EFAU004_01286	Transcriptional regulator, FUR family
	1-3	C→A	Glu*	EFAU004_01802	acetolactate synthase
	1-3	C→A	Asp138Tyr	EFAU004_02036	cardiolipin synthetase
	1-3	G→T	Thr111Lys	*atpB*	ATP synthase subunit C
	1-3	T→C	Ile316Val	*relA*	GTP diphosphokinase

Supplementary Table 3: Mutations identified within day 8 Efm008 Mutant Isolates

Series	Colony	Mutation	AA Change	Gene	Product
1	1	INS	-	*atpE*	ATP Synthase F0 subunit c
	2	INS	-	*atpG*	ATP synthase F1 gamma subunit
	3	DEL	Ile456fs	*atpD*	ATP synthase F1 beta subunit
2	1	C→A	Val323Leu	EFAU004_00970	Uracil permease
		DEL	Gly38fs	*atpF*	ATP synthase F0 B subunit
	2	A→C	Tyr304*	*atpD*	ATP synthase F1 beta subunit
		G→T	Phe3Leu	*yycH*	YycH protein
		C→A	Gly228Val	*aspS*	Aspartyl-tRNA synthetase
	3	INS	-	*atpF*	ATP synthase F0 subunit b
3	1	INS	-	*atpE*	ATP synthase F0 subunit c
	2	T→C	Phe348Leu	EFAU004_00143	Bifunctional glutamate-cysteine ligase/glutathione synthetase
		A→C	Tyr197*	*atpD*	ATP synthase F1 beta subunit
		C→A	Pro197His	*mleA*	Malic enzyme NAD binding domain protein
		C→A	Ala180Ser	EFAU004_02132	Phage portal protein HK97 family
	3	INS	-	*atpB*	ATP synthase F0 subunit a

Supplementary Table 4: Mutations identified within day 58 Efm008 Mutant Isolates

Series	Colony(s)	Mutation	AA Change	Gene	Product
1	1-3	C→A	Ala257Asp	EFAU004_00083	ABC transporter permease protein
	1-3	G→A	Trp201*	EFAU004_00165	M protein trans acting positive regulator
	1-3	C→A	Asn392Lys	*recN*	DNA repair protein RecN
	1-3	A→G	Ile231Thr	EFAU004_01257	PTS system, galactitol specific IIC component
	1-3	C→A	Gly178Cys	*atpD*	ATP synthase F1, beta subunit
	1-3	C→A	Asp49Tyr	EFAU004_02425	PAS domain sensory box histidine kinase
	1-3	C→A	Ser181Ile	*relA*	GTP diphosphokinase
2	1-3	G→T	Glu227*	*pip*	Phage binding protein
	1-3	C→A	Ser76Ile	EFAU004_01744	UDP-glucose-4-epimerase
	1-3	G→T	Gln409Lys	*atpD*	ATP synthase F1 beta subunit
	1-3	C→A	Asp31Tyr	EFAU004_02349	Extracellular solute binding protein
	1-3	G→A	Pro48Leu	EFAU004_02477	GTP diphosphokinase
	1-3	C→A	Arg810Leu	EFAU004_02487	snf2 family protein
	1-3	G→T	Ala24Glu	EFAU004_02618	Serine/threonine protein-kinase
3	1-3	C→A	Ala198Glu	EFAU004_00177	DNA mismatch repair protein
	1-3	G→T	Glu186Asp	EFAU004_00284	Hypothetical protein
	1-3	C→A	Phe161Leu	EFAU004_00640	Hypothetical protein
	1-3	G→T	Ser144Tyr	EFAU004_01007	N-acetylmuramoyl-L-alanine-amidase
	1-3	C→A	Trp363Cys	*gnd*	6-phosphogluconoate dehydrogenase, decarboxylating
	1-3	C→A	Met338Ile	EFAU004_01883	Cation transporter E1-E2 family ATPase
	1-3	C→A	Ala576Ser	*ntpI*	V-type ATP synthase subunit I
	1-3	C→A	Asp99Tyr	EFAU004_02425	Pas domain sensory box histidine kinase

Supplementary Table 5: Mutations identified within final day Sa375 Mutant Isolates

Series	Colony(s)	Mutation	AA Change	Gene	Product
1	1-3	C→T	Leu37Phe	*walK*	Mutli-sensor signal transduction histidine kinase
	1-3	C→T	Pro45Leu	*rpoC*	DNA directed RNA polymerase beta chain protein
	1-3	G→T	Pro82His	*mvaA*	Hydroxymethylglutaryl-CoA reductase
2	1-3	G→A	Gly560Ser	*walK*	Multi-sensor signal transduction histidine kinase
	1-3	G→A	Gly36Arg	SAA6008_00223	oxidoreductase, zinc-binding dehydrogenase family
	1-3	C→A	Thr331Lys	SAA6008_00647	sodium/hydrogen exchanger family protein
	1-3	G→A	Ala814Val	*atl*	bifunctional N-acetylmuramoyl-L-alanine amidase/endo-beta-N-acetylglucosaminidase
	1-3	C→T	Ala210Val	*potD*	spermidine/putrescine ABC superfamily ATP binding cassette transporter, binding protein
	1-3	C→T	Trp124*	SAA6008_01077	conserved hypothetical protein
	1-3	C→T	Arg154*	*efb*	fibrinogen-binding protein precursor
	1-3	T→A	Phe790Leu	*fmtC (mprF)*	oxacillin resistance-related FmtC protein
	1-3	C→T	Ala109Thr	SAA6008_01543	SigmaW regulon antibacterial protein
	1-3	C→T	Thr73Ile	SAA6008_01966	ABC-2 type transport system permease protein
	1-3	G→A	Leu146Phe	*nrgA*	AMT family ammonium or ammonia transporter
	1-3	G→A	Pro231Ser	*rpbB*	50S ribosomal protein L2
	1-3	C→A	Glu154*	SAA6008_02318	acetyltransferase (GNAT) family protein
	1-3	C→T	Gly97Arg	SAA6008_02767	transcriptional regulator, Cro/Cl family
	1-3	G→A	Met365Ile	*ileS*	isoleucyl-tRNA synthetase
	1-3	G→A	Pro116Ser	*murA*	putative UDP-N-acetylglucosamine 1-carboxyvinyltransferase
	1-3	G→A	Gln131*	SAA6008_01768	prolyl oligopeptidase
	1-3	G→A	Gly206Arg	*pabB*	anthranilate synthase component I and chorismate binding protein
	1-3	T→G	Phe88Val	*rsgA*	ribosome small subunit-dependent GTPase A
	1-3	T→C	Leu1461Ser	*yukA*	DNA segregation ATPase like protein
	1-3	A→G	Thr4Ala	*Cap5A*	capsular polysaccharide biosynthesis protein
3	1-3	G→T	Gly30Trp	*walK*	Multi-sensor signal transduction histidine kinase
	1-3	G→A	Ala29Thr	*mvaK2*	phosphomevalonate kinase
	1-3	C→T	Arg207Cys	SAA6008_00647	sodium/hydrogen exchanger family protein
	1-3	G→T	Gly113*	*trkA*	NAD+ binding potassium transporter
	1-3	C→T	Ser42Leu	SAA6008_00679	putative phosphate uptake regulator
	1-3	G→A	Val103Met	SAA6008_00851	phage protein

Supplementary Table 6: Proteins downregulated within Sa057 (≥2-fold) following exposure to BDM-I

Protein ID	Annotation	Log_2 Fold Change (Treated vs WT)	Peptide Count
ADL65445.1	threonine dehydratase	-78.3386864	13
ADL64206.1	bifunctional acetaldehyde-CoA/alcohol dehydrogenase	-60.93074444	55
ADL66445.1	respiratory nitrate reductase, alpha subunit	-52.9772531	59
ADL64332.1	putative membrane protein	-47.25758378	36
ADL65037.1	glycosyl transferase, group 1 family protein	-32.0913884	24
ADL64308.1	cell division and morphogenesis-related protein scdA	-17.49459732	12
ADL64355.1	secreted acid phosphatase	-14.53853543	12
ADL66244.1	6-phospho-beta-galactosidase	-13.61714621	18
ADL64271.1	formate C-acetyltransferase	-10.53505692	68
ADL64107.1	multi-sensor signal transduction histidine kinase, WalK	-9.21419286	15
ADL64288.1	L-lactate dehydrogenase	-8.748175592	15
ADL66644.1	putative dihydroorotate dehydrogenase	-6.855137534	25
ADL66495.1	glycine betaine/choline ABC superfamily ATP binding cassette transporter, ABC protein	-6.841772152	11
ADL64682.1	zinc-binding alcohol dehydrogenase	-6.470065085	19
ADL64301.1	Putative polyribitolphosphotransferase	-6.438815694	24
ADL65200.1	putative dihydroorotase	-5.694503817	25
ADL66097.1	autoinducer sensor protein response regulator protein	-5.674180422	10
ADL65199.1	aspartate carbamoyltransferase catalytic subunit	-5.338100128	14
ADL66344.1	staphylococcal accessory regulator R, SarR	-5.313715031	5
ADL64170.1	immunoglobulin G binding protein A	-5.248837005	5
ADL65201.1	putative carbamoyl-phosphate synthase, pyrimidine-specific, small chain	-4.968032867	14
ADL64335.1	putative secretion system component EssB	-4.76814551	8
ADL65202.1	putative carbamoyl-phosphate synthase, pyrimidine-specific, large chain	-4.449515778	55
ADL65964.1	nitric-oxide synthase, oxygenase subunit	-4.263064876	12
ADL64290.1	inosine/uridine-preferring nucleoside hydrolase	-4.154048896	3

Supplementary Table 6 *continued*

Protein ID	Annotation	Log_2 Fold Change (Treated vs WT)	Peptide Count
ADL65082.1	putative SAM-dependent methyltransferase	-4.078166283	12
ADL66357.1	molybdopterin oxidoreductase	-4.067159972	40
ADL64171.1	staphylococcal accessory regulator A, SarH2	-4.062007357	12
ADL64113.1	rRNA large subunit methyltransferase	-4.008504358	10
ADL64287.1	nitric oxide dioxygenase	-3.954988289	26
ADL66105.1	putative ABC transporter ATP-binding protein	-3.859808138	17
ADL66561.1	D-lactate dehydrogenase	-3.790363083	32
ADL64341.1	conserved hypothetical protein	-3.613467058	3
ADL65204.1	putative orotate phosphoribosyltransferase	-3.599849446	8
ADL64972.1	ATP-dependent nuclease subunit A	-3.553605213	20
ADL65014.1	putative permease	-3.528115076	5
ADL66568.1	L-serine dehydratase, iron-sulfur-dependent, beta subunit	-3.500429185	7
ADL65218.1	Ribosomal RNA large subunit methyltransferase N, Rlmn	-3.497626429	19
ADL64250.1	type-I restriction-modification system restriction endonuclease subunit	-3.483128459	23
ADL66356.1	conserved hypothetical protein	-3.449172577	6
ADL64331.1	ESAT-6/WXG100 family secreted protein EsxA/YukE	-3.328987043	7
ADL66262.1	putative acetolactate synthase	-3.322187076	18
ADL64938.1	D-alanine membrane transfer protein	-3.18006715	2
ADL66655.1	L-lactate dehydrogenase 2	-3.153587563	17
ADL66692.1	immunodominant antigen B	-3.142508865	9
ADL65108.1	inositol monophosphatase	-3.128015277	7
ADL65643.1	Sec family Type I general secretory pathway preprotein translocase subunit YajC	-3.084574195	3
ADL66528.1	DEAD/H helicase / Type III restriction enzyme, res subunit	-2.82182902	30
ADL65203.1	putative orotidine 5'-phosphate decarboxylase	-2.818874378	10
ADL65364.1	amino acid carrier protein (sodium/alanine symporter)	-2.716251467	7

Supplementary Table 6 *continued*

Protein ID	Annotation	Log_2 Fold Change (Treated vs WT)	Peptide Count
ADL64774.1	fructose 1-phosphate kinase	-2.687885938	5
ADL64727.1	dihydroxyacetone kinase, phosphotransfer subunit	-2.628047446	4
ADL64686.1	iron (Fe3+) ABC superfamily ATP binding cassette transporter, binding protein	-2.53994924	13
ADL66529.1	NUDIX hydrolase	-2.511587694	10
ADL66401.1	multidrug resistance protein A, drug resistance transporter	-2.495911693	11
ADL64563.1	pur operon repressor	-2.46218884	11
ADL66654.1	alpha-acetolactate decarboxylase	-2.426411658	5
ADL66233.1	aerobactin biosynthesis protein, IucA/IucC family	-2.393765324	12
ADL64632.1	poly (glycerol-phosphate) alpha-glucosyltransferase	-2.363133898	6
ADL65149.1	putative succinate dehydrogenase iron-sulfur protein	-2.361213793	19
ADL64542.1	alpha, alpha-phosphotrehalase	-2.340916978	23
ADL64481.1	recombinational DNA repair ATPase, RecF 1	-2.286391655	25
ADL66305.1	acetyltransferase (GNAT) family protein	-2.245055566	8
ADL66431.1	conserved hypothetical protein	-2.236593347	13
ADL65847.1	transcriptional regulator Fur family protein	-2.226509728	2
ADL64772.1	putative prolyl-tRNA synthetase	-2.218619038	4
ADL65646.1	crossover junction endodeoxyribonuclease	-2.218522277	12
ADL66390.1	ABC superfamily ATP binding cassette transporter, ABC protein	-2.206746157	14
ADL66567.1	L-serine dehydratase, iron-sulfur-dependent, alpha subunit	-2.202348394	12
ADL64747.1	conserved hypothetical protein	-2.195095231	3
ADL65583.1	radical SAM domain protein	-2.144928234	17
ADL66162.1	ATP synthase subunit gamma, AtpG	-2.134067086	14
ADL64663.1	conserved hypothetical protein	-2.125674099	8
ADL66129.1	alanine racemase 1	-2.093932952	10
ADL64791.1	allophanate hydrolase subunit 1	-2.085491982	12

Supplementary Table 6 *continued*

Protein ID	Annotation	Log_2 Fold Change (Treated vs WT)	Peptide Count
ADL65958.1	adenylosuccinate lyase	-2.077549751	24
ADL64659.1	phosphomevalonate kinase	-2.074897261	18
ADL64715.1	teichoic acid biosynthesis protein B	-2.032342007	7
ADL65975.1	acyl-coenzyme A:6-aminopenicillanic acid acyl-transferase	-2.022737258	7
ADL65501.1	two component transcriptional regulator, winged helix family	-2.019039521	14
ADL64228.1	conserved hypothetical protein	-2.016422082	9
ADL65212.1	primosomal protein N prime	-2.01424942	9
ADL65917.1	conserved hypothetical protein	-2.013212855	5
ADL65063.1	putative quinol oxidase polypeptide II precursor	-2.00312755	29
ADL66301.1	30S ribosomal protein S10	-2.000056663	10
ADL65958.1	adenylosuccinate lyase	-2.077549751	24

Supplementary Table 7: Proteins upregulated within Sa057 (≥2-fold) following exposure to BDM-I

Protein ID	Annotation	Log_2 Fold Change (Treated vs WT)	Peptide Count
ADL66154.1	transglycosylase	34.50375643	6
ADL64875.1	osmotically inducible protein OsmC	13.16270146	7
ADL65629.1	luciferase family oxidoreductase	6.433228181	12
ADL66559.1	glyoxalase/bleomycin resistance protein/dioxygenase superfamily protein	5.437865627	10
ADL65585.1	ribosomal protein L11 methyltransferase	4.910310404	10
ADL64551.1	DNA polymerase III, delta prime subunit	4.227090545	7
ADL66091.1	nitroreductase family protein	4.147105225	9
ADL66741.1	rhodanese domain sulfurtransferase	4.100034435	17
ADL65852.1	Lipid A export ATP-binding/permease protein MsbA	3.949098196	11
ADL64635.1	GlcNAc-PI de-N-acetylase	3.93037638	7
ADL64592.1	D-isomer specific 2-hydroxyacid dehydrogenase family protein	3.810606402	15
ADL66340.1	urease accessory protein UreE	3.737455131	6
ADL65518.1	glyoxalase/bleomycin resistance protein/dioxygenase superfamily protein	3.689545107	7
ADL65343.1	catalase	3.454203144	25
ADL64979.1	ATPase subunit of an ATP-dependent protease, ClpB	3.406325523	54
ADL66074.1	conserved hypothetical protein	3.364733779	2
ADL65282.1	putative CDP-diacylglycerol--glycerol-3-phosphate 3-phosphatidyltransferase	3.212117942	3
ADL64586.1	putative transcriptional regulator, GntR family	3.065023048	4
ADL66739.1	base-induced perplasmic lipid-binding protein	3.05423771	11
ADL64451.1	Nitroreductase family protein	2.970383107	8
ADL65861.1	intracellular protease	2.925664068	10
ADL64397.1	putative bacteriophage envelope protein	2.923949773	2
ADL65531.1	putative exodeoxyribonuclease VII small subunit	2.911255911	3
ADL64257.1	FMN-dependent NADH-azoreductase, AzoR	2.897438876	7
ADL66625.1	beta-lactamase regulatory protein	2.817311488	14

Supplementary Table 7 *continued*

Protein ID	Annotation	Log_2 Fold Change (Treated vs WT)	Peptide Count
ADL64590.1	Firmicute transcriptional repressor of class III stress genes	2.79416438	7
ADL66087.1	co-chaperonin GroEL	2.788330614	35
ADL64593.1	Clp protease ATP binding subunit	2.767540333	79
ADL65515.1	AraC family transcriptional regulator	2.694627491	7
ADL65286.1	conserved hypothetical protein	2.670937981	10
ADL64588.1	pyridoxine biosynthesis amidotransferase	2.664503624	10
ADL66080.1	succinyl-diaminopimelate desuccinylase	2.662257767	10
ADL64961.1	NADH:flavin oxidoreductase / NADH oxidase family protein	2.638600371	24
ADL66210.1	PTS system mannitol-specific IIBC component	2.629936417	8
ADL64921.1	SUF system FeS assembly protein	2.619284294	7
ADL65586.1	chaperone protein DnaJ	2.591884162	14
ADL66339.1	urease, alpha subunit	2.567173323	15
ADL65188.1	alanine racemase	2.54684881	13
ADL65371.1	4-oxalocrotonate tautomerase	2.540961098	2
ADL65716.1	thiol peroxidase	2.515635858	13
ADL65177.1	conserved hypothetical protein	2.51527679	26
ADL64208.1	capsular polysaccharide biosynthesis protein Cap5B	2.504169227	5
ADL65588.1	heat shock molecular chaperone protein	2.470605208	25
ADL64648.1	putative uracil-DNA glycosylase	2.456007626	9
ADL64225.1	putative aldehyde dehydrogenase	2.450589659	29
ADL66650.1	low molecular weight phosphotyrosine protein phosphatase	2.436743015	3
ADL64639.1	putative 6-phospho-3-hexuloisomerase	2.436707181	9
ADL65000.1	transcriptional regulator Spx	2.412416046	7
ADL66615.1	short chain dehydrogenase	2.382488134	8
ADL66088.1	co-chaperonin GroES	2.373084031	7

Supplementary Table 7 *continued*

Protein ID	Annotation	Log_2 Fold Change (Treated vs WT)	Peptide Count
ADL64842.1	putative ATP-dependent Clp protease proteolytic subunit	2.368380809	13
ADL65778.1	arsenate reductase (glutaredoxin)	2.364841024	5
ADL64580.1	redox regulated Hsp33-like chaperonin	2.364639974	14
ADL64578.1	hypoxanthine-guanine phosphoribosyltransferase	2.357999056	11
ADL66464.1	2,3-bisphosphoglycerate-dependent phosphoglycerate mutase	2.28507014	10
ADL66560.1	nitroreductase family protein	2.283796937	15
ADL65587.1	molecular chaperone DnaK	2.282979795	60
ADL65577.1	putative metalloprotease	2.279382837	5
ADL66617.1	putative hydrolase/acyltransferase	2.278951875	23
ADL64722.1	iron (Fe3+) ABC superfamily ATP binding cassette transporter, ABC protein	2.269510151	12
ADL64932.1	conserved hypothetical protein	2.254961682	3
ADL66647.1	3-demethylubiquinone-9 3-methyltransferase	2.248803828	13
ADL65019.1	UDP-glucose diacylglycerol glucosyltransferase	2.246684013	7
ADL64691.1	conserved hypothetical protein	2.243634022	3
ADL65690.1	glyceraldehyde-3-phosphate dehydrogenase (phosphorylating)	2.239396544	14
ADL65620.1	caffeoyl-CoA O-methyltransferase	2.232089552	9
ADL64877.1	nitroreductase family protein	2.230423906	5
ADL65561.1	superoxide dismutase Mn/Fe family protein	2.211703299	17
ADL64223.1	heme-degrading monooxygenase IsdI	2.2001967	4
ADL65437.1	Scaffold protein Nfu/NifU N terminal	2.199657712	7
ADL65735.1	acetyl-coenzyme A synthetase	2.191851199	7
ADL66213.1	putative mannitol-1-phosphate 5-dehydrogenase	2.187265028	20
ADL65715.1	Adenine-specific DNA methylase-like protein	2.1832174	11
ADL65426.1	acetyltransferase, GNAT family protein	2.177895593	4
ADL65209.1	putative guanylate kinase	2.177670498	9

Supplementary Table 7 *continued*

Protein ID	Annotation	Log_2 Fold Change (Treated vs WT)	Peptide Count
ADL65224.1	50S ribosomal protein L28	2.164712451	5
ADL64544.1	acetyltransferase (GNAT) family protein	2.137555556	5
ADL66229.1	iron-dicitrate transporter substrate-binding subunit, FecB	2.128032793	29
ADL65005.1	adenylate cyclase	2.118276879	10
ADL66212.1	phosphoenolpyruvate-dependent sugar phosphotransferase system, EIIA 2, MtlA_1	2.11782364	10
ADL64316.1	glycoside hydrolase, family 1	2.095924561	16
ADL66225.1	conserved hypothetical protein	2.091357282	6
ADL65743.1	UDP-N-acetylmuramate--L-alanine ligase murC	2.090310744	25
ADL66595.1	MerTP family mercury (Hg2+) permease, binding protein MerP	2.070150033	4
ADL65299.1	DNA-directed DNA polymerase III gamma and tau subunits	2.039124622	45
ADL66104.1	redox-sensing transcriptional repressor rex	2.034930665	17
ADL66334.1	iron (Fe+3) ABC superfamily ATP binding cassette transporter, binding protein	2.028436455	27
ADL64939.1	D-alanine-activating enzyme/D-alanine-D-alanyl, dltC protein	2.026606349	2
ADL65681.1	MutT/Nudix hydrolase family protein	2.006159589	14

Supplementary Table 8: Proteins downregulated within Efm008 (≥2-fold) following exposure to BDM-I

Protein ID	Annotation	Log_2 Fold Change (Treated vs WT)	Peptide Count
AFC64337.1	SIS domain protein	-26.65753425	14
AFC63565.1	glycosyl transferase family 8	-18.34897994	14
AFC62125.1	6-phospho-beta-galactosidase	-17.69985836	15
AFC64206.1	L-lactate oxidase	-13.76819181	17
AFC64703.1	Primosomal protein N'	-11.32424812	13
AFC64341.1	PTS system, mannose/fructose/sorbose-specific IIB component	-10.45982677	8
AFC64854.1	D-alanyl-D-alanine dipeptidase	-7.641660784	2
AFC64656.1	PTS system, cellobiose-specific IIB component	-7.6310165	5
AFC64187.1	fructose-1,6-bisphosphatase	-5.212541395	24
AFC63020.1	oxidoreductase family, NAD-binding Rossmann fold protein	-5.117372394	9
AFC62972.1	bacterial extracellular solute-binding protein	-4.931218253	11
AFC62876.1	acetyltransferase	-4.22286793	13
AFC62979.1	amidase	-4.12809139	26
AFC62871.1	PTS system, lactose/cellobiose-specific IIA component	-4.015847339	5
AFC62417.1	zinc-containing alcohol dehydrogenase	-3.803904902	13
AFC62763.1	PTS system, mannose/fructose/sorbose-specific IIB component	-3.755647764	11
AFC62870.1	PTS system, lactose/cellobiose-specific IIB component	-3.742572944	4
AFC63023.1	PTS system, ascorbate-specific IIB component	-3.573722893	3
AFC63024.1	PTS system, ascorbate-specific IIC component	-3.572409326	3
AFC64648.1	16S rRNA pseudouridylate synthase A	-3.534789793	5
AFC62980.1	bacterial extracellular solute-binding protein, family 3	-3.534028866	16
AFC63054.1	Aspartate carbamoyltransferase	-3.400024803	14
AFC62412.1	PTS system, lactose/cellobiose-specific IIB component	-3.205072675	5
AFC62580.1	phosphoenolpyruvate carboxykinase	-3.047501988	28
AFC63240.1	pyridine nucleotide-disulfide oxidoreductase	-3.045390499	16

Supplementary Table 8 *continued*

Protein ID	Annotation	Log_2 Fold Change (Treated vs WT)	Peptide Count
AFC62165.1	cytidine deaminase	-2.985996965	7
AFC62968.1	peroxiredoxin, Ohr family protein	-2.983057004	9
AFC63751.1	hypothetical protein	-2.84221956	6
AFC63850.1	choloylglycine hydrolase family protein	-2.793723077	4
AFC62515.1	transcriptional regulator, PadR family	-2.719153564	4
AFC63052.1	carbamoyl-phosphate synthase, small subunit	-2.686446011	8
AFC63562.1	oxidoreductase, short chain dehydrogenase/reductase family protein	-2.679993499	14
AFC64706.1	hypothetical protein	-2.649911504	3
AFC62598.1	Manganese containing catalase	-2.64033264	17
AFC64752.1	mannosyl-glycoprotein endo-beta-N-acetylglucosaminidase	-2.63634943	15
AFC64195.1	ribonuclease HIII	-2.51457448	8
AFC63566.1	glycosyl transferase family 8	-2.49900728	6
AFC64142.1	ATP synthase F1, gamma subunit	-2.419258373	10
AFC64761.1	Bacterial transcription activator	-2.349567171	8
AFC62461.1	pyridine nucleotide-disulfide oxidoreductase	-2.316142089	8
AFC64381.1	alpha/beta hydrolase fold protein	-2.312429104	11
AFC63143.1	universal stress protein UspA	-2.27554741	9
AFC64111.1	hypothetical protein	-2.263393819	54
AFC63413.1	glycosyl transferase	-2.262510629	2
AFC62528.1	ribokinase	-2.215064147	5
AFC62548.1	cystathionine gamma-synthase	-2.20862705	8
AFC64437.1	hypothetical protein	-2.199606041	8
AFC63006.1	site-specific tyrosine recombinase XerC-family	-2.175168307	8
AFC64522.1	glutaredoxin	-2.152388994	3
AFC64509.1	DNA-binding response regulator	-2.127355247	16

Supplementary Table 8 *continued*

Protein ID	Annotation	Log_2 Fold Change (Treated vs WT)	Peptide Count
AFC62478.1	dihydroxyacetone kinase, phosphotransfer subunit	-2.116424722	6
AFC62344.1	phosphomevalonate kinase	-2.115003575	13
AFC62546.1	glutathione peroxidase	-2.10446904	4
AFC62747.1	Acetyltransferase, GNAT family	-2.092021596	4
AFC62488.1	tyrosine decarboxylase	-2.091990875	28
AFC64739.1	DNA repair protein RadA	-2.089862645	13
AFC62983.1	hypothetical protein	-2.070057016	7
AFC62480.1	dihydroxyacetone kinase, DhaL subunit	-2.058653369	9
AFC62712.1	hypothetical protein	-2.052891436	8
AFC63047.1	orotate phosphoribosyltransferase	-2.045554142	6
AFC62723.1	ABC transporter ATP-binding protein	-2.020137511	4
AFC62594.1	toxin-antitoxin system, antitoxin component, AbrB family	-2.007049054	3

Supplementary Table 9: Proteins upregulated within Efm008 (≥2-fold) following exposure to BDM-I

Protein ID	Annotation	Log_2 Fold Change (Treated vs WT)	Peptide Count
AFC63340.1	Class II Aldolase and Adducin N-terminal domain protein	30.54215653	10
AFC62472.1	coenzyme A disulfide reductase	7.454184564	27
AFC63235.1	LysM domain-containing protein	7.454097246	4
AFC64602.1	adenine deaminase	7.108953144	9
AFC64750.1	nitroreductase family protein	6.581129344	13
AFC63131.1	nitroreductase family protein	4.923962658	18
AFC64516.1	Substrate binding domain of ABC-type glycine betaine transport system	3.869457152	8
AFC63338.1	glyoxalase family protein	3.48252801	9
AFC64005.1	cadmium-translocating P-type ATPase	3.463106231	14
AFC64926.1	Glutathione reductase	3.413432185	27
AFC62308.1	30S ribosomal protein S14	3.223476172	4;1
AFC62693.1	deoxynucleoside kinase	3.115803123	9
AFC63575.1	major cold shock protein CspA	2.962165782	4
AFC64768.1	zinc-binding alcohol dehydrogenase family protein	2.919130909	14
AFC64349.1	ABC transporter, ATP-binding protein	2.819601738	25
AFC64281.1	hypothetical protein	2.77449745	3
AFC63030.1	L-lactate dehydrogenase	2.769151037	16
AFC63645.1	sodium/dicarboxylate symporter family protein	2.762107504	9
AFC63873.1	sulfatase	2.477181745	10
AFC64365.1	oligopeptide ABC superfamily ATP binding cassette transporter, binding protein	2.393125324	10
AFC64569.1	HAD superfamily hydrolase	2.300032418	9
AFC63980.1	hypothetical protein	2.224204534	5
AFC62627.1	tRNA-specific 2-thiouridylase MnmA	2.212	22
AFC64941.1	tRNA modification GTPase MnmE	2.154207069	23
AFC62720.1	putative flavoprotein NrdI	2.142066795	2

Supplementary Table 9 *continued*

Protein ID	Annotation	Log_2 Fold Change (Treated vs WT)	Peptide Count
AFC64409.1	ABC transporter, ATP-binding protein/permease	2.123501098	12
AFC63886.1	acetolactate synthase	2.079857935	26
AFC63794.1	riboflavin biosynthesis protein RibF	2.059165154	11
AFC62623.1	Putative cysteine desulfurase	2.058215674	11
AFC62736.1	uracil-DNA glycosylase	2.056703901	8
AFC62553.1	dihydrodipicolinate synthase	2.044401286	6
AFC63118.1	ABC transporter, permease protein	2.043657765	3
AFC63110.1	(3R)-hydroxymyristoyl-	2.00862528	13

Supplementary Table 10: TPP Raw Data

Protein ID	Annotation[a]	vehiclelogFCheated	treatedlogFCheated	Peptide Count
ADL65759.1	putative flavoprotein	-1.9234386	-0.1826861	2
ADL66624.1	transcriptional repressor	-2.3438984	-0.9501199	2
ADL65633.1	DNA-directed DNA polymerase III gamma and tau subunits	-3.6683702	-1.0059938	3
ADL65578.1	phosphate starvation-inducible ATPase	-3.725101	-0.7705093	4
ADL65793.1	aldo/keto reductase	-1.4047512	-0.6590122	12
ADL65179.1	S-adenosyl-methyltransferase MraW	-1.1105394	-0.3852162	8
ADL64305.1	ribitol-5-phosphate dehydrogenase	-1.589581	-0.5765594	9
ADL64542.1	alpha, alpha-phosphotrehalase	-4.5103661	-2.283215249	7
ADL66181.1	putative transcriptional regulator	-0.9870488	-0.302047412	6
ADL64626.1	deoxynucleoside kinase	-1.6474427	-0.572427227	2
ADL65625.1	exodeoxyribonuclease V alpha chain	-1.0850242	-0.578700808	2
ADL64609.1	methyltransferase small domain protein	-1.8537793	-0.71497432	9
ADL66298.1	50S ribosomal protein L23	-1.4430294	-0.364077475	12
ADL66299.1	50S ribosomal protein L4	-1.1960211	-0.528465019	18
ADL66207.1	haloacid dehalogenase-like hydrolase	-1.8853719	-0.926597717	5
ADL64560.1	dimethyladenosine transferase	-1.1609899	-0.291207266	10
ADL65528.1	putative DNA repair protein	-1.7296668	-0.556939062	13
ADL65629.1	luciferase family oxidoreductase	-1.724091	-0.0722193	7
ADL65511.1	pyrroline-5-carboxylate reductase	-1.9719112	-0.9132596	6
ADL65005.1	adenylate cyclase	-1.8791887	-0.1089413	5
ADL65744.1	FtsK/SpoIIIE (DNA translocase stage III) family protein	-1.2085907	-0.3590943	20
ADL66318.1	molybdenum cofactor biosynthesis protein A	-1.39003	-0.6014978	6
ADL65924.1	phage protein	-2.1239442	-0.3870147	6
ADL65055.1	acetyltransferase, GNAT family	-2.1829768	-0.7389112	4
ADL66712.1	putative flavin reductase	-1.380061	-0.484067	2

Supplementary Table 10 *continued*

Protein ID	Annotation	vehiclelogFCheated	treatedlogFCheated	Peptide Count
ADL64404.1	putative cyclase enzyme	1.94042584	0.88777655	3
ADL64718.1	Serine-type D-Ala-D-Ala carboxypeptidase	2.57674405	1.02454728	2
ADL65267.1	conserved hypothetical protein	2.11247141	0.92036414	6
ADL66358.1	cell envelope-related function transcriptional attenuator, LytR/CpsA family	2.74549852	1.27519418	10
ADL65731.1	Trypsin-like serine endoprotease	2.21904052	0.85659023	5
ADL66329.1	molybdenum (Mo2+) ABC superfamily ATP binding cassette transporter, binding protein	2.30828856	0.84278013	8
ADL64125.1	penicillin-binding protein 2 prime	2.1608036	0.6394437	19
ADL66462.1	amino acid ABC superfamily ATP binding cassette transporter, binding protein	3.03769188	0.86112219	23
ADL65093.1	putative cell-wall binding lipoprotein, YkyA	2.75358204	1.41299675	19
ADL64810.1	ABC-type siderophore binding protein	2.86063992	1.27903032	4
ADL64442.1	putative secreted protease inhibitor	2.36382903	0.42493416	11
ADL65827.1	peptidylprolyl isomerase, PrsA	2.5901633	0.79515768	23
ADL65363.1	DNA topoisomerase (ATP-hydrolyzing) ParC	2.26323987	0.10277375	3
ADL64550.1	conserved hypothetical protein	2.91443879	1.02375092	4
ADL65833.1	transcriptional regulator	0.40793007	0.17115798	9
ADL65931.1	conserved hypothetical protein	1.16678002	0.89471604	8
ADL65592.1	putative 30S ribosomal protein S20	0.61007039	0.09721033	9
ADL64762.1	MarR family transcriptional regulator	1.7521588	0.4372054	11
ADL66123.1	RNA polymerase sigma factor SigB	0.97850859	0.41281521	5
ADL66394.1	isopentenyl-diphosphate delta-isomerase	0.79677979	0.22570414	15
ADL65543.1	glycine dehydrogenase (decarboxylating) subunit 2	1.17451036	0.82575423	21
ADL64411.1	conserved hypothetical protein	0.65849023	0.15664664	3
ADL65918.1	phage protein	1.03567352	0.54949669	3
ADL64798.1	histidinol-phosphate aminotransferase	1.6010087	0.3330248	2

Supplementary table 10 *continued*

Protein ID	Annotation	vehiclelogFCheated	treatedlogFCheated	Peptide Count
ADL66229.1	iron-dicitrate transporter substrate-binding subunit, FecB	1.4163958	0.31233554	7
ADL64513.1	conserved hypothetical protein	0.74036251	0.17797913	2
ADL64284.1	ABC superfamily ATP binding cassette transporter, binding protein	2.42020463	1.477065	7
ADL65953.1	pheromone lipoprotein CamS	3.28015977	1.69404819	9
ADL65390.1	conserved NfeD-like membrane protein	3.39683607	1.60268756	2
ADL65560.1	penicillin-binding protein 3	5.0114709	2.81975724	2
ADL64447.1	conserved hypothetical protein	3.60485327	1.51560631	5
ADL64802.1	NADPH-dependent 7-cyano-7-deazaguanine reductase	2.49451755	1.29771647	4

[a]Annotation derived from *Staphylococcus aureus* strain JKD6008